POLITECNICO DI MILANO
School of Industrial and Information Engineering

Chemistry, Material and Chemical Engineering Department "Giulio Natta"
Master of Science in Chemical Engineering

Preliminary study on green-blue microalgae as organic filler in alkali-activated geopolymer binder

Supervisor: Prof. Stefano TURRI
Co-adivisor: Dr. Riccardo CIAPPONI

Antonio CANNAVACCIUOLO
ID: 842418

Academic Year 2016-2017

Contents

Abstract

The treatment of saline wastewater in presence of organic content represents a challenge for many industrial sectors. Saline wastewater is extremely difficult and expensive to treat, and its discharge represents a major threat to the environment, due to the presence of organic content suspended solids, nutrients (mainly nitrogen and phosphorus) and salt (concentration up to 15%).

SaltGae project has received funding from the European Union's Horizon 2020 research and innovation programme. The aim of the project is to implement and demonstrate at large scale the long-term technological and economic feasibility of an innovative, sustainable and efficient solution for the treatment of high salinity wastewater with the use of algae/bacteria. This kind of solution stands out for its high added value: not only will it provide an effective and ecological solution for wastewater treatment, but also it will represent an innovative way of producing algal biomass, that will subsequently be valorised into different by-products, reducing the economic and environmental impact of the treatment.

The aim of this thesis work was to study and characterize microalgae in order to understand if is feasible the use of algae as organic filler for ceramic or alkali-activated geopolymer, which in recent years has become one of the major alternatives to Portland cement.

Spirulina Platensis and Tetraselmis Seucica have been take into consideration for the characterization and chemical analysis. Thermogravimetric analysis was used to estimate the water content of the lyophilized microalgae and their heat resistance. Infra-red spectroscopy has been also performed in order to study the chemical composition and the main chemical bonds of the microalgae and geopolymer structure. Rheology study has been conducted in order to understand the influence of the microalgae on the geopolymer paste.

Also, a properly modified 3D printer was used in order to carry out several printability tests. In this way samples for the dynamic mechanical analysis and compression tests have been printed.

These tests have been done in +Lab, the 3D Printing Lab of Politecnico di Milano.

Sommario

Il trattamento delle acque reflue industriali con alta concentrazione di sali in presenza di contenuto organico rappresenta una sfida per molti settori. Le acque reflue salate sono estremamente difficili e costose da trattare e, se riversate, rappresentano una grave minaccia per l'ambiente a causa della presenza di sostanze solide in sospensione, sostanze nutritive (principalmente azoto e fosforo) e sale (concentrazione fino al 15%).

Il progetto SaltGae ha ricevuto finanziamenti dal programma di ricerca e innovazione dell'Unione Europea Horizon 2020. Lo scopo del progetto è di attuare e dimostrare su grande scala la fattibilità tecnologica ed economica a lungo termine di una soluzione innovativa, sostenibile ed efficiente per il trattamento di acque reflue ad elevata salinità con l'utilizzo di alghe/batteri. Questo tipo di soluzione si distingue per il suo elevato valore aggiunto: non solo fornirà una soluzione efficace ed ecologica per il trattamento delle acque reflue, ma rappresenterà anche un modo innovativo per produrre la biomassa algale, che sarà successivamente valorizzata in diversi sottoprodotti, riducendo l'impatto economico ed ambientale del trattamento.

Lo scopo di questo lavoro di tesi è stato quello di studiare e caratterizzare alcune specie di microalghe per capire se fosse possibile utilizzarle come filler organico per ceramica o geopolimero, che negli ultimi anni è diventato una delle principali alternative al cemento di Portland.

Spirulina Platensis e Tetraselmis Seucica sono state le due spiecie di alghe prese in considerazione per la caratterizzazione e l'analisi chimica. L'analisi termogravimetrica è stata utilizzata per stimare il contenuto d'acqua della microalga liofilizzata e la loro resistenza al calore. La spettroscopia infrarossa è stata invece eseguita per studiare la composizione e i legami chimici principali nella struttura microalge-geopolimero. Uno studio reologico è stato inoltre condotto per comprendere l'influenza delle microalghe su un impasto fresco di geopolimero e quale effetto avessero sulla viscosità dell'impasto.

Inoltre, è stata utilizzata una stampante 3D correttamente modificata per eseguire diversi test di stampabilità. In questo modo sono stati anche stampati in 3D i campioni utilizzati per diverse analisi meccaniche dinamiche e prove a compressione.

Chapter 1: Introduction

This chapter provides background information on manufacturing processes, especially on additive manufacturing and LDM (Liquid Deposition Modelling) technology. This is followed by a review on the literature with a focus on geopolymer, microalgae and their applications.

1.1 Subtractive and additive manufacturing

Depending upon the physical parameters, design, machining conditions and utilisation of the product, the manufacturing process involved in engineering industries basically can be classified as:

- Subtractive manufacturing;
- additive manufacturing.

Subtractive manufacturing or Machining is defined as a process of removing the material in small amounts from a workpiece by involving various machining processes (drilling, milling, turning, cutting, etc.) to obtain the final finished object. These technologies are done on machines which are operated manually (Drilling, Milling, etc) or computer controlled (CNC machines) [1].

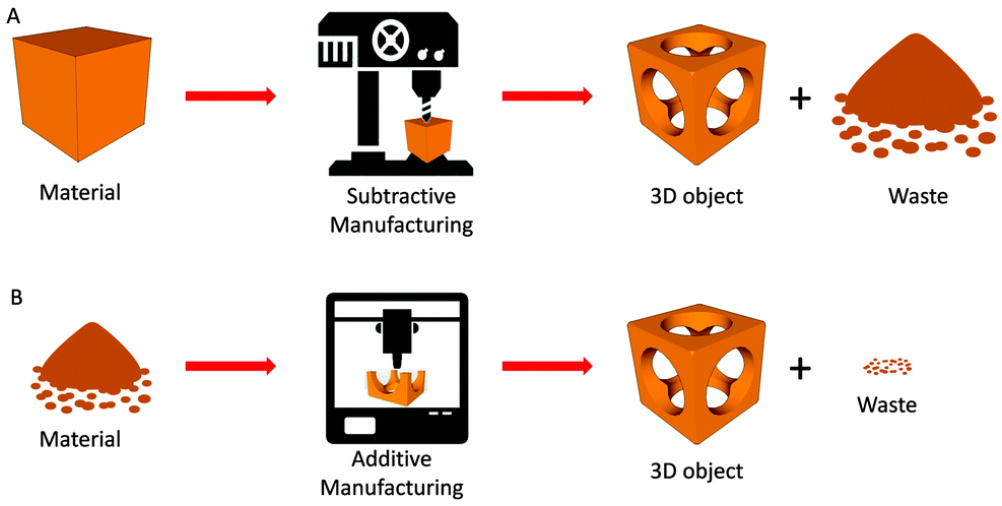

Figure 1. *Subtractive (A) vs. Additive (B) manufacturing.*

The ASTM F42 Technical Committee defines additive manufacturing (AM) as the "process of joining materials to make objects from three-dimensional (3D) model data, usually layer upon layer, as opposed to subtractive manufacturing methodologies". It is also known as additive fabrication, additive processes, direct digital manufacturing, rapid prototyping, rapid manufacturing, layer manufacturing and solid freeform fabrication. The term AM describes additive fabrication processes in the broadest way that includes AM of prototypes (for design verification, form and fit checking), tools, patterns, and concept parts, as well as functional parts with required properties for direct industrial applications and services. Since the late 1980s, AM processes have been investigated, and some have been developed commercially. They include, among others, Stereolithography (SLA), Fused Deposition Modeling (FDM), Selective Laser Sintering (SLS), Laminated Objective Manufacturing (LOM), Three-Dimensional Printing (3DP), and Laser Metal Deposition (LMD). The materials used in these processes include photo-curable resin, polyamide, wax, acrylonitrile-butadiene-styrene (ABS), polycarbonate, metal/ceramic/polymer powders, adhesive coated sheets, etc. [2]. The difference between two technologies is better illustrated in **Figure 1**.

1.2 From 3D modelling to the final object

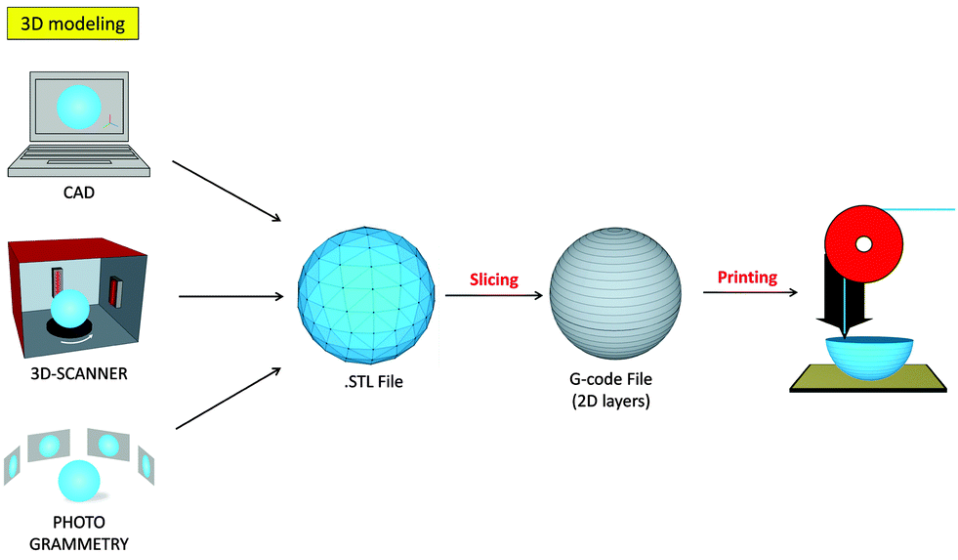

Figure 2. *3D-printing process.*

As **Figure 2** shown, every product development process involving an additive manufacturing machine requires the operator to go through a set sequence of tasks. The seven key steps in the process sequence can summarize as follow:

1. Conceptualization and CAD modelling
2. Conversion to STL
3. Conversion from STL to G-code
4. Machine setup
5. Build
6. Part removal, clean-up of part
7. Application

The first step in any product development process is to come up with an idea for how the product will look and function. If AM is to be used, the product description must be in a digital form that allows a physical model to be made. It may be that AM technology will be used to prototype and not build the final product, but in either case, there are many stages in a product development process where digital models are required. 3D printable models may be created with a computer aided design (CAD) package, via a 3D scanner or via a plain digital camera and photogrammetric software. It is the process of developing a mathematical representation of any three-dimensional surface of an object via specialized software [3].

AM technology would not exist if it were not for 3D CAD. Only after we gained the ability to represent solid objects in computers were we able to develop technology to physically reproduce such objects.

Nearly every AM technology uses the STL file format. The term STL was derived from Stereo Lithography, which was the first commercial AM technology from 3D Systems in the 1990s. STL is a simple way of describing a CAD model in terms of its geometry alone. It works by removing any construction data, modeling history, etc., and approximating the surfaces of the model with a series of triangular facets. The minimum size of these triangles can be set within most CAD software and the objective is to ensure the models created do not show any obvious triangles on the

surface. The triangle size is in fact calculated in terms of the minimum distance between the plane represented by the triangle and the surface it is supposed to represent. In other words, a basic rule of thumb is to ensure that the minimum triangle offset is smaller than the resolution of the AM machine. The process of converting to STL is automatic within most CAD systems, but there is a possibility of errors occurring during this phase. There have therefore been several software tools developed to detect such errors and to rectify them if possible.

Once that's done, the STL file needs to be processed by a piece of software called a "slicer" which converts the model into a series of thin layers and produces a G-code file. The 3D printer follows the G-code instructions to lay down successive layers of liquid, powder, paper or sheet material to build the model from a series of cross sections. Several open source slicer programs exist, including Skein forge, Slic3r, and Cura-engine as well as closed source programs including Simplify3D and KISSlicer. Examples of 3D printing clients include Repetier-Host, ReplicatorG, Print run/Pronterface and Cura. It should be noted here that in practice the client software and the slicer are often combined into one software program. In many case, it’s also possible avoid the use of the client softwares. The latest generation of 3D printers are equipped with an SD slot in which a memory card containing G-code file can be inserted in. In this thesis work in particular Slic3r, Cura and SolidWorks were used in order to make the solid digital model of different samples first, the slicing and conversion to the final G-code file. Finally Repetier-Host was used to better control and adjust different parameters (flow, speed, etc.) during the build process.

1.2.1 Printer setup and build

Before the build process The AM machine must be properly set up. All AM machines will have at least some setup parameters that are specific to that machine or process, like the material constraints, energy source, layer thickness, timings, etc. Some machines are only designed to run a few specific materials and give the user few options to vary layer thickness or other build parameters. Other machines are designed to run with a variety of materials and may also have some parameters that require optimization to suit the type of part that is to be built, or permit parts to be built quicker but with poorer resolution. Such machines can have numerous setup

options available. It is common in the more complex cases to have default settings or save files from previously defined setups to help speed up the machine setup process and to prevent mistakes being made [4].

Although benefitting from the assistance of computers, the first few stages of the AM process are semiautomatic tasks that may require considerable manual control, interaction, and decision making. Once these steps are completed, the process switches to the computer-controlled building phase and AM machine will repeat the layering process until the build is complete. All additive manufacturing (AM) models are built by joining single layers of equal thickness. The layer is shaped (contoured) in an x-y plane two-dimensionally. The third-dimension results from single layers being stacked up on top of each other, but not as a continuous z coordinate. In the strictest sense, additive manufacturing processes are therefore 2½D processes. The models are therefore three-dimensional forms that are very exact on the building plane (x-y direction) and owing to the described procedure are then stepped in the z direction, whereby the smaller the z step is, the more the model looks like the original. Today, the layer thickness is between 0.1 and 0.05 mm. Machines that are used for macroscopic components (characteristic dimensions of several to 100 mm) have a minimum thickness of 0.016 mm, and micro components have layer thicknesses up into the 5 nm range [5].

One of the larger criticisms with subtractive operations is the removal of a little (or a lot) of material from stock material, creating waste. Also in the case of AM technology, the output from AM machine or 3D printer needs to be refined. In all cases, the part must be either separated from a build platform on which the part was produced and it's necessary remove the excess build material or support structures that are eventually made to avoid collapsing or warping during the build process.

1.2.2 Level of applications

Regarding applications, the technology of additive manufacturing/3D printing is divided in two main application levels, so it is very and helpful to make a distinction between Rapid Prototyping (RP) and Rapid Manufacturing (RM).

Regarding the application level "rapid prototyping", two sub-levels can be distinguished: "Solid Imaging" and "Concept Modeling" on the one hand and

"Functional Prototyping" on the other hand. Solid imaging or concept modeling defines a family of parts that are applied to verify a basic concept. The parts resemble a three-dimensional picture or a statue. In most cases, they cannot be loaded. They are used just to get a spatial impression in order to judge the general appearance and the proportions. Because of this the parts are also called "show-and-tell models". Functional Prototyping is applied to allow checking and verifying one or more isolated functions of the later product or to make the production decision, even though the model cannot be used as a final part.

The application level "Rapid manufacturing" summarizes all processes that deliver final products or final parts that need to be assembled to become a product. An AM part is called a product or final part, if it shows all characteristics and functions that are allocated to it during the product development process. If the resulting part is a positive, the process is called "Direct Manufacturing", if it is a negative, which means a die, a mold or a gauge, it is named "Direct Tooling" [6].

The development of innovative, advanced AM techniques has progressed greatly in recent years, yielding broader and broader industry applications. Compared with subtractive manufacturing, AM is particularly suitable for producing low volumes of products, especially for parts with complex geometries.

When compared with conventional manufacturing processes, few of the additive manufacturing processes have seen commercial realization stemming from the ongoing research and development, but additive manufacturing has the following advantages to offer:

- Efficiency in material use: unlike conventional manufacturing based on subtractive principles wherein a large amount of material must be removed, additive manufacturing puts the raw materials to efficient and effective use by building parts layer by layer. The materials that are left over are often reused with minimum processing;
- efficiency in the use of resources: conventional manufacturing processes often require auxiliary resources such as jigs, fixtures, cutting tools, and coolants, in addition to the primary machine tool; however, additive manufacturing does not require such additional resources. As a result, a

variety of parts can be made by small manufacturers that are located close to their customers. This scenario presents an opportunity for improved supply-chain dynamics;

- part flexibility: because additive manufacturing has no tooling constraints, parts having complex features can often be manufactured in a single piece. This has made it possible to not sacrifice the functionality of a part to ensure ease and repeatability in manufacturing. Also, it is currently possible to build a single part with varying mechanical properties, such as a part being flexible at one end and stiffer at the other end. This has opened up new opportunities for novel design innovations;
- flexibility in production: additive manufacturing machines do not require costly setups, so they can be economical for the production of small batches. The overall quality of the part is more dependent on the process used rather than skill-set of the operator, which allows production to be synchronized with customer demand. Also, problems associated with line balancing and production bottlenecks are eliminated because complex parts can be easily produced as a single piece.

The science and technological capabilities of additive manufacturing have made possible its use in a wide spectrum of applications, including the following:

- Cellular machines;
- custom medications;
- flexible electronics;
- high-strength, lightweight aerospace structures having material gradients;
- high-power, high-energy-density microbatteries;
- human organs;
- multifunctional houses;
- products having embedded multi-material sensors and actuators;
- turbine blades having internal cavities [7].

However, 3D-printing could also make a significant impact in the field of chemical synthesis research and manufacturing, in particular because of the ease and economy with which bespoke reactors and complex structures can be designed and compounds manufactured [8]. One of the most important environmental challenges of modern society is to develop new catalysts that make possible chemical processes with reduced environmental impact. Catalyst immobilization is an appealing strategy that, in addition to facilitating catalyst recovery, has proved to give higher catalytic performance, since the solid support usually provides chemical, thermal, and mechanical stabilization to the catalytic species. Catalytic systems and support can be synthesized by 3D printing technology. Ease of preparation of complex shape structures with high surface area make 3D printing technique a good strategy for fabricating different types of heterogeneous catalytic systems [9].

1.3 Classification

AM developed in the 1980s, when a man named Charles “Chuck” Hull invented the first form of 3D printing, called stereolithography (SLA). SLA is a system where an ultraviolet (UV) light source is focused down into an UV photo-curable liquid polymer bath where upon contact, the polymer hardens. Patterns can be drawn using the UV source to semicure the polymer layer. Uncured polymer stays in the bath and provides support to the part being built. After a layer of printing is done, the hardened polymer layer moves down on a build plate in the liquid medium and the next layer of polymer is available on top for the following layer. This process continues until the part is finished based on the CAD design and is removed from the liquid medium. **Figure 3** shows also another configuration of SLA in which a laser beam is scanned from the bottom of the liquid tank through a transparent window. The polymerized layer attaches to the table, which is then moved upwards to refill the gap between the first layer and the window with fresh resin. After these years other innovators started to develop new types of AM machines that used different methods and materials [10].

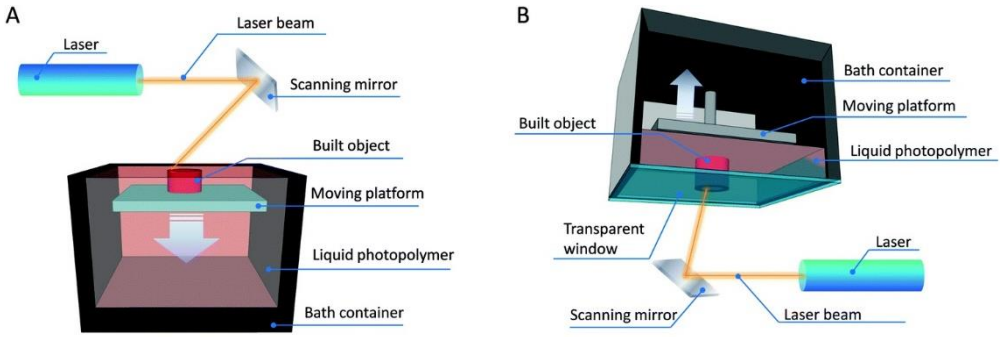

Figure 3. *SLA in a bath configuration (A) and SLA in a layer configuration (B).*

Table 1. *Summary of 3D-printing methods.*

3D-printing process	Technique	Materials	Advantages	Limitations
Photopolymerization	Stereolithography (SLA)	Photopolymers	Simple	Single material
	Material jetting	Photopolymers	Multimaterial structures	High cost
	Continuous liquid interface printing (CLIP)	UV-curable resins	High speed	Single material
	Two-photon polymerization (2PP)	UV-curable resins	Sub-100 nm resolution	Low yield of production
Extrusion	Fused deposition modeling (FDM)	Thermoplastics (ABS, PLA, PC, PA, etc.); glass (new); metal (new)	Simple, multimaterial structures; low cost (for thermoplastic materials)	High cost (for glass and metal)
	Robocasting (DIW)	Plastics, ceramic, food, living cells, composites	Versatile	Requires post-processing; low resolution
Powder based	Selective laser sintering (SLS)	Thermoplastics, metals	No need for support material	Limited mechanical properties of object; high cost
	Selective laser melting (SLM)	Metals	No need for support material	High cost

	Electron beam melting (EBM)	Metals	No need for support material	High cost
	Binder jetting	Any material in particulate form	No need for support material; versatile; lower cost than laser-based methods	Limited mechanical properties
	Selective inhibition sintering (SIS)/inhibitor jetting	Metal	Sintering is performed only once after printing; lower cost than laser-based methods	Low resolution; limited mechanical properties
Lamination	Laminated object manufacturing (LOM)	Paper, metal, plastic, etc. as laminated sheets	Versatile	Limited mechanical properties; some design limitations

Another distinction needs to be made. In this thesis LDM (Liquid Deposition Modeling) process and 3Drag printer are used in order to extrude an alkali-activated ceramic paste.

1.3.1 FDM and LDM

In terms of hardware units sold, the most common 3D printing technology is ‘material extrusion’. This refers to any process that builds up objects in layers by outputting a semiliquid material from a computer-controlled nozzle (**Figure 4**). Many different build materials, including concrete, ceramics, chocolate and even metals can be 3D printed using material extrusion. But the most widely extruded materials are plastics, technically known as thermoplastics that can be temporarily melted for output through a nozzle.

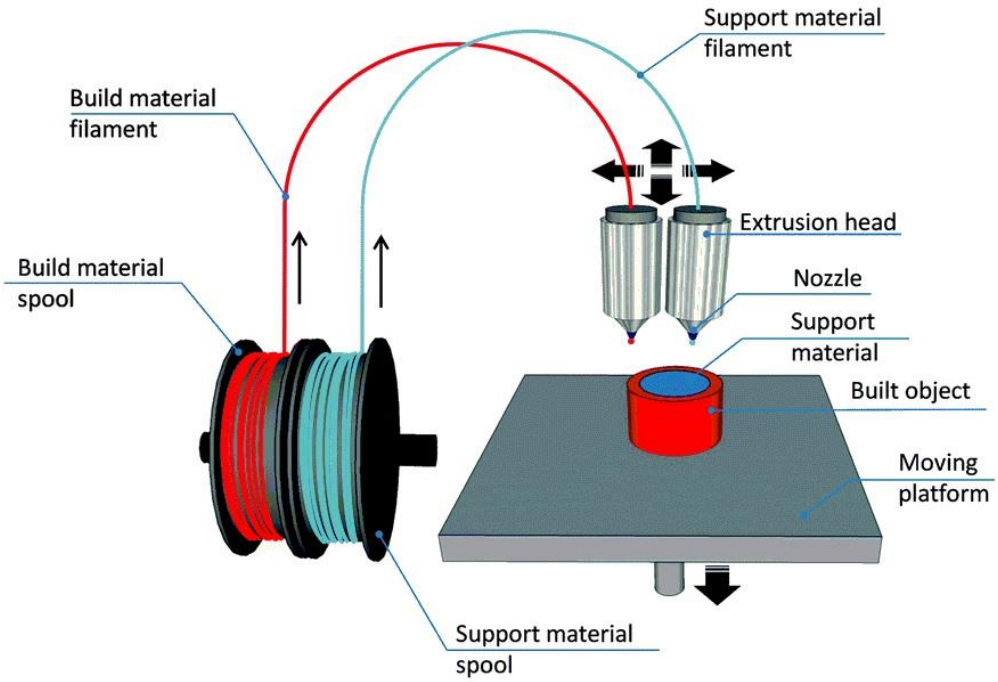

Figure 4. *Schematic diagram of fused deposition modeling (FDM).*

The material extrusion of thermoplastics was invented by a now-market-leading company called Stratasys that labelled the technology 'fused deposition modelling' or 'FDM'. The term FDM has subsequently become widely used (and misused) to refer to the extrusion of thermoplastics, and even to material extrusion technologies more generally. Many build materials can potentially be used in a thermoplastic extrusion 3D printer, the most common is acrylonitrile butadiene styrene, otherwise known as 'ABS', a petroleum-based thermoplastic polymer. Spools of ABS filament are available in a variety of colours, with a typical filament being either 1.75 mm or about 3 mm in diameter. In addition to the aforementioned petroleum-based build materials, another very popular filament is polylactic acid, otherwise known as 'PLA'. This is a bioplastic that is currently made from agricultural produce such as corn starch or sugar cane, and which is subsequently more environmentally friendly than ABS. PLA is also very safe to work with as it does not emit toxic fumes when heated [11].

Extrusion freeforming of ceramics (EFF) is an AM technology based on the continuous deposition of ceramic loaded paste or preceramic precursor extrudates

in a layerwise fashion to build up 3D structures. A variety of synonyms exist that may lead to confusion. For instance, Fused deposition modeling, which was modified in order to fabricate ceramics, is often abbreviated FDC (Fused deposition of ceramics) or LDM (Liquid deposition modeling). In this technology, heated extruder is not needed, but the rheology of the ceramic paste plays an important role during the print process. The feedstock material with a suitable solidification kinetics must be used in order to avoid surface imperfection or collapsing during the built [12]. The extrusion is made by an extruder that may be pressure controlled or volume controlled, whereas pressure control requires calibration of the volume flow, which is highly sensitive to the rheological properties of the feedstock.

1.4 Metakaolin-based geopolymer

The French scientist and engineer Prof. Joseph Davidovits coined the term ‘geopolymer’ in the 1970s. These materials were originally developed as fire-resistant alternative to organic thermosetting polymers, or as a resin in high-temperature carbon-fibre composites. A ‘geopolymer’ is in general defined as a solid and stable aluminosilicate material formed by alkali hydroxide or alkali silicate activation of a reactive precursor that is usually (but not always) supplied as a solid powder, in particular metakaolin (calcined kaolinite clay) or fly ash (a by-product of coal combustion). This results in the formation of a disordered alkali aluminosilicate gel phase, known as the geopolymeric gel binder phase. Embedded within this phase are unreacted solid precursor particles, and the pore network of the gel contains the water that was used in mixing the precursor [13].

Metakaolin (MK) is obtained starting from kaolin after suitable thermal treatments. The name of kaolin is derived from Chinese term ‘Kao-ling’ meaning high ridge, the name for a hill near Jauchau Fu, where this material was mined centuries ago for ceramics.

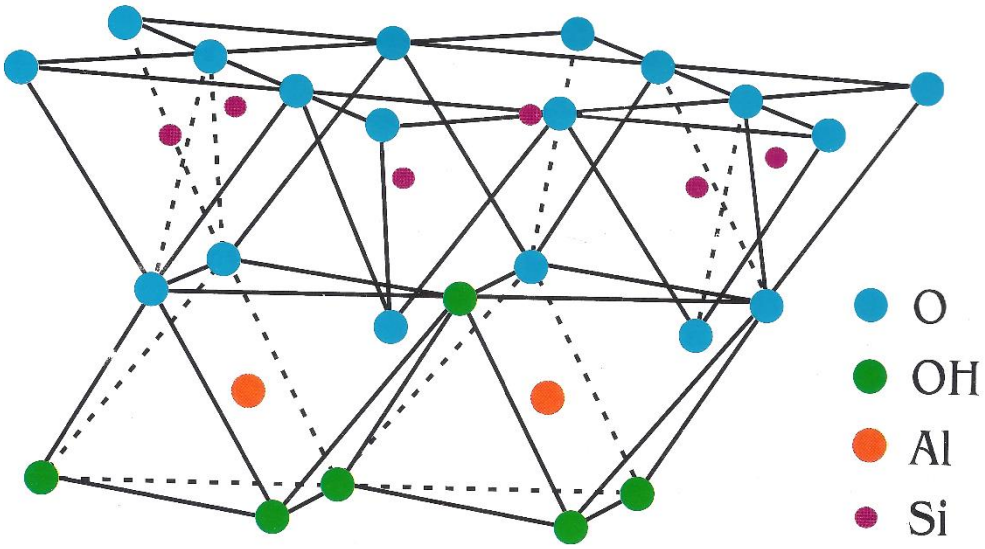

Figure 5. *Semplified kaolinite structure.*

Kaolin is a phyllosilicate, consisting of alternate layers of silica and alumina in tetrahedral and octahedral coordination, respectively (**Figure 5**). This electrically neutral crystalline layer structure, which is a common characteristic of clay minerals, leads to a fine particle size and plate like morphology and allows the particles to move readily over one another, giving rise to physical properties such as softness, soapy, feel and easy cleavage. Kaolinite is the mineralogical term for hydrated aluminium disilicate $Al_2SiO_5(OH)_4$, the primary constituent of kaolin (40-70%).

Under normal environmental conditions, kaolin is quite stable. However, when kaolin heated to temperature of 650-900°C it loses 14% of its mass in bound hydroxylions. This heat treatment, or calcination, breaks down the structure of kaolin such that the alumina and silica layers become puckered and lose their long-range order. Resulting from this dehydroxylation and disorder is MK, a highly reactive transition phase. In metakaolin, the Si – O network remains largely intact while the structure of Al – O network is reorganised.

MK prepared by calcination at 600, 700 or 800°C showed a very similar reactivity. On the other hand, the MK, which was prepared by calcination at 900 ° C, showed lower reactivity due to beginning of sintering [14].

Alkaline activators are the second essential component in alkaline cement design and development. Broadly speaking, the activators used in aluminosilicate

(such as fly ash or metakaolin) based alkaline cements (M_2O-SiO_2-Al_2O_3-H_2O system) are alkaline hydroxides, alkaline silicates or blends of the two, to generate high alkalinity [15]. Alkalis act not only as activators but as structure-forming elements included into the formed phases as well.

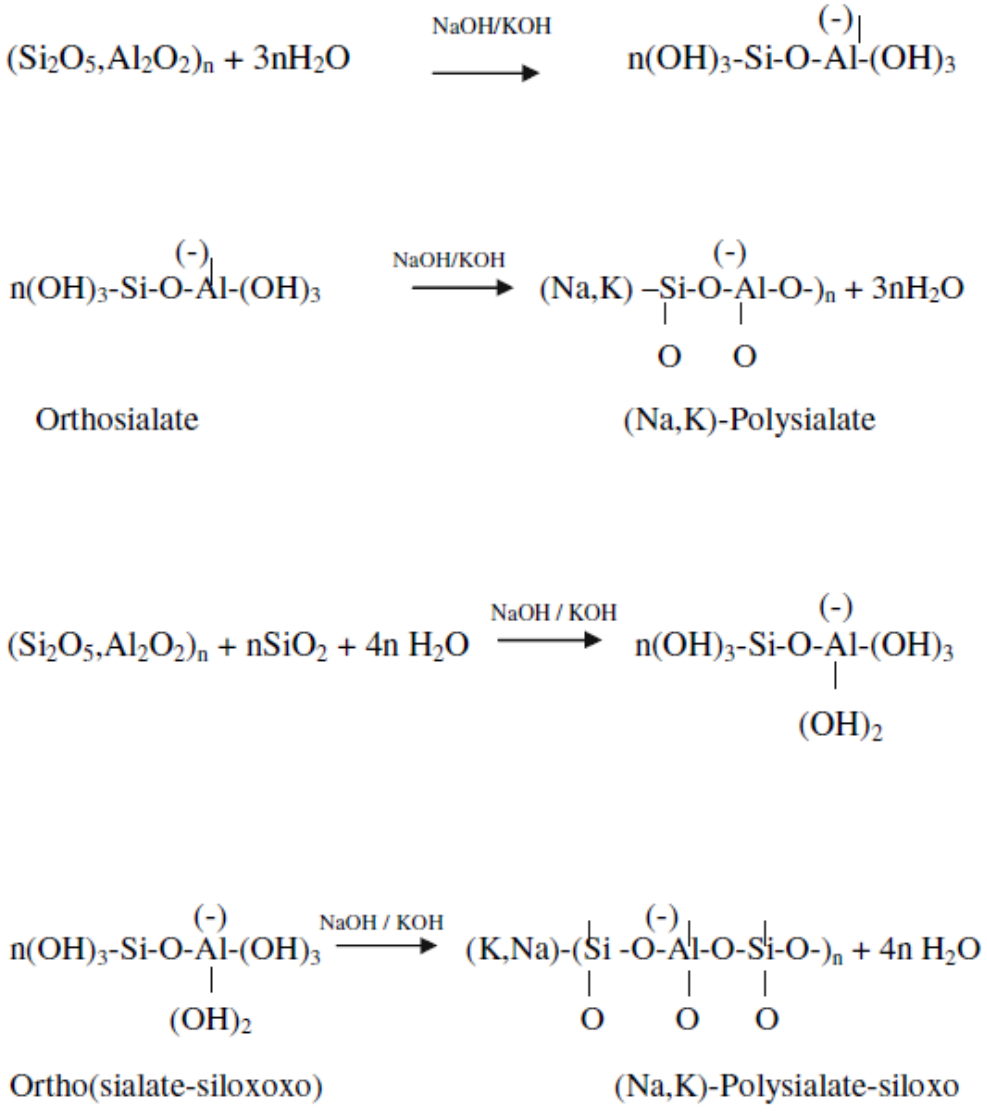

Figure 6. *Reactions involved in geopolymerization [16].*

Figure 6 shows the reactions involved in geopolymerization. The mechanism involves the dissolution of Al and Si in the alkali medium, transportation (orientation) of dissolved species, followed by a polycondensation, forming a 3D network of silico-aluminate structures. These structures can be of three types: poly(sialate) (–Si–O–

Al–O–), poly(sialate–siloxo) (Si–O–Al–O–Si–O) and poly(sialate–disiloxo) (Si–O–Al–O–Si–O–Si–O) [17]. The typical geopolymer composition is generally expressed as $nM_2O{\cdot}Al_2O_3{\cdot}xSiO_2{\cdot}yH_2O$, where M is an alkali metal.

The presence of $[SiO_2(OH)_2]^{2-}$ ions is preferred to $[SiO(OH)_3]^-$ in very high alkaline conditions. Condensation can occur between aluminate and silicate species or silicate species themselves, depending on the concentration of Si in the system. With mixtures with low Si/Al ratios (=1), condensation predominantly occurs between aluminate and silicate species, resulting in mainly poly(sialate) polymer structures. Likewise, when the Si/Al ratio increases (>1), the silicate species formed as a result of the hydrolysis of SiO_2, tend to condense among themselves to form oligomeric silicates. These oligomeric silicates in turn condense with $Al(OH)_4^{4-}$, forming a rigid 3D network of polymer structures [poly(sialate–siloxo) and poly(sialate–disiloxo)] [18]. The final structure consists of aluminum and silica tetrahedrally interlinked alternately by sharing all the oxygen atoms. A polymeric structure of Al–O–Si formed constitutes the main building blocks of geopolymeric structure and the electrical charge balance is maintained by Na, K, Ca and other metallic cations that they are bonded into the matrix via Al–O or Si–O bond or present in the framework cavities [16]. Some terminal hydroxyl groups will doubtless be present at the surface, although this is largely insignificant in the context of the structure of the material [19].

It's not so easy understand the relationship between geopolymer composition, micro e nanostructure and mechanical properties. The mechanical strength of the binder is clearly related to its composition. Theoretically, Si – O – Si linkages are stronger than Si – O – AL and Al – O – Al bonds, meaning that the strength of geopolymers should increase with Si/Al ratio since the density of Si – O – Si bonds increases with Si/Al ratio. But the trend is not monotonically increasing. The decrease in mechanical strength after Si/Al ratio of 1.90 suggests that other factors begin to affect the mechanical properties. Also the unreacted solid aluminosilicate source must to be taken into account, metakaolin in this case. Metakaolin is weak and will be expected to act as a point defect in the structure, locally intensifying the stress in the binder and precipitating failure [20]. Different Si/Al ratio change also the pore distribution and localized gel density, due to the different liability of silica

and aluminium. With Si/Al ratio <1.40 the microstructure exhibits clustered dense particulates with large interconnected pores. With Si/Al >1.65 the porosity appears distributed in small pores [21].

The change in microstructure is a result of variation in the lability of silicate species within the sodium silicate activating solutions that control the rate of strucutural reorganization and densification during geopolymerization. Greater lability allows extensive gel reorganization and densification, and facilitates pores to aggregate resulting in a microstructure comprising dense gel particles and large interconnecting pores, whereas reduced lability promotes a decreased localized gel density and distributed porosity. Lability of the gel during geopolymerization has been linked to the concentration of soluble silicon in the sodium silicate activating solution, with higher lability promoted by low silicon concentration. Grater uniformity in the porous structure explain the increase of compression strength [22].

1.4.1 Alternative to Portland cement

Concrete is the most widely used construction material. Current average consumption of concrete is about 1 t/year per every living human being. Human beings do not consume any other material in such tremendous quantities except for water. Manufacture of ordinary Portland cement (OPC) requires the mining of limestone and releasing of carbon dioxide. For each ton of limestone mined, one-third is released as carbon dioxide that has been locked beneath the surface of the earth for millions of years. Emissions

of greenhouse gases through industrial activities have a major impact on global warming and it is believed that at least 5–7% of CO_2 released to the atmosphere is due to the production of OPC. The release of carbon dioxide is a result of de-carbonation of lime in the kiln during manufacturing of cement (**Figure 7**).

$$5\,CaCO_3 + 2\,SiO_2 \rightarrow 3\,CaO \cdot SiO_2 + 2\,CaO \cdot SiO_2 + 5\,CO_2$$

Figure 7. *De-carbonation of lime [16].*

This has led to significant research on eco-friendly construction materials such as geopolymers and binary- and ternary-blended OPC concretes. The demand for worldwide cement production is increasing by approximately 30% per decade as of 2016. The need for new infrastructure construction in developing nations is projected to force the demand up for cement in the coming years. Manufacture of Portland cement is the fourth largest contributor to worldwide carbon emissions and is only behind petroleum, coal, and natural gas in releasing carbon dioxide that has been locked beneath the earth's surface for millions of years. The new cement factories that are being built mostly in developing nations to meet this forthcoming demand are unsustainable in the long term for the following reasons:

1. Capital Intensive: Cement factories are extremely capital-intensive developments. Once the capital is invested, the investor is committed to cement-production tonnages to recoup their capital investments. Cement manufacturers are notoriously well connected in the construction industry and are resistant to any new low-carbon technologies to protect their investments. Once capital investments are locked into new cement factories, there is little incentive for the cement manufacturers to embrace low-carbon technologies;
2. low Employment/Capital Dollars Invested: Cement manufacture is largely automated with low labor intensity. Despite large capital investments, it offers very few employment opportunities. A modern plant usually employs less than 150 people;
3. energy Intensive: Each ton of cement produced requires 60–130 kg of fuel oil or its equivalent, depending on the cement variety and the process used, and about 110 kWh of electricity [23].

Theoretically, any material composed of silica and alumina could be alkali-activated. The investigations performed worldwide have used the following materials as sources for the needed silica and alumina, for example:

- Kaolinitic clays [24];

- metakaolin [25];
- fly ashes [26];
- blast furnace slag [27];
- mixtures of fly ashes and slag [28];
- mixtures of fly ashes and metakaolin [29];
- mixtures of slag and metakaolin [30].

Accordingly, alkali-activation (geopolymerization) could be considered as an economically viable technology for the transformation of industrial wastes and/or products of aluminosilicate composition into attractive beneficial construction materials. Several studies have been devoted to investigate the durability of geopolymers and their response toward various affecting environments [31].

There are different advantages showed by geopolymeric materials or alkali-activated binders: resistance to acid attack, resistance to high temperature and fire, resistance to freeze-thaw and a very high durability [32].

One of the major unanswered questions in the field of geopolymer technology relates to the long-term performance of geopolymeric materials in cement replacement applications. There are many different mechanisms by which traditional concretes become corroded and eventually fail, and the successful introduction of a new alternative to ordinary Portland cements (OPC) will require that the new product is at least as resistant to each of these forms of attack as the traditional technology. Experience has established that OPC-based concrete is not a material of endless durability due to the increasingly common occurrence of structural and material degradation throughout the world. The main reasons given to explain the poor durability of OPC-based concretes are its brittleness, high permeability, low tensile strength, low ductility, volume instability (shrinkage), weak resistance to acid and reasonably low strength to weight ratio [33]. Most of the degradation problems of Portland cement are a direct consequence of its chemistry and microstructure, which is mainly composed of calcium silicate hydrate (CSH), calcium hydroxide (CH), calcium aluminate (CA), tetracalcium aluminoferrite (C_4AF) and calcium sulfoaluminates [34].

Durability testing and acid diffusion testing are therefore a major research focus at present, and preliminary results are very promising in many areas, although data related to the durability of geopolymers under severe conditions and for extended period of time is limited due to the relatively short timeframe in which geopolymer research has been conducted [35].

Concretes degrade by a large variety of mechanisms, with probably the most significant in most parts of the world being chloride attack leading to corrosion of steel reinforcing. In the case of geopolymer phase, it was observed a reduction of chloride ingress due to a very low permeability. This is likely to be of significant value in the development of geopolymer technology for applications ranging from bunkers for nuclear waste storage to coatings for protection of transport infrastructure [36]. In order to explain the durability and also the resistance to the acid attack of the geopolymer binder, different studies were carried out regarding the microstructure and in particular of the aggregate interfacial porosity evaluated by a method for combining scanning electron microscopy and energy dispersive X-ray. In the case of OPC-based concretes, the porosity of the binder phase in contact with natural siliceous aggregate (used for this kind of measurement), the interfacial transition zone (ITZ), is much higher than that of the bulk material. Previous work on the interface between geopolymers and siliceous aggregates has shown the absence of a significant porous ITZ region. This will then allow slow penetration of the aggressive dissolved species throughout the material, degrading its mechanical properties more slowly [37].

1.5 Wastewater treatment with algae

Microalgae have received substantial attention in recent years due to their effective role in the uptake of pollutants from the environment as well as their ability to produce valuable biomass that can be used in different industrial applications such as food processing, pharmaceuticals, organic fertilizer, animal feed, biofuel and biogas.

Discharge of wastewater that is rich in nutrients can cause eutrophication which is a serious problem that occurs particularly in enclosed water bodies.

Eutrophication occurs when a dense bloom of algae grow in water due to presence of high concentrations of nitrogen and phosphorus, the main nutrients of concern. This reduces the level of oxygen in the aquatic system to less than the natural level that is required by aquatic organisms causing their death (**Figure 8**). The ability of microalgae to grow quickly in water that is rich in nutrients can be positively used in wastewater treatment to remove the nutrients from wastewater before discharge to the river [38].

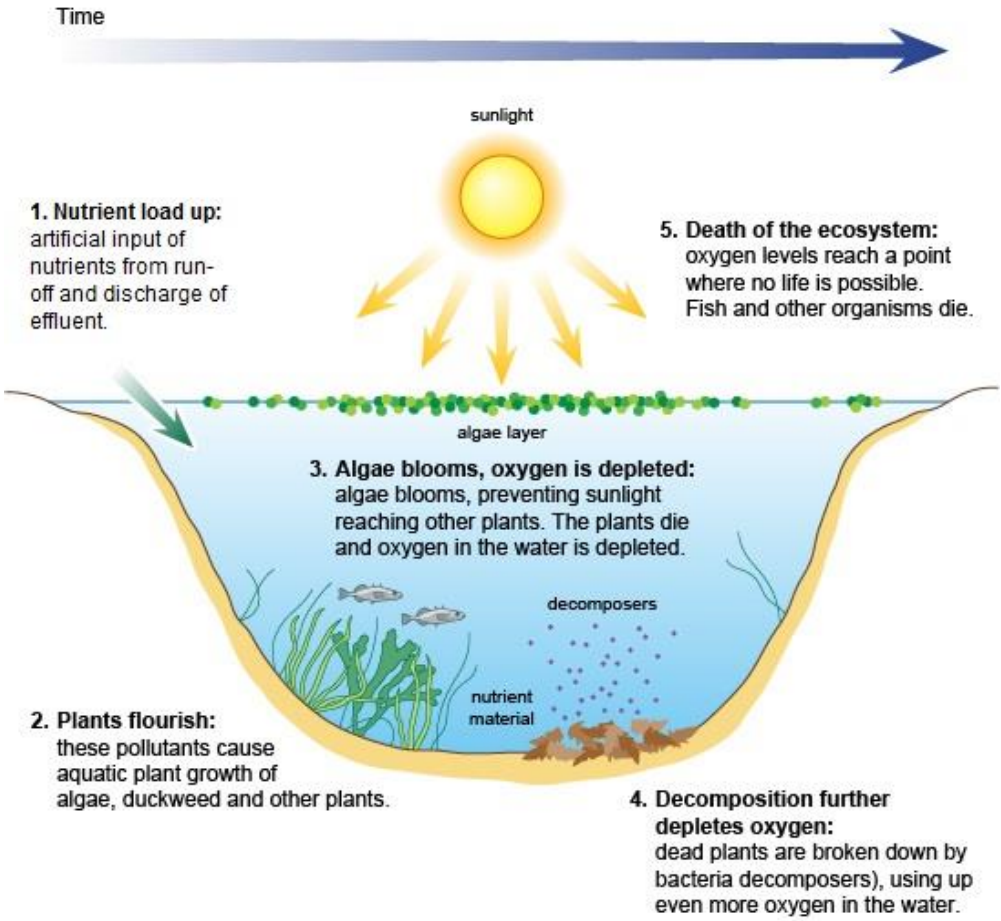

Figure 8. *Steps of Eutrophication Process.*

The term microalgae refers to all algae too small to be seen properly without microscope, and often includes both eukaryotic microalgae and the prokaryotic cyanobacteria [39]. Majority of algae are living in aquatic (saline or freshwater) environments, whereas some of them can be found in other environments such as

snow, desert soils, and hot springs. They can be either autotrophic or heterotrophic. Autotrophic algae require only carbon dioxide, light, and salts to grow, whereas heterotrophic require an organic source of carbon, like glucose, as well as nutrients. Microalgae also can be either phototrophic or chemotrophic.

Phototrophic algae use light as an energy source, whereas chemotrophic type use oxidizing compounds. Additionally, some algae are capable of behaving in both autotrophic and heterotrophic modes. These are called mixotrophic algae [40]. **Table 2** shows a scheme of classification based on the most recently published classifications [41].

Table 2. *Classification Scheme of the Different Algal Groups [41].*

Kingdom	Division	Class
Prokaryota eubacteria	Cuanophyta	Cyanophyceae
	Prochlorophyta	Prochlorophyceae
Eukaryota	Glaucophyta	Glaucophyceae
	Rhodophyta	Bangiophyceae
		Florideophyceae
	Heterokontophyta	Chrysophyceae
		Xanthophyceae
		Eustigmatophyceae
		Bacillariophyceae
		Raphidophyceae
		Dictyochophyceae
		Phaeophyceae
	Haptophyta	Haptophyceae
	Cryptophyta	Cryptophyceae
	Dinophyta	Dinophyceae
	Euglenophyta	Euglenophyceae
	Chlorarachniophyta	Chlorarachniophyceae
	Chlorophyta	Prasubiohyceae
		Chlorophyceae
		Ulvophyceae

	Cladophorophycee
	Bryopsidophyceae
	Zygnematophyceae
	Trentepohliophyceae
	Klebsormidiophyceae
	Charophyceae
	Dasycladophyceae

Microalgae are made up of eukaryotic cells. Microalgae cells consist of cell wall, plasmatic membrane (**Figure 9**), cytoplasm, nucleus and organelles, such as mitochrondria, lysosomes and golgi. Microalgae also have plastids, the bodies with chlorophyll that carry out photosynthesis. However, various strains of microalgae have different combinations of chlorophyll molecules - some have only Chlorophyll A, some A and B, while other strain, A and C. The biomass of microalgae contains three main components: proteins, carbohydrates and lipids in different percentage, depending on different factors because the microalgae growth is influenced by chemical factors (nutrients and carbon dioxide), physical factors (light and temperature of the production environment), but also by operational factors, basically concerns bioreactor design, mixing and dilution rate [42]. A stoichiometric formula for the most common elements in an average algal cell is $C_{106}H_{181}O_{45}N_{16}P$, and the elements should be present in these proportions in the medium for optimal growth.

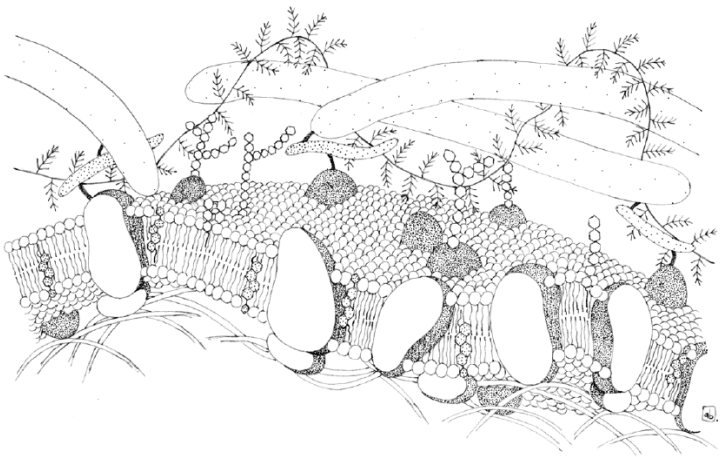

Figure 9. *Schematic drawing of a simple cell membrane [41].*

1.5.1 Cultivation and production methods

There are different production methods. Suspended cultures, including open ponds and closed reactors, and immobilized cultures, including matrix-immobilized systems and biofilms, are the two main methods [43].

The most common large-scale production systems in practice are high rate algal ponds, also known as HRAPs or raceway ponds (

Figure 10). In use since the 1950s, a raceway pond is made of a closed loop recirculation channel that is typically about 0.3 m deep to provide sufficient sunlight to allow photosynthesis by microalgal cells. Mixing and circulation are produced by a paddlewheel. Flow is guided around bends by baffles placed in the flow channel. Raceway channels are built in concrete, or compacted earth, and may be lined with white plastic. During daylight, the culture is fed continuously in front of the paddlewheel where the flow begins. Broth is harvested behind the paddlewheel, on completion of the circulation loop. The paddlewheel operates all the time to prevent sedimentation. In raceways, any cooling is achieved only by

evaporation. Temperature fluctuates within a diurnal cycle and seasonally. Evaporative water loss can be

significant. Because of significant losses to atmosphere, raceways use carbon dioxide much less efficiently than photobioreactors. Productivity is affected by contamination with unwanted algae and microorganisms that feed on algae. The biomass concentration remains low because raceways are poorly mixed and cannot sustain an optically dark zone [44].

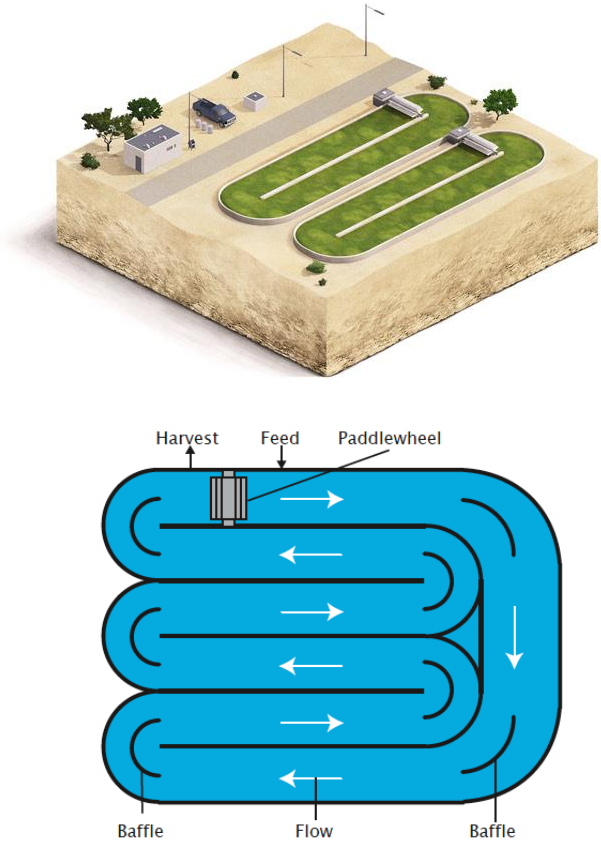

Figure 10. *Schematic examples of raceway algal ponds.*

Compared with open ponds, the design of closed reactors helps avoid water evaporation and contamination, and increases photo- synthesis efficiency. Typical closed reactors include flat plate reactors, tubular photobioreactors, and bag systems and are suitable for photoautotrophic, mixotrophic or heterotrophic algae [45].

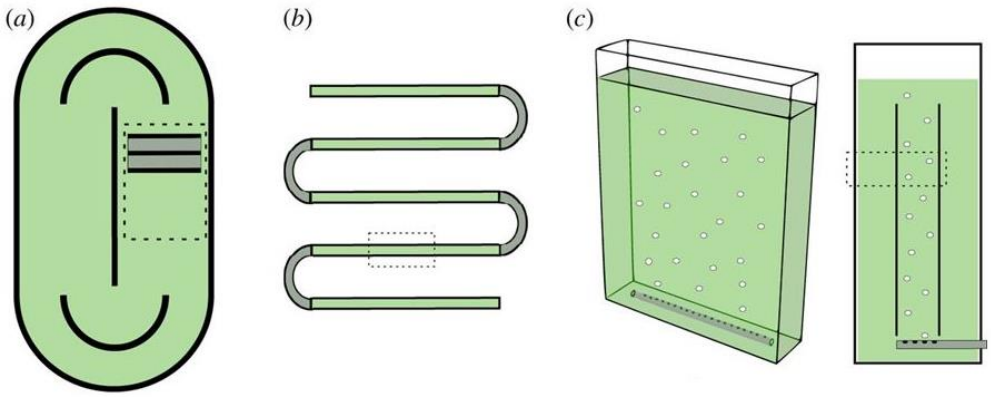

Figure 11. *Raceway pond (top view) (a); tubular photobioreactor, where suspensions are typically driven by a pump (b); flat plate reactor (three-dimensional and cross-sectional view) (c).*

The two basic designs are the flat plate reactors and the tubular photobioreactors (**Figure 11**) with an optimum thickness of the algal culture in these reactors is between 2 and 4 cm. These reactors are designed in order to reduce the light path and thus to increase the amount of light available to each cell. These reactors are also well mixed to ensure optimum light availability to the cells and to enhance gas exchange. These closed reactors have several advantages such as 'clean' algal culture, high light utilisation efficiency leading to high productivities as high sustainable biomass, temperature control and the ability to be used outdoors in natural daylight. This means that a much wider range of species can be cultivated as contamination is avoided and the reactors can be operated over a much wider climatic range that the open-air systems. There is also a greater ability to control the culture conditions so that the final product is of more consistent composition and quality. Finally, these systems are able to operate in continuous mode. Continuous culture and good control over the growth environment results in a consistent product quality and the higher operating cell densities also mean that harvesting costs are reduced and there is a smaller requirement for land [46]. **Table 3** shows several type of photobioreactor and their advantages and disadvantages.

Table 3. *Cultivation of microalgae species in closed photobioreactor systems [42].*

Type of photobioreactor	Strain	Capacity (L)	Biomass concentration	Advantage	Disadvantage
Tubular	*Phaeodactylum tricornutum*	200	1.19 g/L	1. Very effective light use, 2. Excellent temperature control, 3. Reasonable scale up.	Fouling with some growth along walls.
	Phaeodactylum tricornutum	75	1.38 g/L		
	Porphyridium cruentum	6000	35 g/m^2/d		
	Spirulina sp.	10000	25 g/m^3/d		
	Spirulina platesnsis	5.5	0.62 g/L		
	Spirulina platensis	65	32.5 g/m^2/d		
	Spirulina sp.	100	0.01 g/L/g		
Airlift	*Botryococcus braunii*	3	2.31 g/m^3/d	1. Good light use, 2. High temperature control, 3. High mass transfer coefficient	1. Low hydrodynamic stress on algae, 2. Difficult to scale up.
	Chaetoceros sp.	170	0.80 g/L		
	Chlorella sp.	n/a	109–264		
	Chlorella vugaris	2	0.28-0.89 g/L/d		
	Haematococcus pluvialis	3	4.09 g/L		
	Nannochloropsis sp.	n/a	32.5–95.3 g/m^3/d		
Bubble column	*Aphanothece microscopica*	3	0.77 g/L/d	1. Scalable; homogeneous culture environment, 2. Low cooling requirement, 3. Effective light use.	Increased shear stress by pumps limiting biomass productivity.
	Chaetoceceros sp.	170	3.31 g/L		
	Chlorella vulgaris	1.8	1.41 g/L		
	Cyanobium sp.	1.8	0.071 g/L		
	Phaeoductylum sp.	1.9	n/a		
	Isochrysis aff. Galbana	5	n/a		
	Monodus sp.	64	0.03–0.20 g/L		
	Monoraphidium sp.	4.5	23 g/m^3/d		
	Scenedesmus obliquus	1.8	2.12 g/L		
	Spirulina sp.	3.5	4.13 g/L		
Flat plate	*Chlorella vulgaris*	1.5–3.0	0.027–0.045 g/L/h	1. Excellent light use and temperature control, 2. Low cooling requirement, 3. High gas transfer coefficient.	Difficult to scale up.
	Dunaliella sp.	3.4	1.5 g/L		
	Dunaliella tertiolecta	30	3.42 g/d		
	Nannochloropsis sp.	200	0.225 g/L		
	Nannochloropsis sp.	440	0.27 g/L		
	Phaeodactylum sp.	5	1.38 g/L		
Plastic bag	*Tetraselmis* sp.	50	20–30 g/m^3/d	-	-

One of the limitations for the development of wastewater treatment systems based on suspended cultures of microalgae is the recovery of the biomass at the end of the treatment process. However, the immobilization of cells can represent an alternative for solving the problem as well as providing advantages such as an increase in the cell retention time within bioreactors and higher metabolic activity [47]. An immobilized cell is defined as a living cell that, by natural or artificial means, is prevented from moving independently from its original location to all parts of an aqueous phase of a system. Several immobilization methods have been defined and most of the general immobilization techniques for microorganisms can be easily modified and applied to microalgae, adding a design factor that these are photosynthetic microorganisms that require light. The most commonly used method is immobilization in polymers. In these systems, the microorganisms are immobilized to the bedding material, while the

treated fluid flows through it and a separation between the microorganism and the treated waste occurs [48]. After absorption of the contaminants by the microalgae, the cleaner waters diffuse out of the polymers and are collected and reused and the process is repeated for several cycles. Both synthetic (acrylamide, polyurethane, polyvinyl, resins) and natural polymer derivatives of algal polysaccharides (alginate, carrageenan, agar, agarose) can be used in this process. Regardless of the polymers used, the material must be hydrophilic, allowing wastewater to diffuse into the bead. The most commonly used polymers are the natural polymers alginate and carrageenan, even though natural polymers are less stable in wastewater than synthetic polymers and they can dissolve in highly contaminated wastewater but diffusivity is higher and they are less hazardous to produce. Alginates (polymers made of different proportions and sequences of mannuronic and guluronic acids extracted from brown algae) are the polymers of choice in most systems of immobilization because they are easy to handle, nontoxic to humans, the environment, and the entrapped microorganisms, legally safe for human use, available in large quantities, and inexpensive. From a physiological perspective, a major advantage of alginate is that immobilized cells do not suffer extreme changes in physicochemical condition during the procedure of

immobilization and the gel is transparent and permeable. Regarding the general effect on microalgae, immobilization in alginate beads of the hydrocarbon-rich microalgae yielded a significant increase in chlorophyll, carotenoids, dry weight, and lipids during the stationary and resting growth phases, compared to free-living cells. In other cases a polymeric matrix leads to an increase of the glycerol or ammonia production and the cell walls are also protected against toxic chemical species [49].

1.6 Wastewater treatment

Today, although the strategic importance of fresh water is universally recognized more than ever before, and although issues concerning sustainable water management can be found almost in every scientific, social, or political agenda all over the world, water resources seem to face severe quantitative and qualitative threats. The pollution increase, industrialization and rapid economic development, impose severe risks to availability and quality of water resources, in many areas worldwide. Pollution is a man-made phenomenon, arising either when the concentrations of naturally occurring substances are increased or when non-natural synthetic compounds (xenobiotics) are released into the environment. Watercourses receive pollution from many different sources, from towns and villages; discharge from manufacturing or industrial plants; run-off from agricultural land; and leachates from solid waste disposal sites. The composition of wastewater is a complex mixture of natural organic and inorganic materials as well as man-made compounds. Three quarters of organic carbon in sewage are present as carbohydrates, fats, proteins, amino acids, and volatile acids. The inorganic constituents include large concentrations of sodium, calcium, potassium, magnesium, chlorine, sulphur, phosphate, bicarbonate, ammonium salts and heavy metals [50]. Also, the high salt wastewater released by food industries (i.e. pickled pickles production) is a serious problem for the environment. High salt wastewater refers to the total salt (NaCl content meter) for at least 1% of the wastewater and a large number of inorganic salts, such as Cl^-, Na^-, Ca^{2+} and SO_4^{2-}. If this high salts concentration is released into soil system can cause the collapse of the soil ecological

system destroying the organisms and plants due to dehydration and bringing an acceleration of eutrophication process in the lakes and rivers [51].

The aims of wastewater treatment are to convert the waste materials present in wastewaters into stable oxidised end products which can be safely discharged to inland or coastal waters without any adverse ecological effects; to protect public health; to ensure wastewater is effectively disposed of on a regular and reliable basis without nuisance or offence; to provide an economical method of disposal; and to recycle and recover the valuable components of wastewater. A wastewater treatment plant is a combination of separate treatment processes or units designed to produce an effluent of specified quality from a wastewater (influent) of known composition and flow rate. Unit treatment processes can be classified into four stages:

1. Preliminary treatment: the removal and disintegration of gross solids, the removal of grit and the separation of storm water. Oil and grease are also removed at this stage if present in large amounts
2. Primary (sedimentation) treatment: the first major stage of treatment following preliminary treatment, which usually involves the removal of settleable solids which are separated as sludge
3. Secondary (biological) treatment: the dissolved and colloidal organics are oxidised in the presence of micro-organisms
4. Tertiary treatment: further treatment of a biologically treated effluent to remove BOD5, bacteria, suspended solids, specific toxic compounds or nutrients to enable the final effluent to comply with a standard more stringent than 20:30 before discharge

A general layout of wastewater treatment is showed in **Figure 12**.

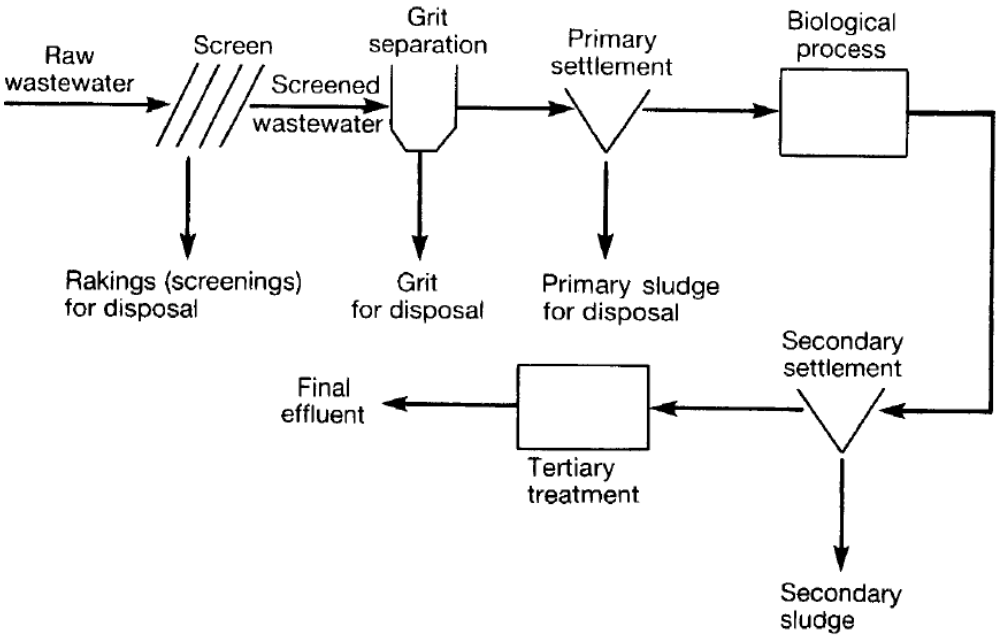

Figure 12. *General layout of wastewater treatment showing primary, secondary and tertiary treatment stages [52].*

1.6.1 Preliminary and primary treatment

In order to avoid damage of the pumps and blocking of the tubes, coarse solids (floating solids, rags, paper, wood, plastic) that are contained in the raw sewage, need to be removed prior to treatment. Most plants employ simple screens comprising vertical rows of steel bars which can be curved, vertical straight or inclined straight in design, to physically remove such solids from the influent wastewater. Screens are in four sizes, coarse, fine, very fine, or micro and usually they are angled at 60° to the flow to facilitate manually cleaning, of if the flow exceeds approximately 1000 m^3d-1, then mechanically operated rakes are used. Mechanical raking systems operate either on a time basis or by depth using some form of water level detector (e.g. float switch) because as the solids are retained, thereby blocking the screen, the flow is impeded so that the level of the wastewater downstream of the screen rises. **Table 4** shows several categories of industrial screens and their applications.

Table 4. *Typical size range of screens used in wastewater treatment [52].*

Category	Spacing (mm)	Application
Coarse screens	> 10	Removal of large material
Fina screens	1.5–10	Used as substitute for primary sedimentation for extended aeration plants
Very fine screens	0.2–1.5	Used as substitute for primary sedimentation Used in conjunction with series of larger screens
Micro-screens	0.001–0.3	Effluent polishing. Treatment of inert quarry washings

The materials removed from screens are generally called screenings or rakings. Many plants use macerators or disintegrators in order to chop up the screenings and after this operation they are co-settled with raw sludge in the primary sedimentation tank.

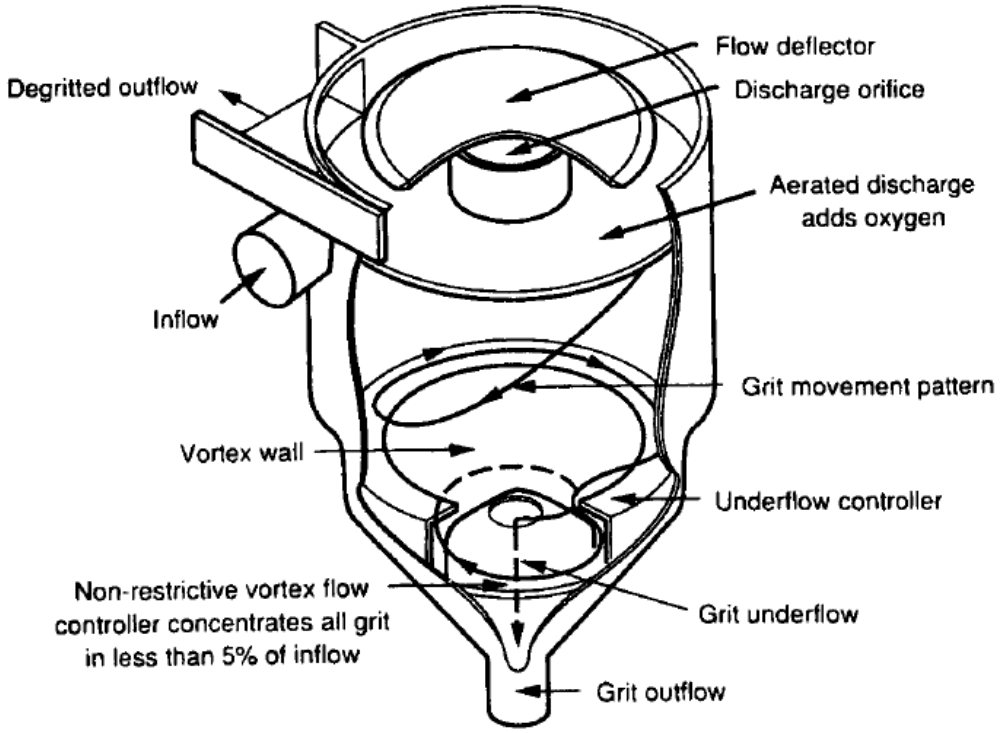

Figure 13. *Grit separation using vortex-type systems [52].*

After maceration, the wastewater contains a mixture of silt, sand and gravel and fragments of metal and dense plastic. This mixture is called grit and his density is greater than wastewater, for this reason the separation can be easily carry out

with detritors or vortex separators that are the most commonly used systems based on sedimentation.

In many plats, after the grit separation, special units that employ dissolved air and nitrogen are used. Compressed air is fed into wastewater and small bubbles are formed in order to allow the flotation of suspended particles that have a specific gravity less than water, in this way a thick surface layer of solids know as float is formed out of the water and it can be removed by a mechanical skimming device that pushes the solids into a collection chamber. Dissolved air flotation (DAF) units are generally used to remove emulsified fats, oil and grease (FOG). In some cases, chemical flocculants (e.g. polyacrylamide, iron and aluminium salts) are used to improve the DAF performance.

The primary treatment is based on the sedimentation and it can significantly reduce the organic loading to the secondary treatment stage. The settleable solids which are heavier than water are removed from wastewater by allowing the particles to gravitate to the floor of a specially constructed tank to form a sludge that is removed as primary sludge. The sedimentation or settlement process is also used after the second treatment to remove material converted to settleable solids during the biological phase of treatment, such as the removal of humus from filter effluents and the recovery of activated sludge [52].

1.6.2 Secondary treatment

Typically, the preliminary and primary processes are not able to produce a treated effluent which can meet the discharge limits due to the presence of colloidal and soluble pollutants that are organic in nature and biodegradable, so further treatment is needed. In the industrial application, the secondary treatment is often biological in nature and it can be used to provide partial and subsequently almost complete stabilization of the biodegradable substances by using a staged treatment with anaerobic and aerobic processes. Both these processes depend on microorganisms to provide the functional basis for the treatment processes which include carbon oxidation, nitrification and denitrification, acidogenesis, and methanogenesis. Bacteria are the micro-organisms of principal interest and the bulk of these would be both heterotrophs and autotrophs, in this way organic and

inorganic carbon (e.g. carbon dioxide) can be used for cell synthesis. Although treatment processes are generally identified as aerobic and anaerobic, the bacteria in the "aerobic" processes are in fact largely facultative. Obligate aerobes would have required the presence of molecular oxygen to thrive, so it's better to have bacteria able to function under both anaerobic and aerobic conditions in order to perform denitrification, where combined oxygen in nitrites and nitrates are removed releasing nitrogen gas. These aerobic, facultative, and anaerobic bacteria have several distinct shapes or morphology. Many bacteria species common and important to wastewater treatment belong to the cocci or spherical shaped bacteria and the bacilli or rod-shaped bacteria, but it is usually desirable, in wastewater treatment, to have such mixed cultures so that a wide range of pollutants can be handled. A mixed culture is also likely to be more robust when challenged with changing wastewater characteristics [53].

There are different industrial plant configurations to carry out this treatment based on the state of biomass fixation.

Reactors with suspended biomass: activated sludge (several variants); sequencing batch reactor; membrane reactor.

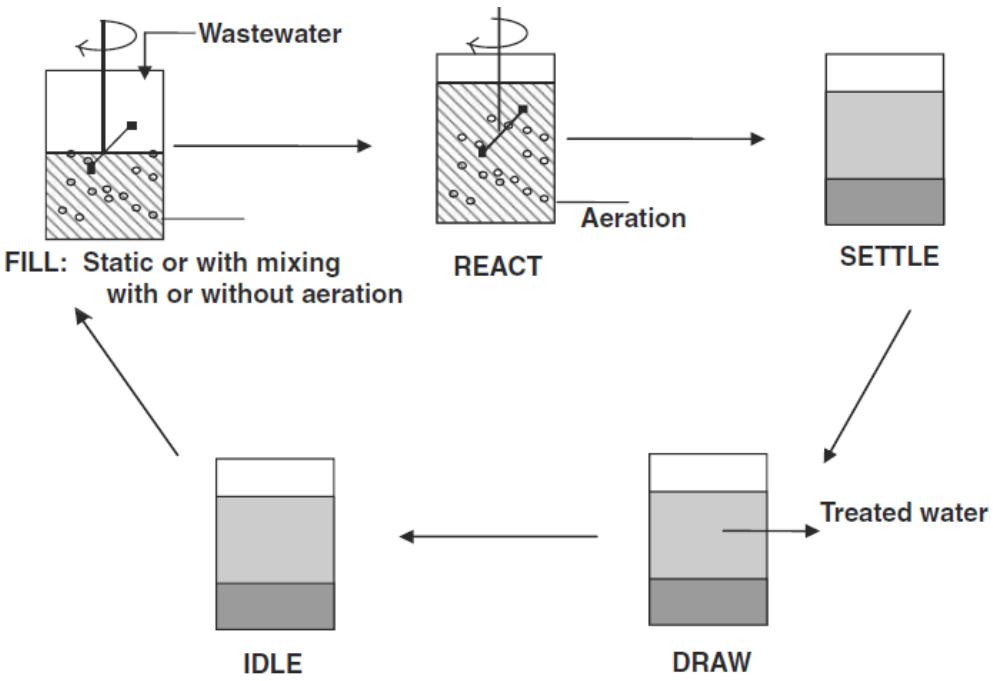

Figure 14. *Schematic operation on a SBR during a cycle [54].*

The term SBR (sequencing batch reactors) is given to wastewater treatment systems, operated on a sequence of fill and draw cycles (**Figure 14**) and it can work with attached biomass. Usually an SBR-type bioreactor operates under five well-defined phases: fill, react, settle, draw, and idle. The settle and draw phases are fixed in duration by the characteristics and constraints of the activated sludge and the reactor itself while the duration of the other phases is usually determined by an expert operator based on his/her experience and exhaustive testing in the laboratory with a pilot plant. The SBR system can be also fully automated using the oxygen uptake rate to determine the end of the reaction phase and an optical or ultra sound device to detect settling [54]. Benefits and advantages of this process can be summarizing as follow:

- less land required than conventional methods;
- lower cost than conventional biological treatment methods;
- capable of handling wide swings in hydraulic and organic loadings;
- easier to control filamentous growth and settling problems;
- less equipment to maintain;
- less operator attention required;
- greater operator flexibility;
- powdered activated carbon (PAC) can be added [55].

The term MBR is applied to the system developed for the wastewater treatment that combines a biological stage and a membrane module bioreactor. A membrane as applied to water and wastewater treatment is simply a material which allows some physical, chemical, or biological components to pass more readily through it than others. Thus, a membrane is permselective, since it is more permeable to those constituents passing through it (which then become the permeate) than those which are rejected by it (which form the retentate) (**Figure 15**).

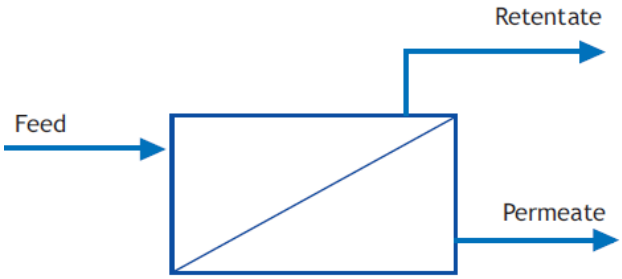

Figure 15. *Schematic of membrane [56].*

The degree of selectivity depends on the membrane pore size. The coarsest membrane, associated with microfiltration (MF), can reject particulate matter and retain bacteria. A tighter ultrafiltration (UF) membrane can also reject viruses. An even tighter nanofiltration (NF) membrane is more selective than reverse osmosis (RO), rejecting a high amount of bulk organic matter and many micropollutant, while tightest/least selective RO can also reject singly-charged (i.e. monovalent) ions, such as sodium (Na^+) and chloride (Cl^-). Membrane bioreactors specifically are a combination of bio treatment with membrane separation by MF or UF. On the simple basis of cost, the preferred membrane materials are polymeric and the common materials are cellulose acetate; polysulphone, polypropylene, PTFE, polyamide (0.04 – 0.1 µm of pore diameter); ceramic materials (0.1 – 0.2 µm), zirconium dioxide (0.05 µm), and alumina (0.2 µm). Regarding the plant configuration, there are two types of configuration for the MBR: the membranes can be placed either outside (sMBR) or inside (iMBR) the bioreactor.

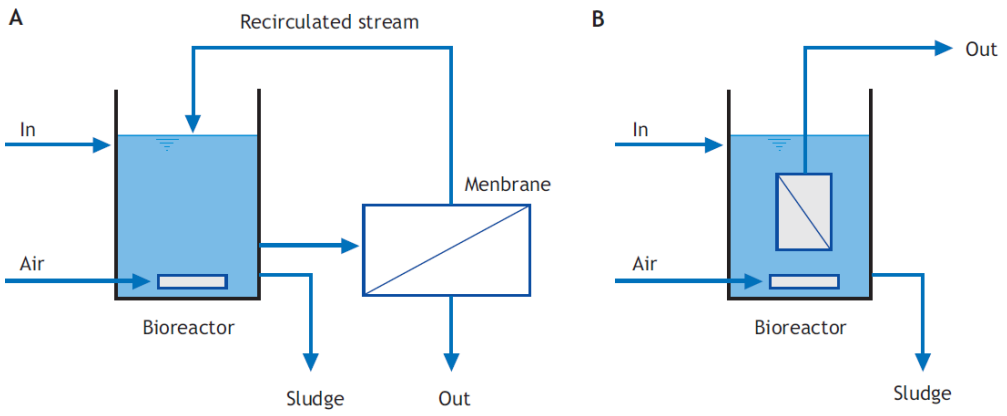

Figure 16. *MBR process conigurations: sidestream MBR (sMBR) (A) and submerged or immersed MBR (iMBR) (B) [56].*

For the external configuration, the mixed liquor is filtered under pressure in a specific membrane module, whereas for the submerged configuration, the filtration is carried out in the aeration basin by suction removal of the effluent, in this case the transmembrane pressure (TMP) is about 0.5 bar. There are also two modes of hydraulic operation: pumped (positive pressure) and air-lift (vacuum pressure), the latter almost exclusively used for immersed systems and the former for side streams.

The rejection of contaminants ultimately places a fundamental constraint on all membrane processes. The rejected constituents in the retentate tend to accumulate at the membrane surface, producing various phenomena which lead to a reduction in the flux (flow per unit area) of water through the membrane at a given transmembrane pressure (TMP), or conversely an increase in the TMP for a given flux (reducing the permeability, which is the ratio of flux to TMP). These phenomena are collectively referred to as fouling. It has been demonstrated that there exists a critical flux, below which the membrane fouling can be neglected and thus membrane cleaning is not required. It is important, therefore, to choose an adequate initial permeate flux or TMP. Conventional techniques for limiting membrane fouling are as follows:

- Reduction of membrane fouling by aeration near membranes by filtration below the critical flux, by the addition of coagulants, by high-frequency backpulsing, or by utilizing a high recycle velocity;
- removal of the fouling material after formation by chemical washing (backwashing or back-pulsing);
- operation in crossflow mode, where the feedwater flows tangentially with the membrane surface and thus applies a degree of scouring which tends to limit fouling deposits on the membrane.

The advantages offered by the process over conventional bio treatment processes are widely recognised, and of these the ones most often cited are:

- Production of a high quality, clarified and largely disinfected permeate product in a single stage, (the equivalent of tertiary filtration);
- absolute and dependent control of solids retention time (SRT) and hydraulic retention time (HRT), parameters which are normally coupled in a conventional treatment plant;
- operation at higher mixed liquor suspended solids (MLSS) concentrations, which both reduces the required reactor size and promotes the development of specific nitrifying bacteria and thus enhancing ammonia removal;
- operation at longer sludge retention time (SRT) providing an opportunity to select for slow-growing bacterial populations with possible enhanced treatment (e.g. organic micro-pollutant degradation);
- reduced sludge production [56].

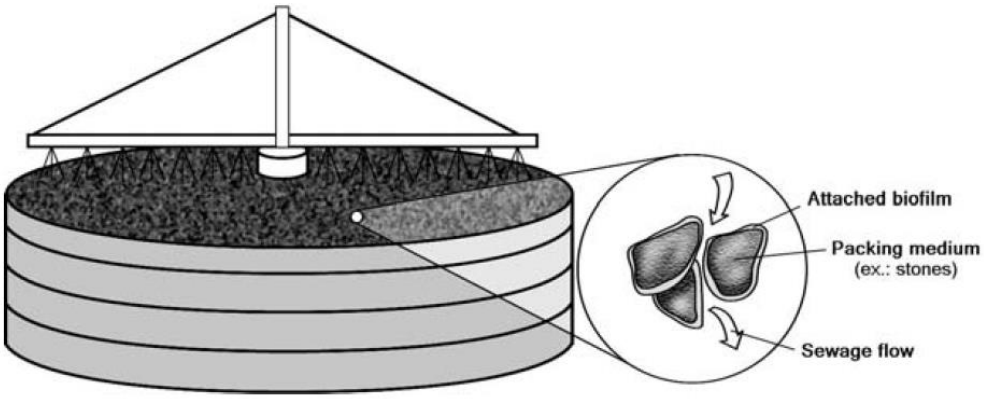

Figure 17. *Schematic representation of a trickling filter [57].*

Reactors with attached biomass, or simply biofilm reactors, now include, besides trickling filters (**Figure 17**) and rotating biological contactors, several other types of reactors with fixed or moving beds. Processes with moving beds have the support medium in permanent movement, hydraulically or mechanically driven. They generally use a material with large specific surface area for the attachment of the biomass, that can be grains of small diameter (0.2 to 2 mm) or a material with high porosity (e.g., sponges). High biomass concentrations are reached in these processes, resulting in a high treatment capacity. Their main advantage with relation to fixed bed processes is the absence of clogging of the filter medium, and their main

disadvantages are the high operational costs (especially energy) and the sophisticated devices necessary for appropriate flow distribution and aeration [57].

Biofilters are characterized by bacteria being attached to a solid surface in the form of a biofilm. Biofilms are a dense layer of bacteria characterized by their ability to adhere to a solid medium and form a fixed film of polymers in which the bacteria are protected against sloughing off. Biofilters have a short hydraulic retention time and hence free bacteria in the water will be washed out [58].

In this type of process, several technologies with the use of microalgae have been developed. The term “algal biofilms” therefore refers to microalgae dominated biofilm communities that colonize illuminated surfaces in the presence of moisture and nutrients. Algal biofilms are usually utilized for tertiary wastewater treatment [59].

1.6.3 Tertiary treatment

In tertiary treatment, additional processes are used to remove constituents, such as nitrogen or phosphorus, that are not reduced significantly by the secondary treatment [60].

Biochemical reactors play an important role in the biochemical industry. In order to employ a most appropriate reactor for an industrial operation, reaction rate should be high and the reactor configuration should be simple. Under optimized parameters such as pH, temperature, substrate, and medium components, reaction rate can be increased by increasing cell mass concentration in the reactor. There are two methods commonly used for increasing cell mass concentration inside the reactor; first, use of a permeable membrane to retain cells; and the other, use of immobilized cell technique. Membrane reactors allow passing of liquid, substrate, and product out of the reactor while retaining the cells. In these reactors, high cell concentrations can be achieved. Unfortunately, for some processes such as waste water treatment, these reactors are not preferred due to their high cost and problems with fouling. A comparison is reported in the following table:

Table 5. *A comparison of different types of reactors with biofilm reactors [61].*

Reactor Type	Comments
Membrane reactor	
Advantages	High productivities, high cell concentration can be achieved inside the reactor, clear permeates for further separation
Disadvantages	Fouling with cells, cost prohibits their use in low cost large volume chemical production
Immobilized cell reactors	
Covalent bond formation	
Advantages	High cell concentration may be achieved, high productivity
Disadvantages	Cell growth inside matrix may be restricted, cells leach out of the matrix and hence centrifugation of effluent may be required, chemical may affect the cells
Entrapment	
Advantages	High cell concentration may be achieved, high productivity
Disadvantages	Matrix often starts disintegration with time, cells leach out of matrix, centrifugation of reactor effluents is required for further separation
Biofilm	
Advantages	Comparatively high reactor productivities and high cell concentrations are achieved, reactors run longer and are economic to operate
Disadvantages	Effluent centrifugation is required

Other types of reactors that offer high reaction rates are immobilized cell reactors. In these reactors, high cell concentrations are achieved by fixing them on various supports. Cells can be immobilized by three different techniques; namely, adsorption, entrapment, and covalent bond formation. The third technique is of natural origin as cells "adsorb/and adhere" to the support naturally and firmly. In addition to being a natural process, adsorption can be performed in place, and economical adsorbents are available. Adsorbed cells form cell layers that are called “biofilms”. Biofilms can be used in various types of reactors such as continuous stirred tank reactors (CSTRs), packed bed reactors (PBRs), fluidized bed reactors (FBRs), airlift reactors (ALRs), upflow anaerobic sludge blanket (UASB) reactors, and expanded granular sludge bed (EGSB) reactors etc. (**Figure 18**)

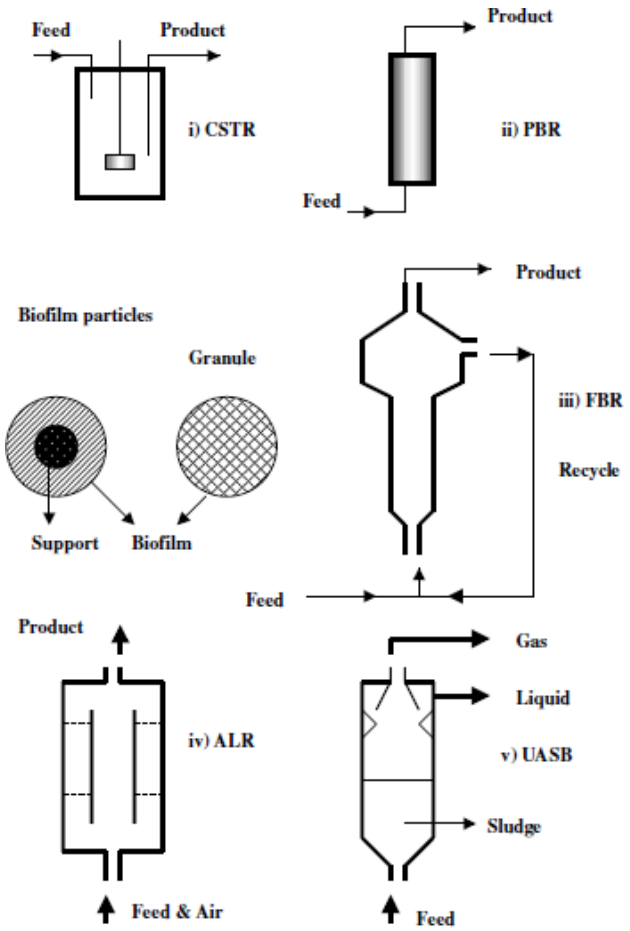

Figure 18. *Schematic diagrams of various types of biofilm reactors and biofilm particles [61].*

The application of biofilm technology in wastewater treatment originated from the industrial operation of trickling filters in the early 1880s in Wales, Great Britain. Biofilm processes in wastewater treatment can be divided into two categories:

- The fixed-medium systems where the biofilm media are static in the reactors and the biological reactions take place in the biofilm developed on the static media;
- the moving-medium systems where the biofilm media are kept continually moving by means of mechanical, hydraulic, or air forces.

The moving-medium systems include rotating biological contactors, moving-bed biofilm reactors, vertically moving biofilm reactors, and fluidized bed biofilm

reactors; while the fixed-medium systems include trickling filters and biological aerated filters.

Rotating biological contactors (RBC) have been widely used in biological treatment of wastewater for reducing chemical oxygen demand (COD)/biological oxygen demand (BOD) and nitrification/denitrification purposes. Rotating biological contactors treat wastewater streams using a thin biofilm of aerobic microorganisms on rotating cylinders or biodiscs. The rate of rotation is selected to provide optimum contact of the waste stream with the biofilm for efficient oxygen transfer and bioactivity.

The fluidized bed biofilm reactors (FBBR; also called as FBR) (in which particles move up and down within the expanded bed in the well-defined zone of the reactor) have been used for more than two decades for treating industrial wastewater. Immobilized bacterial systems configured as fluidized bed biofilm reactors (FBBRs) offer some technical advantages. Since chemical wastes are injected into the recycle, toxic chemicals are immediately diluted, which make the microorganisms more resistant to direct chemical toxicity than many conventional treatment systems. In addition, since FBBRs are usually oxygenated by supplying air into the recycle loop, a high level of microbial activity may be supported with minimal air stripping of volatile chemicals [61].

Table 6 shows the benefits and limitations of different technology for algae production.

Table 6. *Benefits and limitations of design approaches for algae production [43].*

Design	Culture density ($g\ l^{-1}$)	Gas exchange	Scalability	Culture control
Raceway pond	0.25–1	Low	High	Low
Tubular reactor	1.5–1.7	Very low	Medium	High
Biofilm system	70	High	High	Low

1.6.4 Nutrient removal

Effluent produced from the secondary treatment plant contains more amounts of nutrients (nitrogen and phosphorus) and if these effluents are

discharged into water bodies; it causes eutrophication and affects the ecosystem. To remove these nutrients, several processes are used, but the disadvantages of this type of treatment are high cost and increased sludge production. As an alternative to the conventional treatment methods, microalgae are suggested to remove the nutrients from wastewater. The use of microalgae or macroalgae (seaweeds) to remove pollutants and nutrients from the wastewater is called phycoremediation. Microalgae wastewater treatment is eco-friendly and offers the advantage of a cost-effective way of nutrient removal and biomass production.

Wastewater contains different types of materials like soluble organic, inorganic, insoluble inorganic materials, macro solids, toxins, etc. By processing, it is ensured that only the soluble fraction of the waste like carbon, nitrogen and phosphate are used for the microalgae cultivation. Besides pollutants, bacteria and protozoa are also present in wastewater. If this wastewater is used as a culture medium, microbes present in it will compete for microalgae growth and nutrition [62].

Micro-algae play a key role in converting inorganic nitrogen to its organic form through a process called assimilation. Cyanobacteria can assimilate nitrogenous compounds like ammonium, nitrate, nitrite, urea, and amino acids. Diazotrophic cyanobacteria can also assimilate atmospheric nitrogen (N_2) [63].

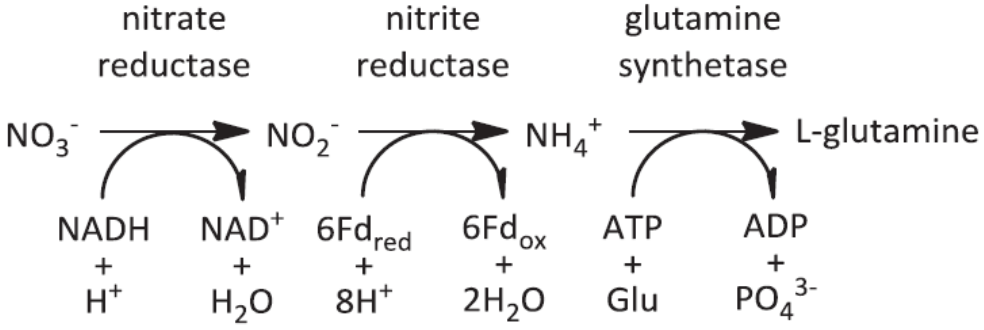

Figure 19. *Simplified schematic of the assimilation of inorganic nitrogen [45].*

Assimilation requires inorganic nitrogen be only in forms of nitrate, nitrite and ammonium. Translocation of the inorganic nitrogen occurs across the plasma membrane, followed by the reduction of oxidized nitrogen and the incorporation of

ammonium into amino acids. Intracellular nitrate is sequentially reduced to nitrite and ammonium by nitrate reductase and nitrite reductase. Cyanobacterial nitrite reductase is homologous with ferredoxin-dependent higher-plant nitrite reductase and contains a [4Fe-4S] cluster and sirohaem as prosthetic groups. Electrons from reduced ferredoxin are transferred to the iron–sulphur cluster and then to sirohaem, where nitrite is reduced to ammonium. Cyanobacterial nitrate reductase is homologous with Mo-containing bacterial oxidoreductases but is unique in that it uses ferredoxin as an electron donor, forming tight 1:1 complexes [12]. The Mo cofactor is of the Mo-bis-molybdopterin guanine dinucleotide type, and the enzyme also contains a [4Fe-4S] cluster. In this enzyme system, electrons flow from reduced ferredoxin to the iron–sulphur cluster and then to the Mo cofactor, where nitrate is reduced to nitrite. Thus, all forms of inorganic nitrogen are ultimately reduced to ammonium prior to being incorporated into amino acids within the intracellular fluid. Finally, using glutamate (Glu) and adenosine triphosphate (ATP), glutamine synthase facilitates the incorporation ammonium into the amino acid glutamine [64].

Phosphorus has been identified as the other main nutrient of concern in eutrophication and it is also an essential nutrient for algal growth [65]. During algae metabolism, phosphorus, preferably in the forms of $H_2PO_4^-$ and HPO_4^{2-}, is incorporated into organic compounds through phosphorylation, much of which involves the generation of ATP from adenosine diphosphate (ADP), accompanied by a form of energy input. Energy input can come from the oxidation of respiratory substrates, the electron transport system of the mitochondria, or in the case of photosynthesis, from light. Phosphates are transferred by energized transport across the plasma membrane of the algal cell. Some varieties of algae are able to use also phosphorus found in organic esters for growth. It should be noted that phosphorus removal in wastewater is not only governed by the uptake into the cell, but also by external conditions such as pH and dissolved oxygen [66]. **Table 7** shows nitrogen and phosphorus removal by different species of microalgae.

Table 7. *Nitrogen and phosphorus removal by various genera of microalgae and cyanobacteria [45].*

Category	Genus and species	Waste stream	Process type	Removal time (d)	Total nitrogen (TN)		Total phosphorus (TP)	
					Initial conc. (mg L^{-1})	Removal efficiency (%)	Initial conc. (mg L^{-1})	Removal efficiency (%)
Chlorophyte	*Chlorella* sp.	Digested manure	Batch	21	100–240	76–83	15–30	63–75
	C. kessleri	Artificial medium	Batch	3	168	8–19[b]	10–12	8–20[c]
	C. pyrenoidosa	Industrial wastewater	Fed-batch	5	267	87–89	56	70
	C. sorokiniana	Municipal wastewater	Batch	10	–	–	22	45–72
	C. vulgaris	Artificial medium	Batch	1–10	13–410	23–100[a]	5–8	46–94[c]
	C. vulgaris	Industrial wastewater	Batch	5–9	3–36	30–95[a]	112	20–55
	C. vulgaris	Municipal wastewater	Batch	2–10	48–1550	55–88	4–42	12–100
	C. reinhardtii	Artificial medium	Batch	10–30	129	42–83[a]	120	13–14[c]
	Scenedesmus sp.	Artificial medium	Batch	0.2–4.5	14–44	30–100[a,b]	1.4–6.0	30–100[c]
	S. dimorphus	Industrial wastewater	Batch	9	–	–	112	20–55
	S. obliquus	Municipal wastewater	Batch	0.2–8	27	79–100[a]	12	47–98
Cyanobacteria	*Arthrospira* sp.	Animal wastewater	Semi-cont.	–	–	84–96[a]	–	72–87[c]
	A. platensis	Industrial wastewater	Batch	15	2–3	96–100[a]	18–21	87–99[c]
	Oscillatoria sp.	Municipal wastewater	Continuous	14	498	100	76	100
Diatom	*P. tricornutum*	Municipal wastewater	Continuous	14	498–835	80–100	76–116	50–100
Haptophyte	*I. galbana*	Artificial medium	Batch	8	377	99	–	–

[a] Ammonia nitrogen (NH_4^+–N).
[b] Nitrate (NO_3^-–N), Nitrite (NO_2^-–N).
[c] Total orthophosphates (PO_4^{3-}–P).

Inorganic pollutants include also heavy metals, commonly defined as metals having a specific density of more than 5 g/cm^3 (Fe, Mn, Cu, Mo, Zn and Co). They are required in traces as nutrients by the living organisms, but they become toxic at higher concentrations and if they are released to the environment, they can create serious damage to the aquatic life. The other group of metals like Cd, Hg and Pb exert their potential toxic effects even at extremely lower concentrations [67]. A number of methods have been developed for the removal of heavy metals from liquid wastes such as precipitation, evaporation, electroplating, ion exchange, membrane processes, etc. However, these methods have several disadvantages such as unpredictable metal ion removal, high reagent requirement, generation of toxic sludge, etc. The innovative process for the metal removal is called biosorption, that exploit the ability of microalgae to incorporate heavy metal inside cell [68], because they are necessary for the microalgae as co-factors of enzymatic reactions [69]. Algae accumulate high concentrations of metals depending on their concentration in the external environment and the concentration factor for heavy metals varies greatly in different algal species, but it increases as the metal concentration in the water decreases. The mechanism of metal biosorption is a complicated process and it

involves steps: an initial rapid (passive) uptake followed by a much slower (active) uptake. During the passive uptake, metal ions adsorb onto the cell surface by extracellular cell-associated materials (e.g. polysaccharides and mucilage) and cell wall components (e.g. carboxyl and hydroxy groups as well as sulphate and phosphate) within a relatively short span of time (few seconds or minutes) [70], and the process is metabolism independent (**Figure 20**).

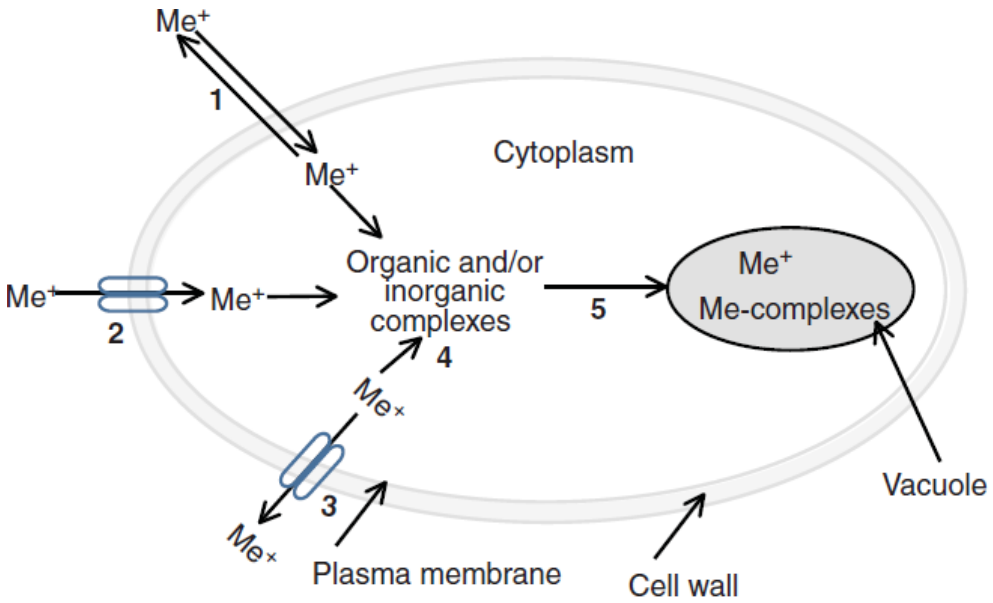

1 – Diffusion (inactive process); 2 – active uptake via ion transporters; 3 – active efflux of free metal ions; 4 – Formation of complexes of the free metal ions with various organic and/or inorganic compounds in the cytoplasm; 5 – transport to the vacuole and stored either as free metal ion or as complexes.

Figure 20. *Metal ions uptake and detoxification processes (absorption) occurring inside living cells [70].*

Active uptake is metabolism-dependent, causing the transport of metal ions across the cell membrane into the cytoplasm. In some instances, the transport of metal ions may also occur through passive diffusion owing to metal-induced increase in permeability of the cell membrane. The assimilation is possible thanks to the algal cell wall which has many functional groups such as, hydroxyl (-OH), phosphoryl (-PO_3O_2), amino (-NH_2), carboxyl (-COOH), sulphydryl (-SH), etc. which confer negative charge to the cell surface. Since metal ions in water are generally in the cationic form, they are adsorbed onto the cell surface and it dissociates into corresponding anion and proton at a specific pH. These functional groups are found associated with

various cell wall components, e.g., peptidoglycan, teichuronic acid, teichoic acids, polysaccharides and proteins [71]. It should be noted that the biosorption can be affect by several factor: temperature, pH, initial metal ion concentration, biomass concentration and other factors like nutrient level, growth rate and illumination.

1.7 Applications of microalgae

Nowadays, there are numerous commercial applications of microalgae. For example, microalgae can be used to enhance the nutritional value of food and animal feed owing to their chemical composition, as **Table 8** shows.

Table 8. *Genral composition of different human food sources and algae (% of dry matter) [72].*

Commodity	Protein	Carbo-hydrate	Lipid
Bakers' yeast	39	38	1
Meat	43	1	34
Milk	26	38	28
Rice	8	77	2
Soybean	37	30	20
Anabaena cylindrica	43–56	25–30	4–7
Chlamydomonas rheinhardii	48	17	21
Chlorella vulgaris	51–58	12–17	14–22
Dunaliella salina	57	32	6
Porphyridium cruentum	28–39	40–57	9–14
Scenedesmus obliquus	50–56	10–17	12–14
Spirulina maxima	60–71	13–16	6–7
Synechococcus sp.	63	15	11

The high protein content of various microalgal species is one of the main reasons to consider them as an unconventional source of protein. In addition, the amino acid pattern of almost all algae compares favourably with that of other food proteins. As the cells are capable of synthesizing all amino acids, they can provide the essential ones to humans and animals. They also play a crucial role in aquaculture and they can be incorporated into cosmetics: some microalgal species are established in the skin care market, the main ones being Arthrospira and Chlorella. Protein-rich extract from Arthrospira repairs the signs of early skin aging, exerts a

tightening effect and prevents stria formation; and an extract from Chlorella vulgaris stimulates collagen synthesis in skin, thereby supporting tissue regeneration and wrinkle reduction. Another important application is in the colorant field (**Figure 21**). In many markets, microalgal carotenoids are in competition with the synthetic form of the pigments. Although the synthetic forms are much less expensive than the natural ones, microalgal carotenoids have the advantage of supplying natural isomers in their natural ratio. It is accepted today that the natural isomer of β-carotene is superior to the synthetic all-trans form.

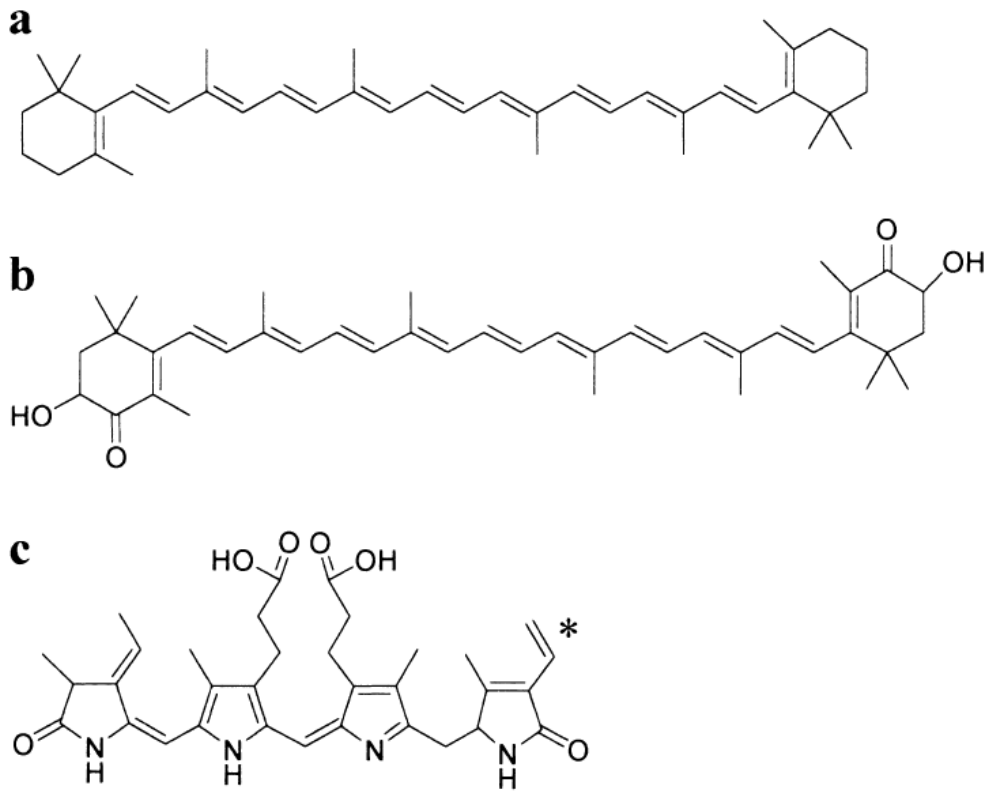

Figure 21. *Chemical structures of microalgal pigments: β-Carotene (a), astaxanthin (b), phycoerythrin (in phycocyanin, the CH=CH2 group noted an asterisk is replaced by CH3-CH2) [72].*

Pharmaceutical applications also have to be considered [72]: phycobiliproteins are a group of coloured proteins commonly present in cyanobacteria and red algae possessing a spectrum of applications. They are extensively commercialized for fluorescent applications in clinical and

immunological analysis. They are also used as a colorant, and their therapeutic value has also been categorically demonstrated [73].

Other potentiality of microalgae can be exploited in the field of renewable biofuels. Sustainable production of renewable energy is being hotly debated globally since it is increasingly understood that first generation biofuels, primarily produced from food crops and mostly oil seeds are limited in their ability to achieve targets for biofuel production, climate change mitigation and economic growth. These concerns have increased the interest in developing second generation biofuels produced from non-food feedstocks, such as microalgae, which potentially offer greatest opportunities in the longer term [74]. The use of microalgae is desirable since they are able to serve a dual role of bioremediation of wastewater as well as generating biomass for biofuel production with concomitant carbon dioxide sequestration, as **Figure 22** shows [75].

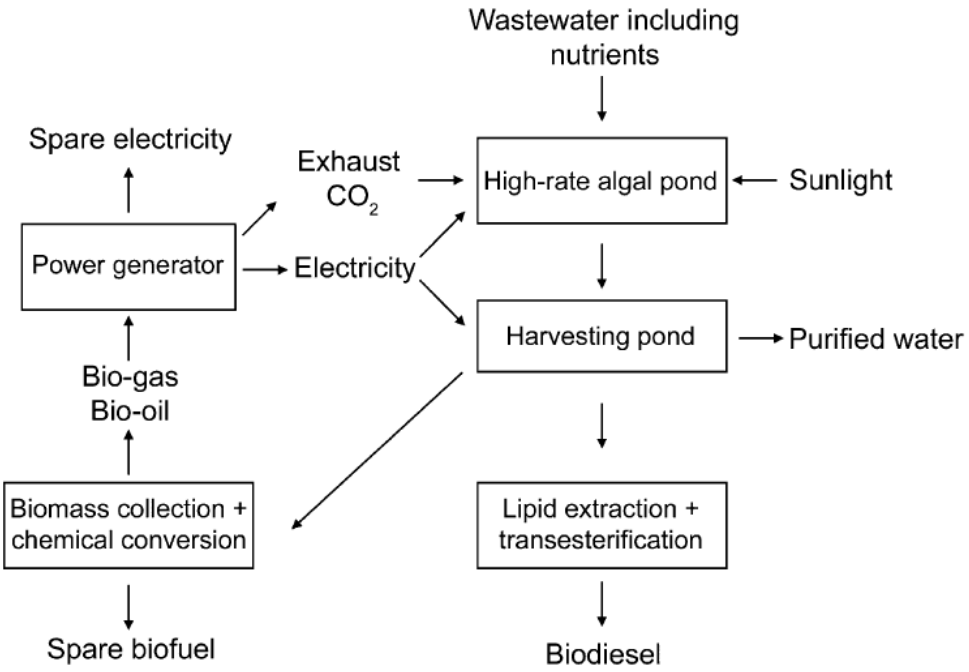

Figure 22. *A flow-diagram showing how wastewater resources could be utilised for sustainable algal-based biofuel production [76].*

The ability of microalgae to grow well under certain wastewater conditions and their high biomass productivity and in some cases high lipid productivity demonstrated in many of the reviewed studies of wastewater-grown microalgae,

suggests that there is real potential in the utilisation of these high nutrient resources for cost-effective biofuel production. However, there are some limitations that need to be addressed [76]. Several issues have to be overcame in order to make microalgal biofuel a commercial reality, and further researches are needed on:

- Wastewater nutrients removal process by microalgae;
- tolerance capacity of microalgae to various wastewaters and environmental stresses;
- augmentation of environmental parameters and combined heterotrophic and mixotrophic cultivation;
- development of innovative, efficient and cost-effective algae harvesting and conversion technologies;
- comprehensive life cycle assessment for economic viability, carbon foot print and sustainability [77].

1.8 Aim of the work

The aim of the project was to characterize microalgae in order to understand if is feasible the use of algae as passive filler or supplementary material for alkali-activated geopolymer, which in the recent yeas has become one of the major alternatives to Portland cement.

Lyophilized Spirulina Platensis and Tetraselmis Seucica have been used for the analysis and tests. First of all, standard characterization analysis was performed. Thermogravimetric analysis and differential scanning calorimetry were used to estimate the water content of the microalgae and their thermal resistance. Infra-red spectroscopy on microalgae and metakaolin powder and on the final geopolymer structure, with and without algae, have been performed to verify and estimate the influence of the microalgae on the chemical structure after and before the geopolymerization. A rheological study has been conducted in order to understand the influence of the microalgae on the fresh geopolymer paste. Several shear tests were performed on fresh geopolymer paste with and without microalgae, to observe

the influence of algae during the geopolymerization and study the evolution in time of the hardness of the paste.

Also, a properly modified 3D printer was used to carry out several printability tests. In this way samples for the dynamic mechanical analysis have been printed. These tests have been done in +Lab, the 3D Printing Lab of Politecnico di Milano.

Chapter 2: Materials and methods

2.1 3Drag

3Drag (**Figure 23**) is a 3D Printer compatible with all the RepRap software and firmware available for free. It is made by aluminium profiles designed for fastening interlocking and designed to give lightness and rigidity for the suppression of vibrations and unwanted resonances.

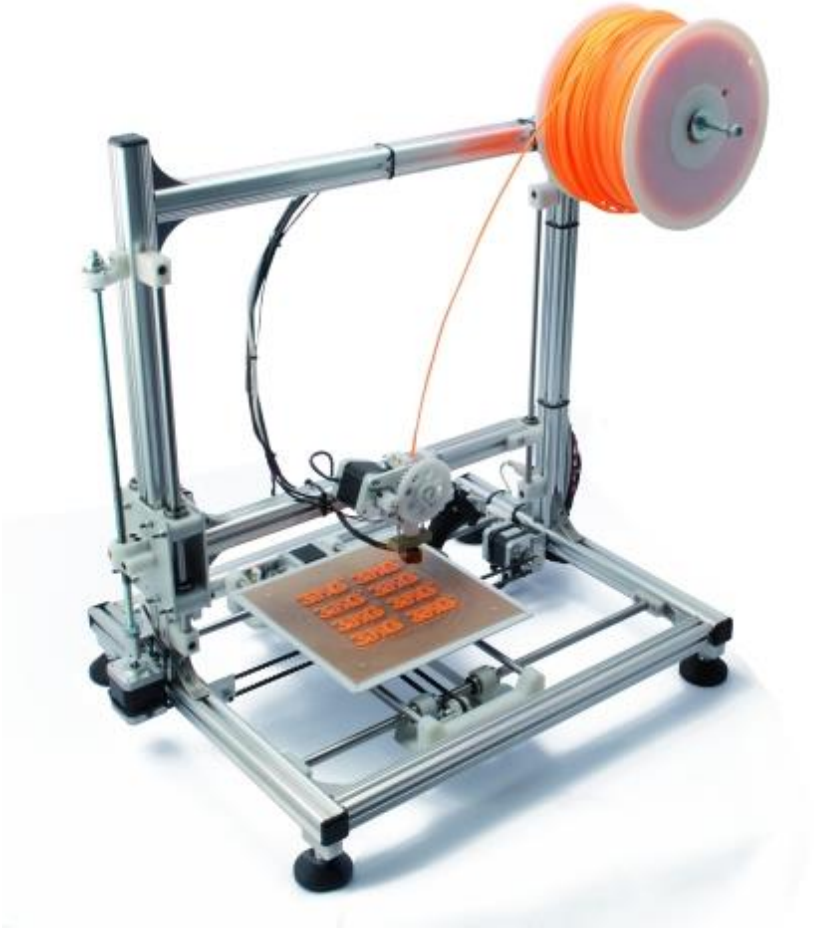

Figure 23. *3Drag printer with PLA filament.*

The printer uses the X/Y system to the platen, and Z for the cart. This particular configuration allows to simplify the extrusion system which, no longer having to move on a horizontal axis, it is simply attached to the structure that moves on the axis Z. 3Drag was designed in order to print PLA or ABS filament. For this work

this printer has been properly modified for LDM technology, instead of FDM. In the standard configuration showed in **Figure 23**, three stepper motors NEMA 17 are necessary to move all the mechanical parts. In the modified configuration, another stepper motor was added and the heated extruder has been replaced by a syringe which can be filled with ceramic or geopolymeric material (**Figure 24**). The added motor, thanks to plastic gears and mechanical interconnections, push down the piston inside the syringe and the material can be extruded.

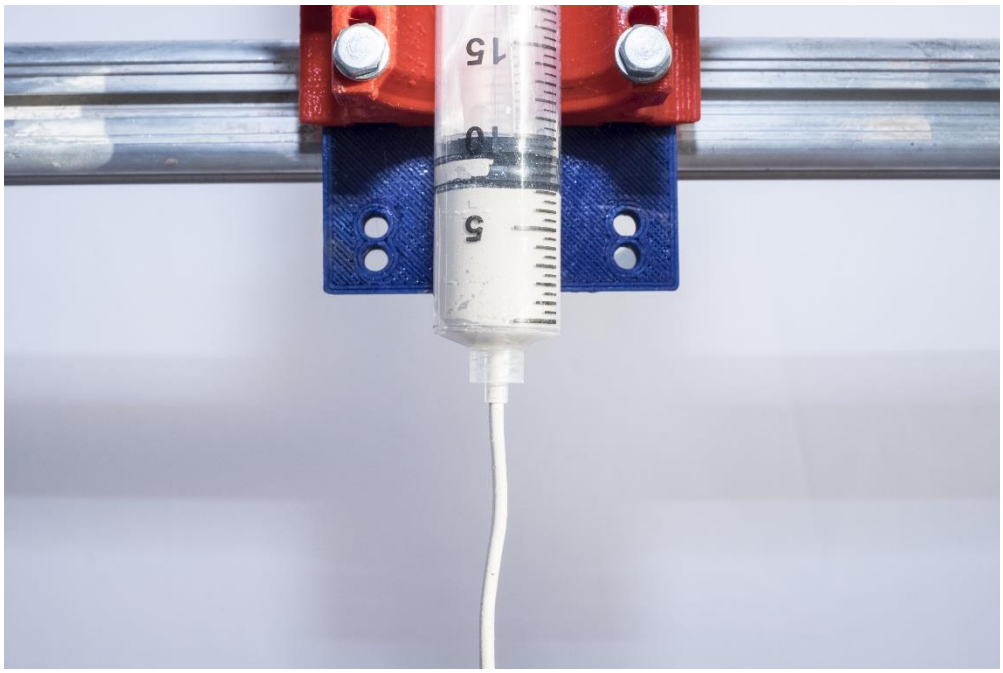

Figure 24. *Modified 3Drag configuration during the print.*

In this way, several geopolymeric samples were printed in order to carry out mechanical and printability tests that are described in the following paragraphs.

2.2 Dosage and preparation of geopolymer paste

Several printability tests were performed in order to obtain the optimum formulation for a printable geopolymer paste. Geopolymer paste was prepared in a plastic becker by mixing with a spatula all the components in the following order: metakaolin, bentonite, water and activator. **Table 9** shows the dosage used to

perform mechanical and rheological analysis described in the following paragraphs, while the typical paste formulation used for a 20 ml syringe is reported in **Table 10**.

In this study, bentonite was used as supplementary material. It simply acts as a filler to make the geopolymer more compact [78] and with a suitable viscosity for the print.

Table 9. *Dosage of a geopolymeric paste.*

Metakaolin [%]	Bentonite [%]	Activator [%]	Distilled Water [%]
37.6	22.6	30	9.8

Spirulina Platensis and Tetraselmis Suecica are the microalgal species used in this thesis work, provided by Archimede Ricerche, and the percentage of microalgae added to the geopolymer paste was calculated by considering only the amount of metakaolin and bentonite. 1%, 3% and 5% are the percentages used.

Table 10. *Typical paste formulation for a 20 ml syringe.*

Metakaolin [g]	Bentonite [g]	Activator [g]	Distilled Water [g]
18.8	11.3	15	4.9

The chemical composition and the characterization of the materials are reported in the following chapter.

2.3 Mechanical analysis

Different mechanical tests have been carry out in order to evaluate flexural modulus, storage and loss modulus and compressive resistance of samples. For the three-point bending and shear test, DMA/SDTA861 (Mettler-Toledo®) instrument was used (**Figure 25**). While AllroundLine (Zwick Roell®) machine was used to perform the compression tests.

Figure 25. *DMA/SDTA861 (Mettler-Toledo®) instrument.*

2.3.1 Three-point Flexural test

In three-point bending mode, the ends of the sample rest on two knife-edges and an oscillatory force is applied to the middle by a moving knife-edge (**Figure 26**) [79]. Flexural modulus can be evaluated with the following formula:

$$\sigma_f = \frac{3PL}{2bd^2} \; ; \; \varepsilon_f = \frac{6Dd}{L^2} \; ; \; E_f = \frac{L^3 m}{4bd^3}$$

Where:

- σ_f = stress in outer fibers at midpoint, [MPa];
- ε_f = strain in the outer surface, [mm/mm];
- E_f = flexural Modulus of elasticity, [MPa];
- P = load at a given point on the load deflection curve, [N];
- L = support span, [mm];
- b = width of tested beam, [mm];
- d = depth of tested beam, [mm];
- D = maximum defletion of the center of the beam, [mm];

- m = the gradient (i.e., slope) of the initial straight-line portion of the load deflection curve, (P/D), [N/mm].

Figure 26. *Example of three-point bending configuration* [79].

Rectangular cross-section geopolymeric specimens were designed with SolidWorks softaware and they were printed with 3Drag. **Figure 27** shows the 3D modelled specimen and his size, while printing parameters are reported in **Table 11**.

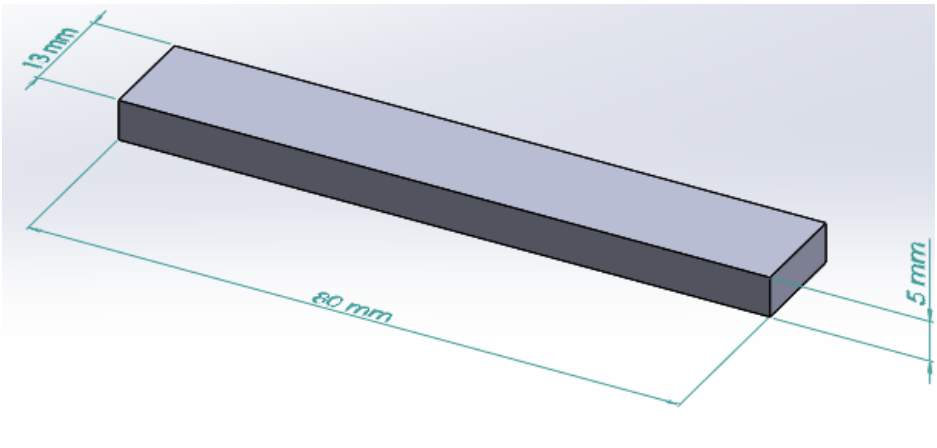

Figure 27. *Three-point bending specimen designed with SolidWorks software.*

Table 11. *Printing parameters for a 20 ml syringe (three-point bending specimens).*[1]

Flow	Layer height [mm]	Printing speed [mm/s]	Nozzle [mm]	Inner diameter [mm]	Infill [%]
100	1.25	15	2.25	18.6	100

Cura 3D Printing Slicing Software (Ultimaker), version 14.12.1, was used to setup the paramters and generate the G-code file.

The test was performed at room temperature by setting a force of 0.7 N with 0.1 Hz of frequency and a displacement ranging from 0.1 up to 100 µm.

After the print, the samples have been covered with a plastic film in order to reduce the water evaporation avoiding the cracks formation and propagation into the geopolymer structure. The three-point bending test then was performed after 28 days, in order to carry out the test on a well-crosslinked geopolymer structure.

2.3.2 Shear test

Two identical samples are clamped symmetrically between two outer fixed parts and the central moving part providing the oscillatory force (**Figure 28**). Because a sinusoidal force is applied, the storage modulus can be expressed as an in-phase component and the loss modulus of the material can be expressed as an out of phase component [80].

Figure 28. *Example of shear configuration* [79].

[1] The nozzle and inner diameter reported are related to the type of syringe used.

The storage and loss modulus are defined as follow:

$$M' = \frac{\sigma_0}{\varepsilon_0}\cos\delta \;\; ; \;\; M'' = \frac{\sigma_0}{\varepsilon_0}\sin\delta$$

Where:

- M’ = storage modulus;
- M’’ = loss modulus;
- δ = phase lag between stress and strain.

According to ISO 6721-1, the storage modulus M’ represents the stiffness of a visco-elastic material and is proportional to the energy stored during a loading cycle. It is roughly equal to the elastic modulus for a single, rapid stress at low load and reversible deformation.

In the same ISO standard, the loss modulus M’’ is defined as being proportional to the energy dissipated during one loading cycle. It represents, for example, energy lost as heat, and is a measure of vibrational energy that has been converted during vibration and that cannot be recovered [81].

The test was performed in order to understand the mechanical property related to the printability of a fresh geopolymer paste and the variation of the modulus in the time.

Discs of fresh material with 8 mm of diameter and 5 mm of thickness were made and clamped inside the instrument and the moduli have been evaluated at t_0 (immediately after the paste was done) with frequency ranging from 0.01 Hz up to 1 Hz. Other measurements were also done at higher frequencies and different time steps. The Moduli have been evaluated also at t_0, after 60 min, 120 min and 240 min by setting a force of 10 N, a displacement of 0.5 µm and a frequency ranging from 0.1 Hz up to 100 Hz.

2.3.3 Compression test

Several geopolymer samples were tested in order to evaluate the compression strength of the material and the microalgae effect.

Compressive strength or compression strength is the capacity of a material or structure to withstand loads tending to reduce size, as opposed to tensile strength, which withstands loads tending to elongate. In other words, compressive strength resists compression (being pushed together), whereas tensile strength resists tension (being pulled apart). A compression test for a material involves at least two opposing forces directed towards each other applied to opposite face of the test sample so that the sample is compressed.

The tests were performed with Zwick Roell ProloLine Z010 and square plates (**Figure 29**) with a load cell of 10 kN was used. Two types of samples were analysed. In one hand 3D-printed cylindrical geopolymer samples (see **Table 12**) have been tested with 1%, 3% and 5% of microalgae content after 7 days and 28 days. A 20 ml syringe was used to print the samples and the printing parameters are reported in **Table 13**.

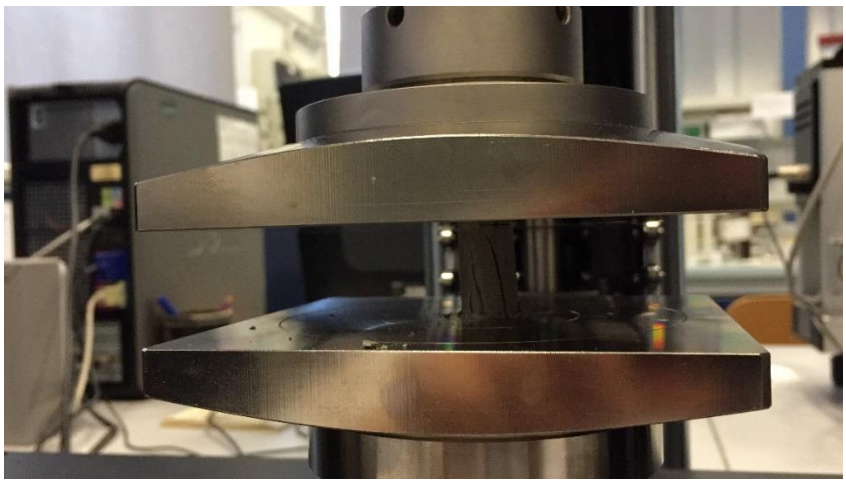

Figure 29. *Square compression plates.*

Table 12*. Sizes of 3D-printed compression samples.*

Height [mm]	Inner diameter [mm]	Outer diameter [mm]
25	7.5	15

Table 13*. Printing parameters for a 20 ml syringe (compression specimens).*

Flow	Layer height [mm]	Printing speed [mm/s]	Nozzle [mm]	Inner diameter [mm]	Shell thickness [mm]
130	0.9	20	2.25	18.6	2.25

In the other hand, syringe-casted specimens were tested with the same test procedure. A 1 ml syringe was filled with fresh geopolymer paste in order to obtain compact full-cylinder geopolymer samples with 5 mm of diameter and 13.5 mm of height.

Then, two types of analysis were done. Compression tests were performed on thermally cured samples and ambient cured (uncured) samples. This last have been covered with a plastic film to avoid cracks formation and propagation. The first ones have been cured at 800°C as shown in **Table 14**.

Table 14. *Curing steps.*

Time [hours]	Temperature
1	Room temperature to 800°C
2	800°C
2	800°C to 550°C

At 550°C the samples were taken from the oven. The thermal curing was performed with a muffle furnace (CONTROLS®, **Figure 30**) with maximum settable temperature of 1200°C. Finally the size of the samples were properly choose, compliant with ASTM C1424-15 standard [82].

Figure 30. *Controls® muffle furnace.*

2.4 Characterization analysis

Several characterization analyses were performed on the materials used in this work.

2.4.1 Thermogravimetric analysis

Thermogravimetric analysis (TGA) was performed on microalgal samples in order to characterize the different decomposition steps [83] and on alkali activator in order to evaluate the amount of water contained in solution. The TGA instrument is able to measure with high precision mass change, temperature change and temperature. The sample is loaded on a pan and continuously weighted by a precision balance. A furnace can increase or equilibrate the temperature.

The experiments were carried out with a TGA Q 500 (TG Instruments®) (**Figure 31**).

Figure 31. *Q 500 thermogravimetric analyzer.*

In each experiment, Spirulina and Tetraselmis samples were spread uniformly on the bottom of the platinum crucible of the thermal analyser. The pyrolysis experiments were performed at heating rates of 10°C/min and air was fed at a constant flow rate of 90 ml/min. The temperature of the furnace was programmed to rise from room temperature to 800°C. In the case of alkali solution, the settings

are the same, but the temperature was programmed to rise from room temperature to 300°C.

2.4.2 Differential Scanning Calorimetry

Differential Scanning Calorimetry (DSC) is a technique used to detect the temperatures at which transitions occur in the materials, for example fusions, evaporations.

A DSC 823e (Mettler-Toledo®) instrument was used (**Figure 32**) and the microalgal samples were analysed with three runs: from 25°C to 175°C 20°C/min, from 175°C to -50°C -20°C/min, and from -50°C to 300°C 20°C/min.

Figure 32. *Mettler-Toledo® DSC 823e.*

2.4.3 X-ray Diffraction

Elemental analysis on alkali activator and on metakaolin powder was done. X-ray diffraction is based on constructive interference of monochromatic X-rays and a crystalline sample. These X-rays are generated by a cathode ray tube, filtered to produce monochromatic radiation, collimated to concentrate, and directed toward the sample. The interaction of the incident rays with the sample produces constructive interference (and a diffracted ray) when conditions satisfy Bragg's Law:

$$n\lambda = 2d \sin\theta$$

This law relates the wavelength of electromagnetic radiation to the diffraction angle and the lattice spacing in a crystalline sample. These diffracted X-rays are then detected, processed and counted. By scanning the sample through a range of 2θangles, all possible diffraction directions of the lattice should be attained due to the random orientation of the powdered material. Conversion of the diffraction peaks to d-spacings allows identification of the mineral because each mineral has a set of unique d-spacings. Typically, this is achieved by comparison of d-spacings with standard reference patterns [84].

XRD analysis was performed with D8 Advance (Brukel®) instrument with a radiation generated at 40kV and 40 mA and 2θ ranging from 2° to 80° with a step size of 0.02°. Intensity peaks of diffracted X-rays were continuously recorded with scan step time 1.2 s at room temperature. In this thesis work the alkali activator was analysed in order to qualitatively evaluate his formulation and the main compound of the solution.

2.4.4 Fourier Transform Infra-Red Spectroscopy

Fourier transform infrared spectroscopy (FT-IR) was performed on different samples in order to evaluate the influence of microalgae in the geopolymer structure [85], knowing that molecules absorb specific frequencies which match the transition energy of the bond that vibrates. This can be used to identify functional groups or bonds, whose vibrations have characteristic frequencies and intensities.

Due to Beer-Lambert law (Eq. 3), absorbance depends on the thickness of the analysed film *l*, on the concentration of the solution *c* and on the molar extinction coefficient *ε*, which depends on the nature of the harmonic oscillators of the analyte. Therefore, in order to compare different specimen spectra, which have different thicknesses, it is necessary to normalize the peaks height with the height of another peak, taken as reference.

$$A = \varepsilon c l$$

Thermo Nicolet NEXUS 470 FTIR (GMI Inc.) was used. The analysed powders were blended with potassium bromide (KBr) powder, ground together and then pressed with a hydraulic press (PerkinElmer) into thin disks of diameter 13 mm under 8 tons for 3 min. Then, IR spectra region 4000 – 400 cm^{-1} were recorded at room temperature. Each spectrum was an average of 64 scans at a resolution of 4 cm^{-1}. Spectra analysis was done using OMNIC Specta Software (Thermo Scientific®).

2.5 Rheology

Several tests were performed in order to understand the influence of the two microalgal species on geopolymer viscosity, which is a measure of a fluid's resistance to flow and its definition is related to Newton's Law of Viscosity that, for a Newtonian fluid, is:

$$\tau = \eta\dot{\gamma}$$

Where:

- τ = shear stress [Pa];
- η = viscosity [Pa s];
- $\dot{\gamma}$ = shear rate [1/s].

Distinction between Newtonian and non-Newtonian fluids must be made. A Newtonian fluid behaves according to Newton's Law and his viscosity is constant at a given temperature and independent on shear strain rate and time [86]. Non-Newtonian fluids are also classified as time-dependent or time-independent. Fluids in which rheological behaviour depends only on the shear stress (at constant temperature) are considered time-independent. Time-dependent fluids are those in which the viscosity depends, not only on the shear stress, but also on the amount of time the stress has been applied to the fluid [87]. Geopolymer paste belongs to the last-mentioned class and it is showed with the results reported in the following chapter.

The experiments were performed at room temperature with Dynamic Stress Rheometer DSR200 (Rheometrics). Viscosity of fresh geopolymer paste with different algae content (1%, 3% and 5%) and also of distilled water containing 5%, 10% and 20% of microalgae was evaluated.

2.6 Printability test

Printability study was performed by printing overhanged objects with 3Drag printer in order to qualitatively evaluate the effect of microalgae as process coadjutant or thickener material. The objects were designed with SolidWorks software as **Figure 33** shows, the result is an overturned truncated cone.

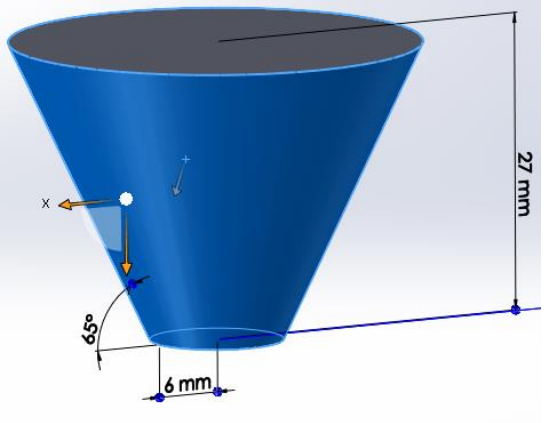

***Figure 33**. Sample with 65° of inclination designed with SolidWorks.*

Four samples for each inclination angle (65°, 55° and 45°) and for each formulation were printed: 0%, 1%, 3% and 5% of microalgae content. Another test was also done: substitution of 2% in weight of bentonite with microalgae. In **Table 15** and **Table 16** size and all the printing parameters are reported.

***Table 15.** Size of truncated cones.*

Inclination [°]	Base radius [mm]	Height [mm]
65	6	27
55	6	24.4
45	6	21.1

Table 16. *Printing parameters.*

Inclination [°]	Flow	Layer height [mm]	Printing speed [mm/s]	Nozzle [mm]	Inner diameter [mm]	Shell thickness [mm]
65	150	0.9	15	2.25	18.6	2.25
55	160	0.9	10	2.25	18.6	2.25
45	180	0.9	8	2.25	18.6	2.25

Chapter 3: Results and discussion

3.1 Chemical composition

A commercial metakaolin powder (MEFISTO L05) provided by Ceské Lupkové Zàvody a.s. was used as aluminosilicate source of geopolymer, and a commercial sodium silicate solution provided by the same supplier was used as alkaline activator. Commercial bentonite powder provided by Sigma-Aldrich was used as supplementary material in the geopolymer paste.

The chemical and physical properties of MK powder are reported in **Table 17** and **Table 18**, while **Figure 34** shows the typical particles size distribution curve.

Table 17. *Typical chemical composition of metakaolin MEFISTO L05 powder.*

Al_2O_3 [%]	SiO_2 [%]	K_2O [%]	Fe_2O_3 [%]	TiO_2 [%]	MgO [%]	CaO [%]
41.90	52.90	0.80	1.10	1.80	0.18	0.13

Table 18. *Physical properties of metakaolin MEFISTO L05 powder.*

Moisture [%]	Specific surface [m2/g]	Pozzolan activity [°C]	Whiteness [%]
0.5	12.69	4.30	60

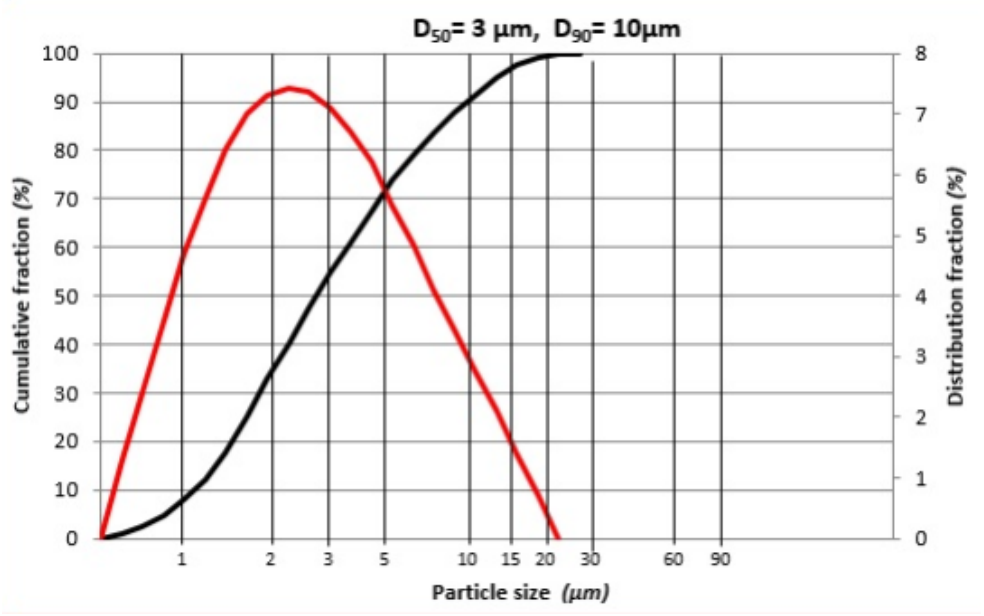

Figure 34. *Typical size distribution curve of metakaolin MEFISTO L05 powder.*

Spirulina Platensis and Tetraselmis Suecica provided by Archimede Ricerche Srl are the two green-blue microalgal species used in this study. **Table 19** shows the chemical composition of algae based on the characterization analysis done by Extractis.

Table 19. *Chemical composition of algae after centrifugation.*

Algae	Tetraselmis Suecica	Spirulina Platensis
DM [%]	95.16	97.49
Ash [%/DM]	17.05	9.12
Proteins [%/DM]	37.89	67.78
Total sugars [%/DM]	14.49	9.31
Total free sugars [%/DM]	4.19	2.79
Lipids [%/DM]	12.82	6.26
Other [%/DM]	13.56	4.74

3.2 X-ray Diffraction results

Alkaline activator used for the geopolymer paste preparation is a highly basic solution of different component. XRD analysis have been performed on alkaline activator sample, after a dehydration process carried out in order to briefly reduce the water content. **Figure 35** shows the obtained spectrum.

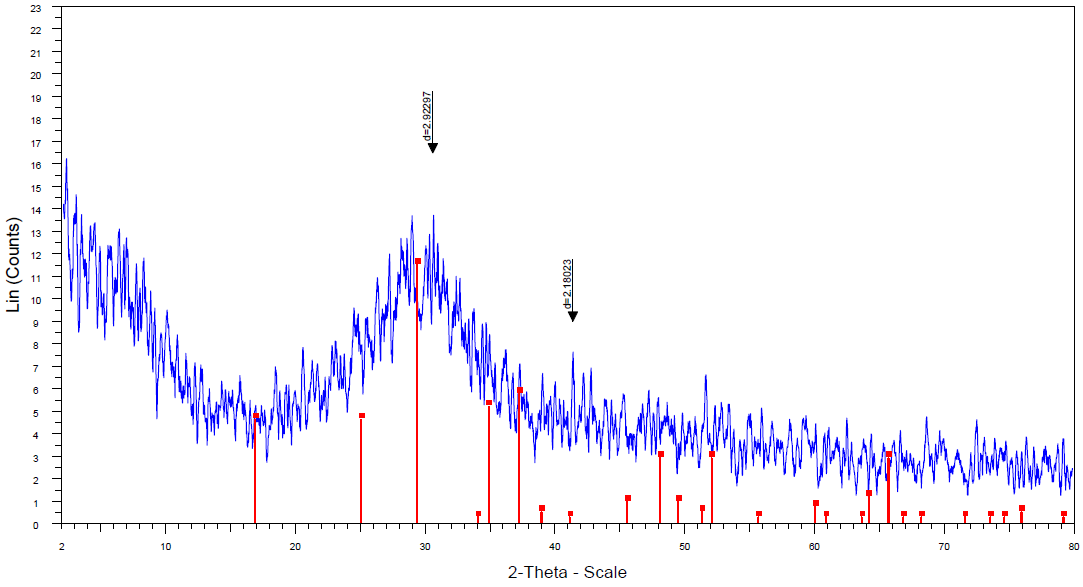

Figure 35*. XRD pattern of alkaline activator.*

An high sodium silicate (Na_2SiO_3) concentration was detected by software and database comparison analysis based on the main peaks at 2θ=2.92297 and 2θ=2.18023, in agreement with bibliography [88].

The same analysis was performed on metakaolin powder sample. The related spectrum is provided in **Figure 36**.

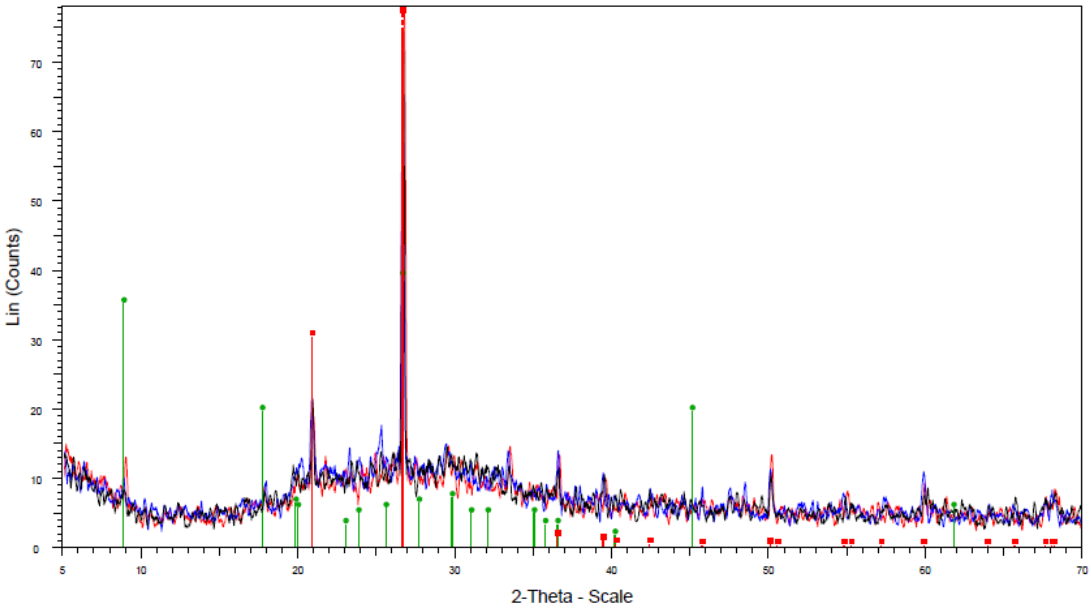

Figure 36. *XRD pattern of metakaolin.*

The MK shows an apparent amorphous phase between 20° and 35° in its structure with the characteristic peaks of quartz, SiO_2 and illite, (K, $H_3O)Al_2Si_3AlO_{10}(OH)_2$ [89].

3.3 Thermogravimetric analysis results

Figure 37 and **Figure 38** show the weight loss curve obtained by TGA curve and the derivative of the TGA curve (DTG) obtained for the two microalgal species, with a heating rate of 10°C/min in air.

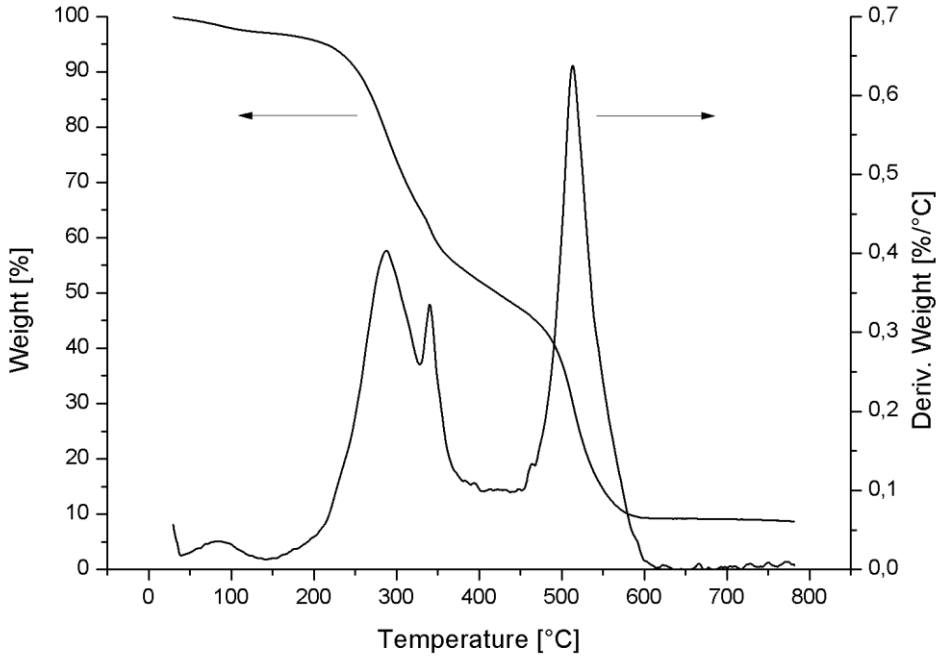

Figure 37. *The TGA and DTG curve of Spirulina Platensis at the heating rate of 10°C/min.*

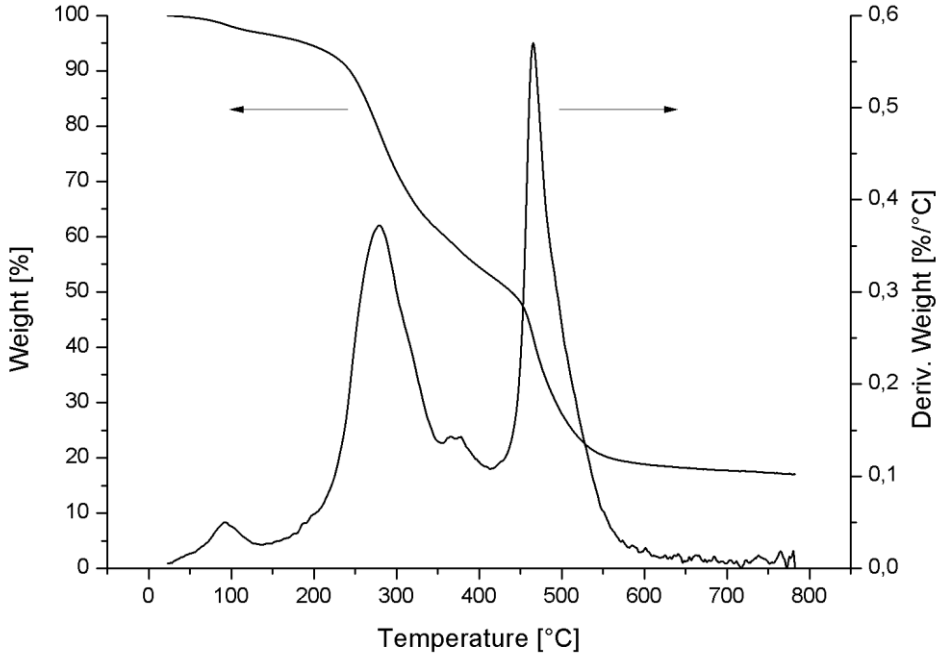

Figure 38. *The TGA and DTG curve of Tetraselmis Suecica at the heating rate of 10°C/min.*

For the two microalgae, similar trend can be noted and three main decomposition steps can be identified: <180°C corresponding to loss of water in the algae cells or it can be called dehydration process. At this stage only small weight loss can be observed.

The second stage, known as devolatilization stage, started after 180°C and ended almost at 540°C. This stage corresponds to the decomposition of protein, carbohydrate and lipid present in microalgae, and the main weight loss can be observed. Finally, the last stage occurs after 540°C during which a slow continued loss of weight revealed that the carbonaceous matters in the solid residue continuously decomposed at a very slow rate and the solid residue reached an asymptotic value.

TGA was performed also on alkali activator used for this work. The **Figure 39** shows the result.

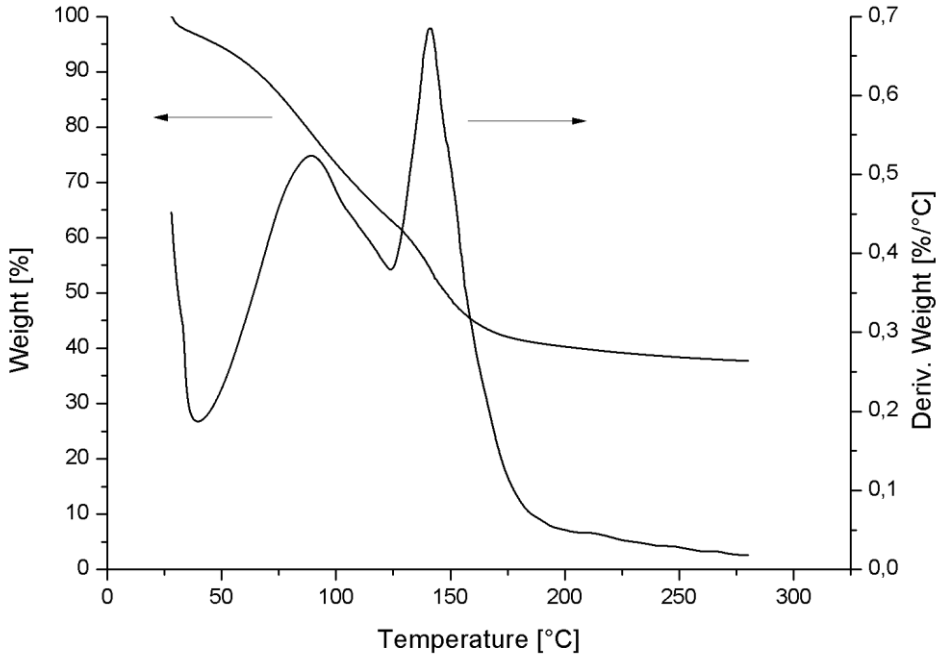

Figure 39. *The TGA and DTG curve of alkali activator at the heating rate of 10°C/min.*

The first major peak around 100°C is due to the dehydration process. The commercial solution of alkali activator used is rich in water, so a considerable weight loss can be observed. Then decomposition occurs.

3.4 Differential Scanning Calorimetry results

Figure 40 and **Figure 41** provide the DSC curves of Spirulina Platensis and Tetraselmis Suecica.

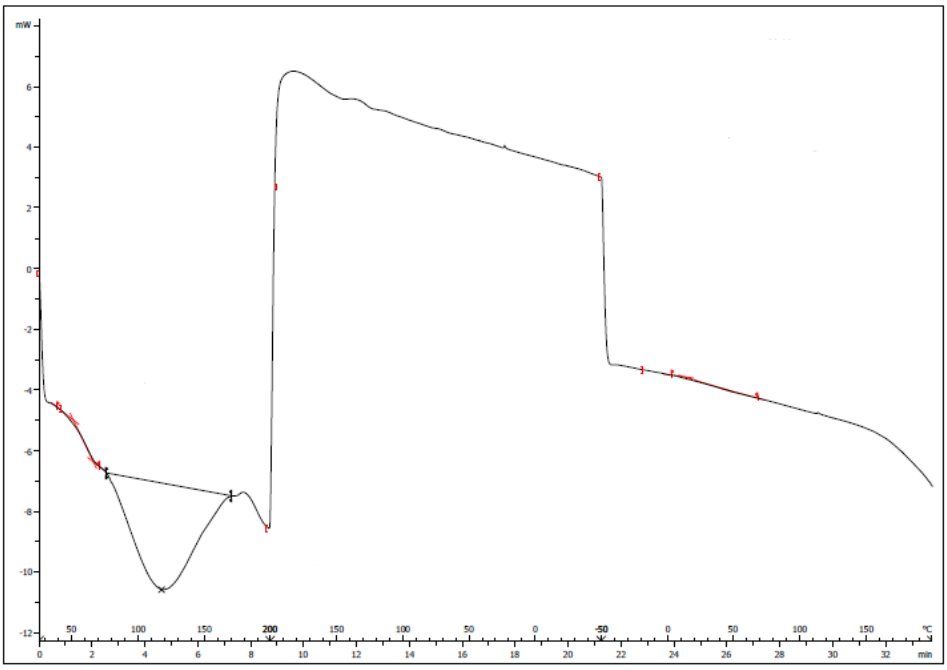

Figure 40. *DSC curve of Spirulina Platensis at heating rate of 20°C/min.*

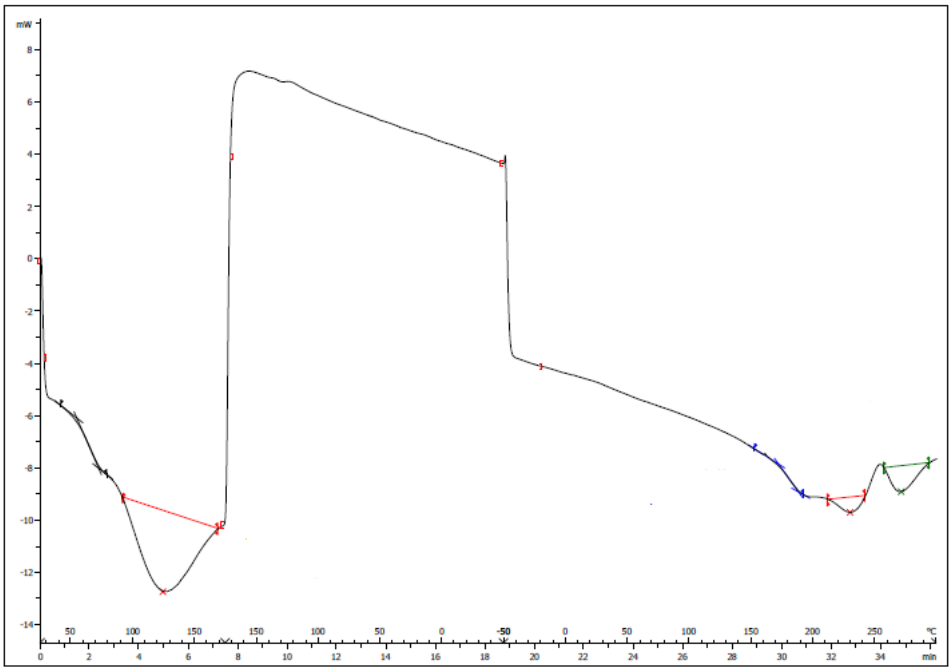

Figure 41. *DSC curve of Tetraselmis Suecica at heating rate of 20°C/min.*

Characteristic peak related to water evaporation was detected in the two analyses. The endothermic phase transition can be noted at 117°C in the case of Spirulina and at 92°C in the case of Tetraselmis.

No other relevant phase transitions were observed in the measurement.

3.5 Fourier Transform Infra-Red Spectroscopy results

Spirulina Platensis and Tetraselmis Suecica have been analysed in order to see the main and characteristic bonds of these two microalgal structures. The results are reported in **Figure 43**.

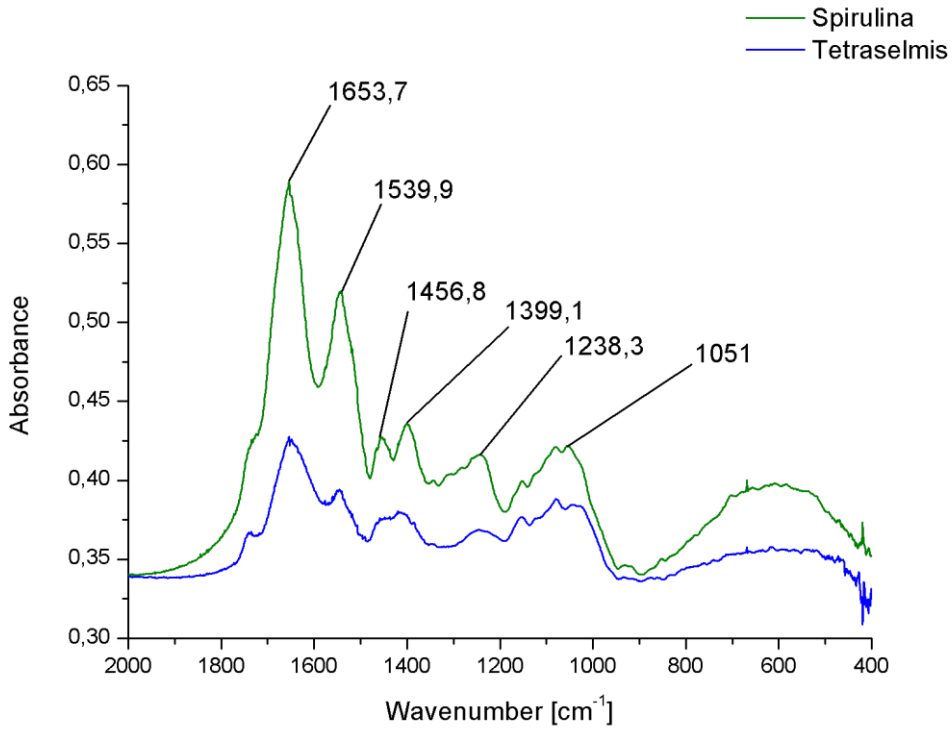

Figure 42. *Fourier Transform Infrared (FT-IR) Analysis of Spirulina Platensis and Tetraselmis Suecica.*

The peaks from 4000 cm^{-1} to 2000 cm^{-1} are not considered in this analysis since they are the characteristic peaks of water O-H stretching.

Considering Spirulina is a mixture of complex compounds, its infrared spectrum is complex and contains several bands from the contribution of different

functional groups in proteins, saccharides and other nutrients. The principal components all have their own infrared characteristic peaks. The IR peaks at 1653 cm^{-1} and 1539 cm^{-1}, which represent the vibrations of amides I and II, are from the protein in Spirulina powder and the IR peak at 1051 cm^{-1}, which represent C-O or C-C vibrations, are from saccharides. The intensity of the characteristic peak at 1653 cm^{-1}, which represents the C=O bond in proteins is the strongest because proteins are the dominant component of Spirulina.

The detailed spectral band assignments from the literature [85] of Spirulina Platensis and Tetraselmis Suecica are provided in **Table 20**.

Table 20. *Major absorption peaks in infrared spectra of control Spirulina and Tetraselmis powder sample.*

Frequency [cm^{-1}]	Group	Vibration mode	Main attribution
1653	Amide I (C=O)	Stretching	Protein
1539	Amide II (N-H, C-N)	In-plane bending	Protein
1456	Methyl (-CH_3)	Out-of-plane bending and stretching	Protein, lipids, saccharides
1399	N-O	Stretching	Presence of nitro compouds
1238	C-O	Stretching	Presence of alchols, carboxylic acids, esters, ethers
1051	C-O, C-C, C-O-C	Stretching	Saccharides

Geopolymer powder was also analysed, after and before the geopolymerization. **Figure 43** shows the IR spectra of the powders, before the geopolymerization, while **Figure 44** shows the spectra after geopolymerization.

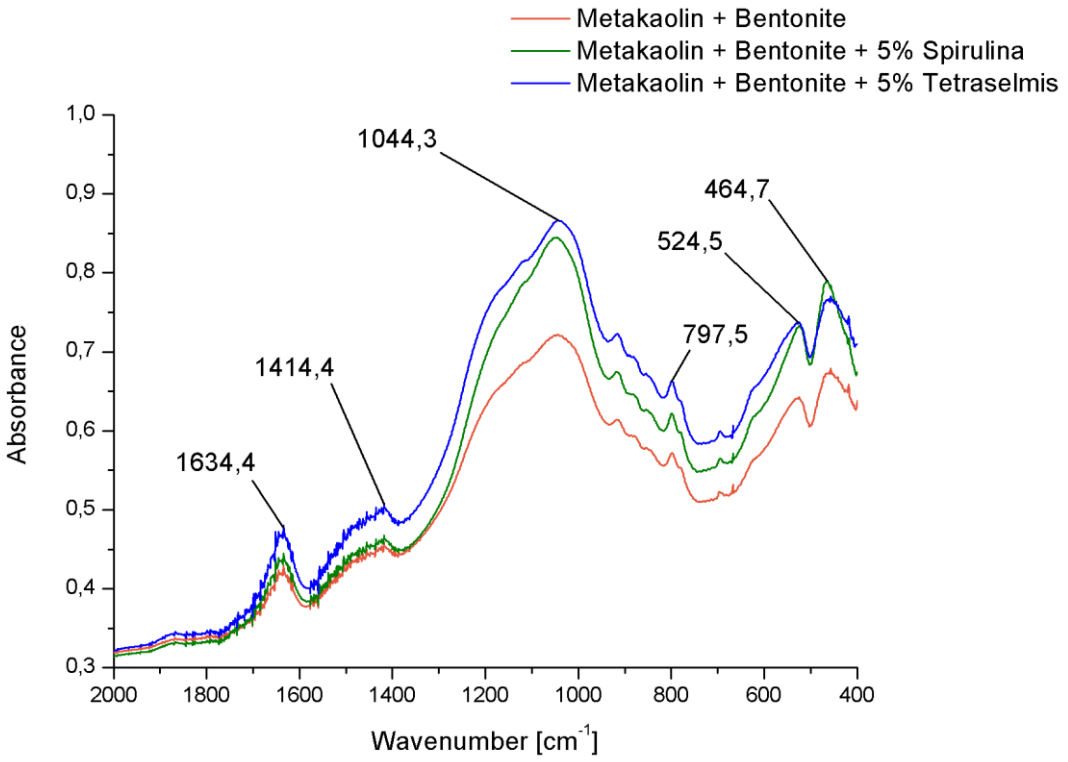

Figure 43. *Fourier Transform Infrared (FT-IR) Analysis of powders before the geopolymerization.*

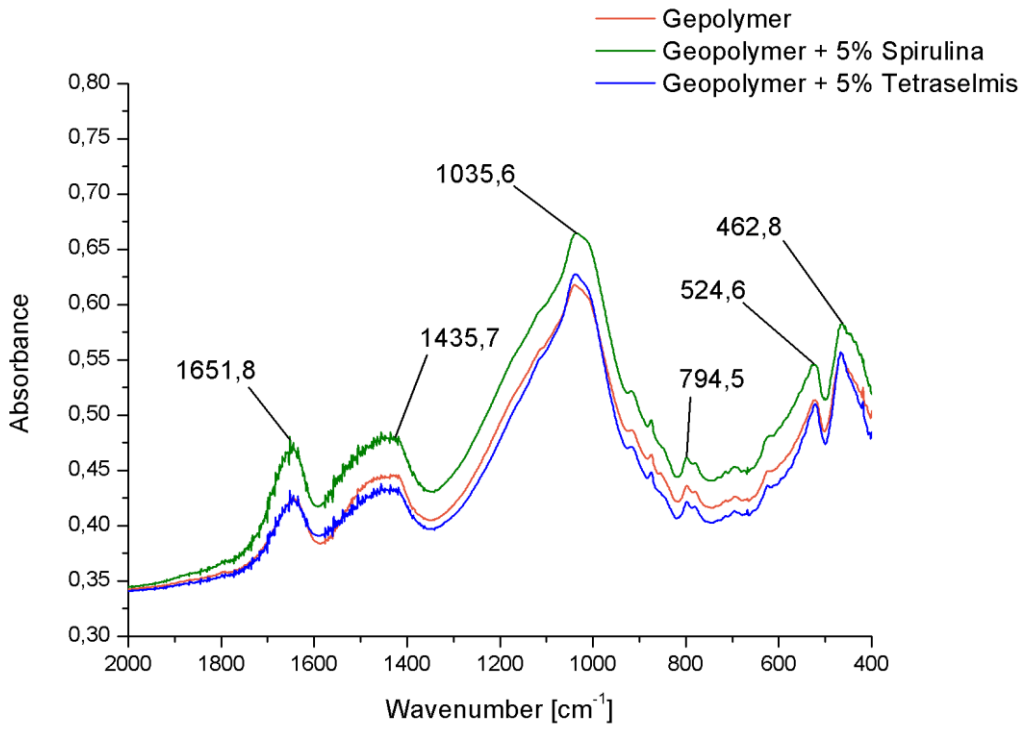

Figure 44. *Fourier Transform Infrared (FT-IR) Analysis after geopolymerization.*

The geopolymer FTIR spectra presents the strongest vibration typical of all aluminosilicates, which are assigned to internal vibrations of Si-O-Si and Si-O-Al. A strong Si-O stretching vibration can be noted at about 1080-1100 cm^{-1} and Si-O bending vibration at about 450-470 cm^{-1}. The peak at 1035 cm^{-1} is the characteristic peak of a bentonite based geopolymer. Moreover, the bands between 600-800 cm^{-1} are due to Al-O-Si vibrations: the bands at 794 cm^{-1} are due to Al-O stretching vibrations [90].

In both cases, before and after geopolymerization, there is no formation of other peaks. Microalgal species do not act as a chemical filler, but as passive filler since there is no chemical interaction or chemical bonds formation between microalgae and the geopolymer structure.

3.6 Three-point Flexural test results

Three-point bending was performed on several 3D-printed samples (**Figure 45**) in order to observe the microalgae effect on a well-crosslinked geopolymer structure.

Figure 45. *Geopolymer sample used for the three-point flexural test.*

The **Figure 46** shows the Flexural Moduli versus the filler content (microalgae).

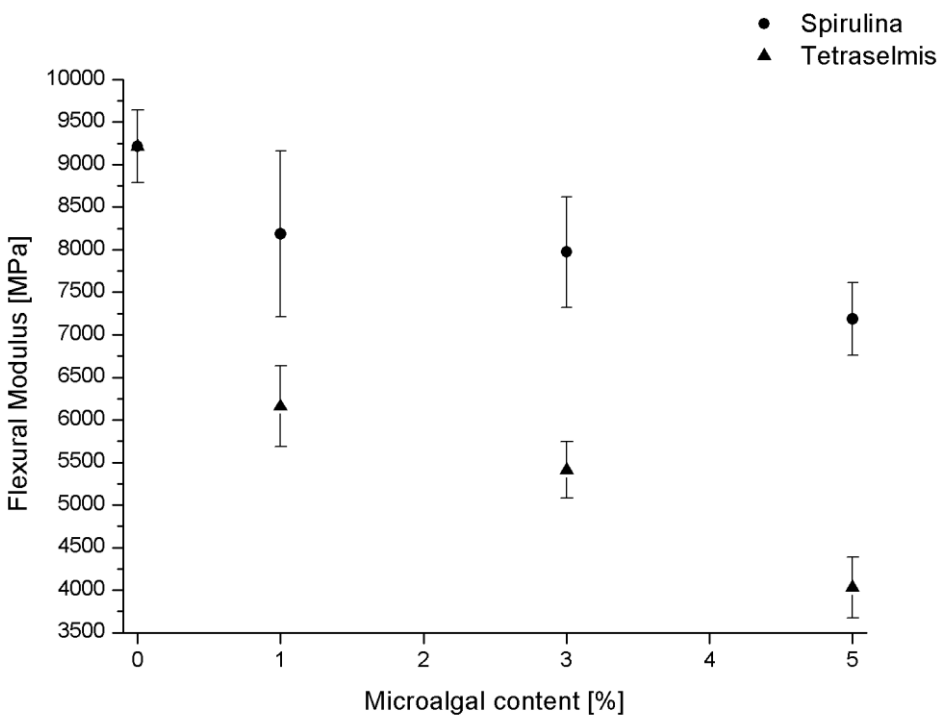

Figure 46. *Flexural Modulus, E_f versus microalgae content.*

A Flexural Modulus around 9200 MPa can be observed with 0% of microalgae content. The graph (**Figure 46**) shows also a decreasing profile with increasing microalgae content and a different influence of the two microalgal species on the mechanical properties. Modulus reduction of only 20% can be noted, despite the highest percentage of Spirulina was used. By using Tetraselmis a reduction of around 60% occurs. The different effect on the Flexural Modulus is due to the different chemical composition of the two microalgal species used in this work.

3.7 Shear test results

Dynamic mechanical analysis in shear mode was performed at different frequency intensities. **Figure 47** shows Storage Modulus, M' and Loss Modulus, M'' of fresh geopolymer paste without microalgae addition.

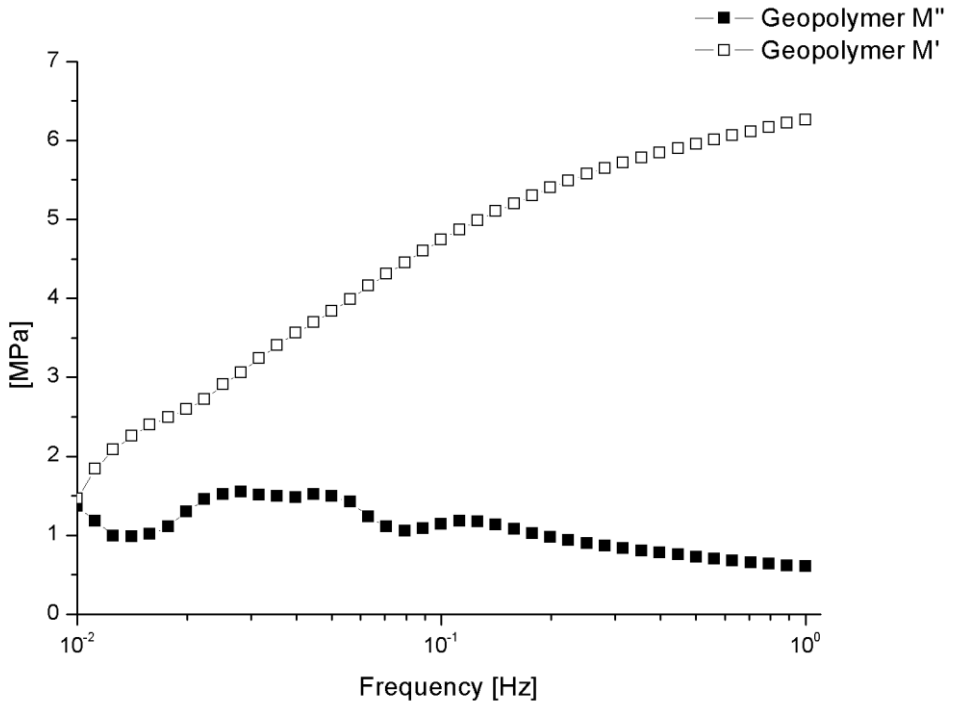

Figure 47. *Storage Modulus, M' and Loss Modulus M'' of fresh geopolymer paste at t_0, from 0.01 Hz up to 1 Hz.*

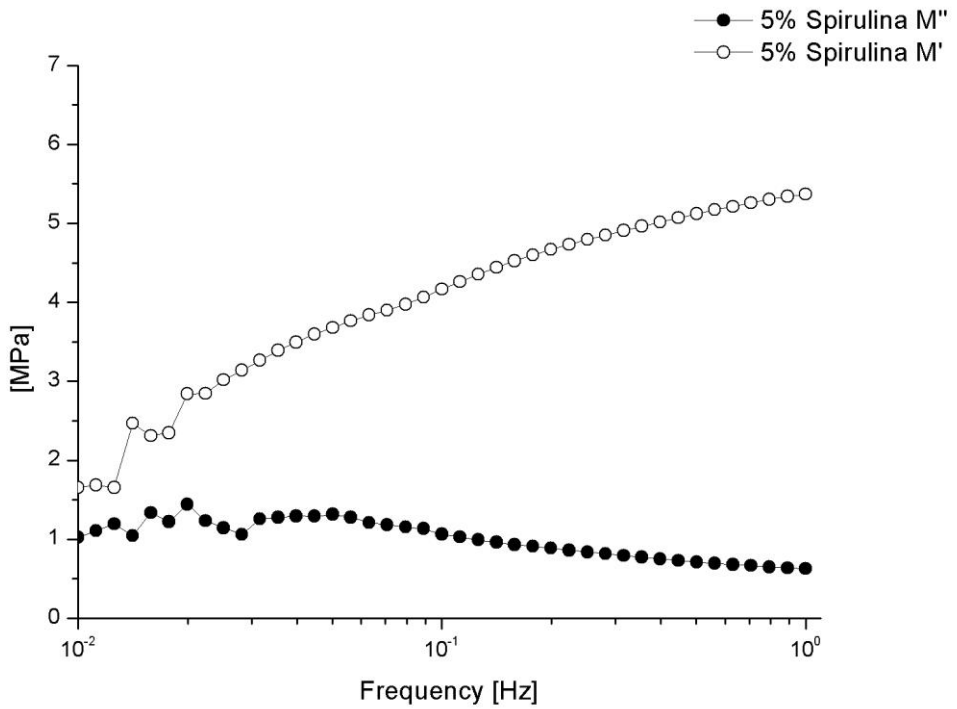

Figure 48. *Storage Modulus, M' and Loss Modulus, M'' of fresh geopolymer paste with 5% of Spirulina at t_0, from 0.01 Hz up to 1 Hz.*

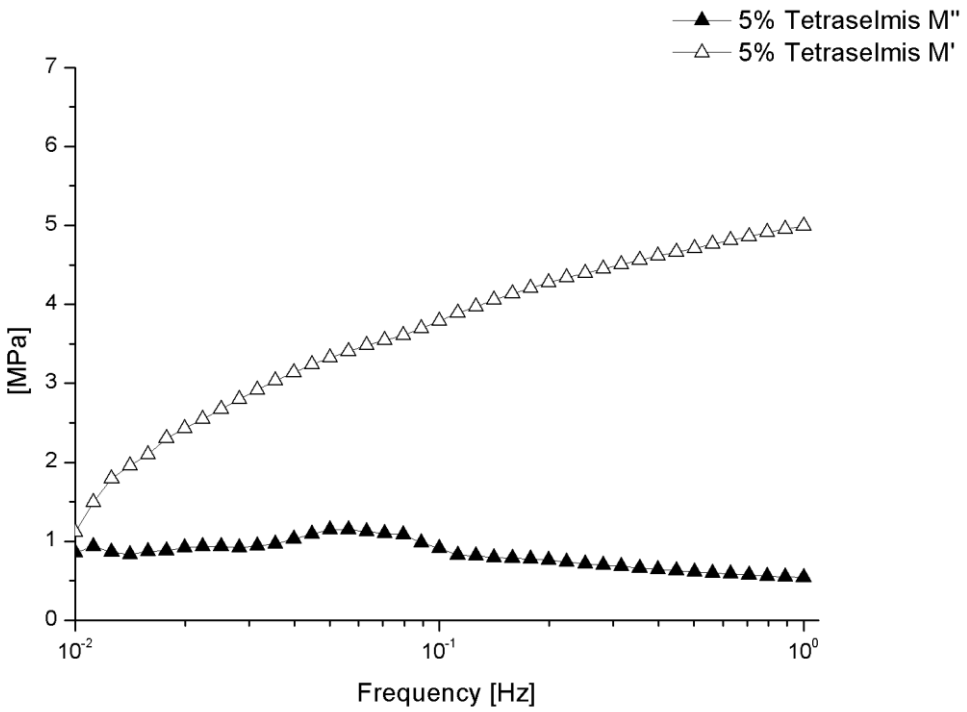

Figure 49. *Storage Modulus, M' and Loss Modulus M'' of fresh geopolymer paste with 5% of Tetraselmis at t_0, from 0.01 Hz up to 1 Hz.*

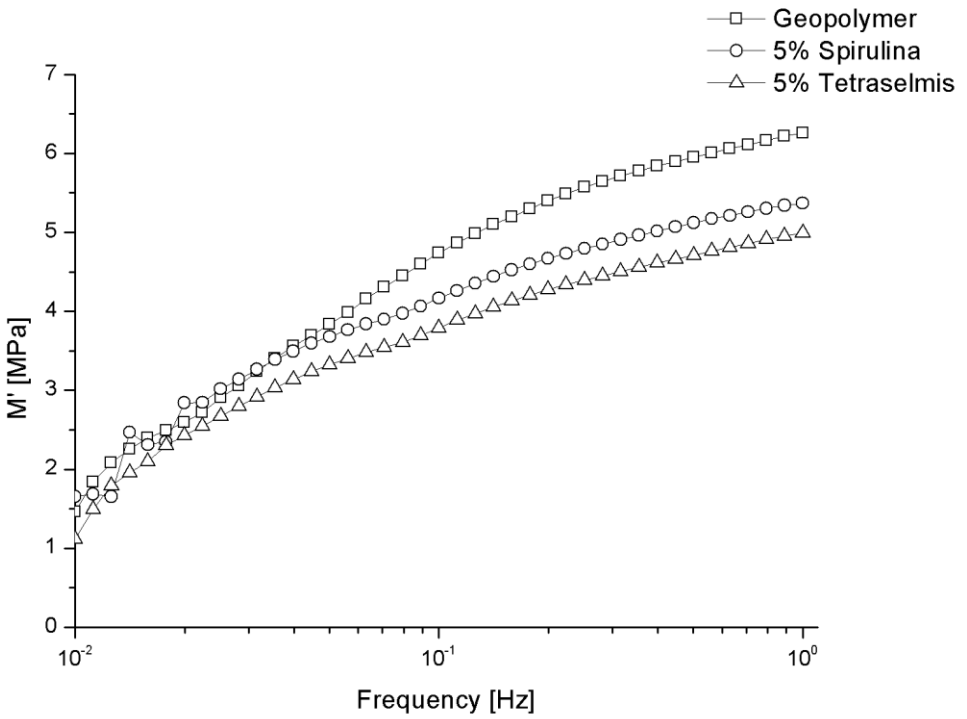

Figure 50. *Comparison between Storage Moduli at t_0, from 0.01 Hz up to 1 Hz.*

There is no intersection between the two Moduli. Fresh geopolymer paste behaves as a solid material, also at very low frequency and at time zero. The same results have been observed with the addiction of microalgae (see **Figure 48** and **Figure 49**). **Figure 50** shows a comparison between the Storage Moduli, M'.

There is no an appreciable difference between the three formulations. The addiction of the microalgae does not have a great effect on the Storage Modulus of geopolymer paste.

The evolution of Moduli versus time is also studied. All the results are reported in **Figure 51**, **Figure 52**, **Figure 53** and **Figure 54**.

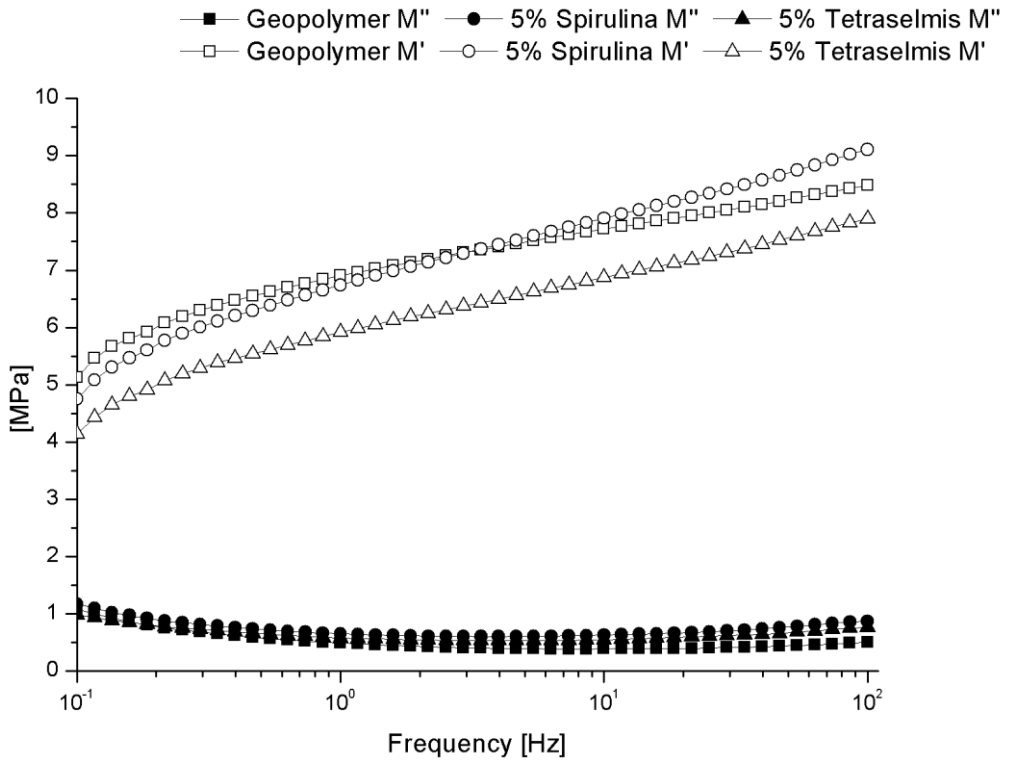

Figure 51. *Storage Modulus, M' and Loss Modulus, M'' at t_0, from 0.1 Hz up to 100 Hz.*

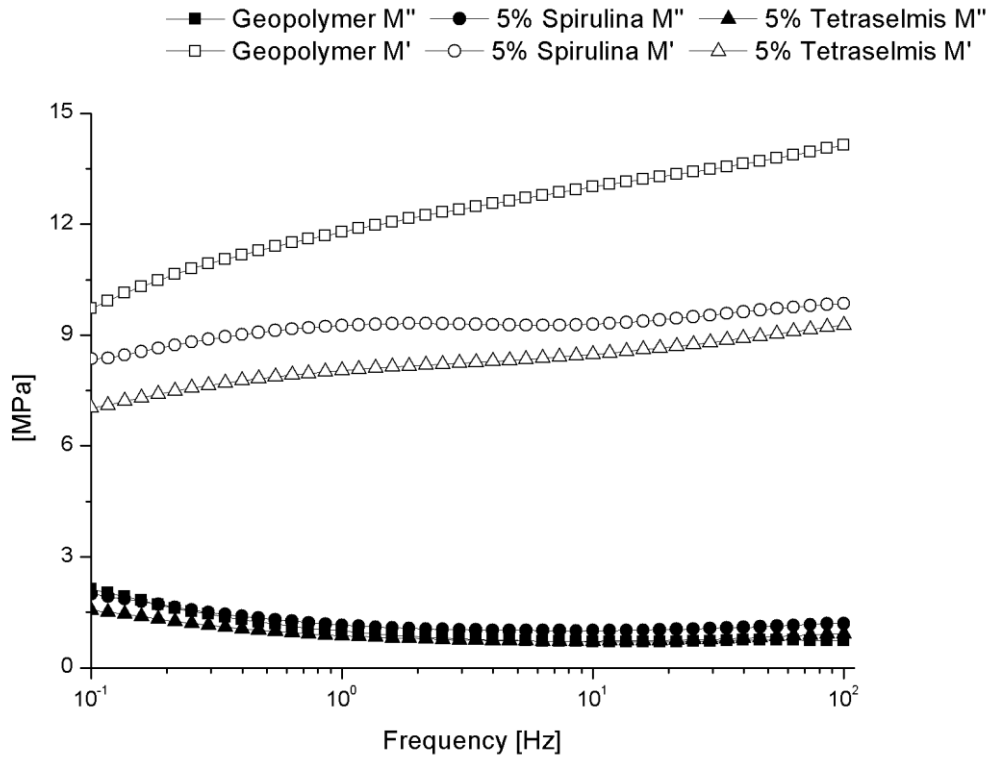

Figure 52. *Storage Modulus, M' and Loss Modulus, M'' after 60 min, from 0.1 Hz up to 100 Hz.*

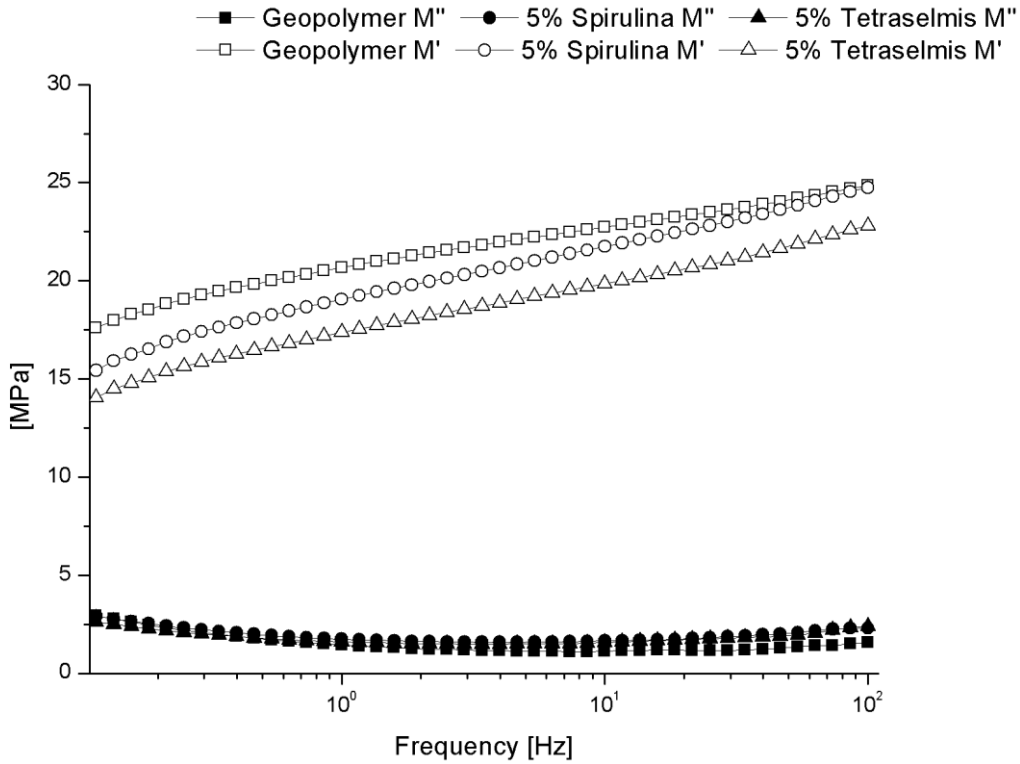

Figure 53. *Storage Modulus, M' and Loss Modulus, M'' after 120 min, from 0.1 Hz up to 100 Hz.*

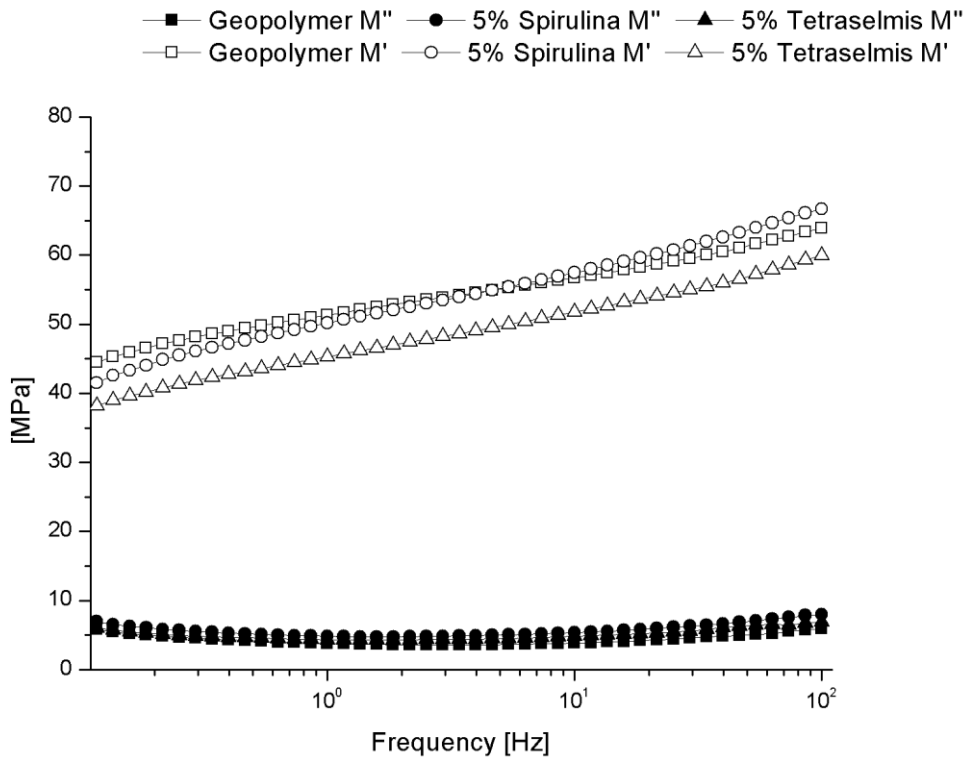

Figure 54. *Storage Modulus, M' and Loss Modulus, M'' after 240 min, from 0.1 Hz up to 100 Hz.*

On the one hand, the relatively constant Loss Modulus, M'' can be observed during the several measurements. On the other hand, the increase of Storage Modulus, M' can be clearly noted. During the measurements, the geopolymerization occurs which increases the hardness of the samples leading to a very high M' after four hours.

3.8 Compression test results

Several compression tests were carried out. The maximum stress was calculated by considering the maximum force divided by the exposed surface, so the compressive strength was evaluated.

Figure 55 and **Figure 56** show the results obtained by using thermal uncured 3D-printed samples, tested after 7 and 28 days.

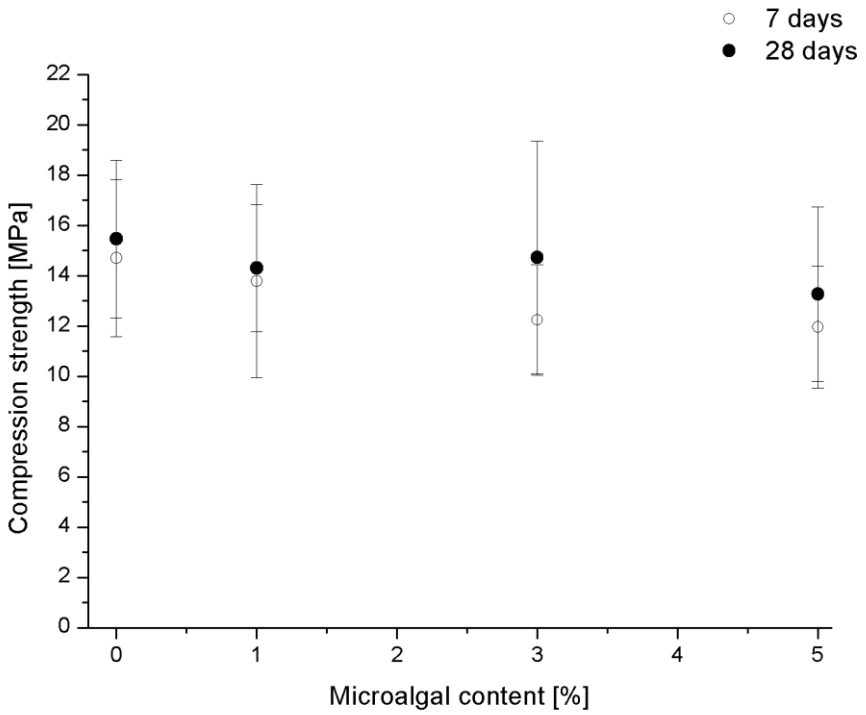

Figure 55. *Compressive strength of 3D-printed samples after 7 and 28 days of ambient curing with different content of Spirulina.*

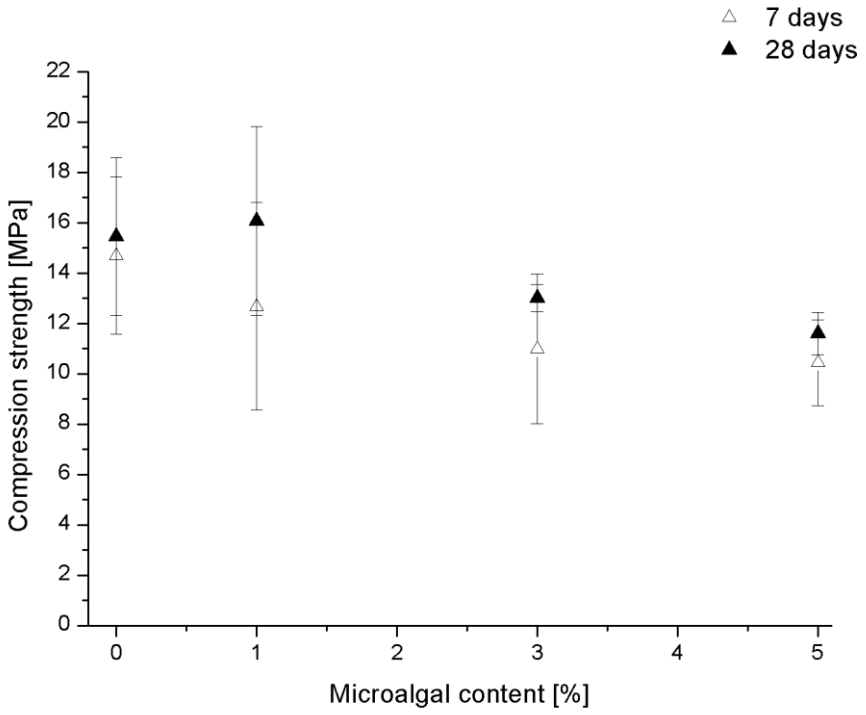

Figure 56. *Compressive strength of 3D-printed samples after 7 and 28 days of ambient curing with different content of Tetraselmis.*

It was observed that the compressive strength increases with the increase in the ambient curing period in accord to several bibliography studies [91], regardless from the microalgal species and content. The recorded improvement by increasing the ambient curing is due to an increase of the degree of geopolymerization versus time that leads to a gradual increase in compression strength.

By increasing the microalgal content a slight decrease of compressive strength can be noted, except for the case of 3% Spirulina after 28 days of ambient curing (see **Figure 55**). The mechanical propertis of the material decreases due to the addition of filler less performing than the geopolymer.

It should be noted that some printing defects and operating printing conditions (humidity, temperature, drying speed, etc.) have to be taken into account. Cracks and printing defects in the samples could affect the measurement and lower the mechanical properties.

A more remarkable difference can be noted by considering thermally cured 3D-printed samples as **Figure 57**, **Figure 58**, **Figure 59** and **Figure 60** show.

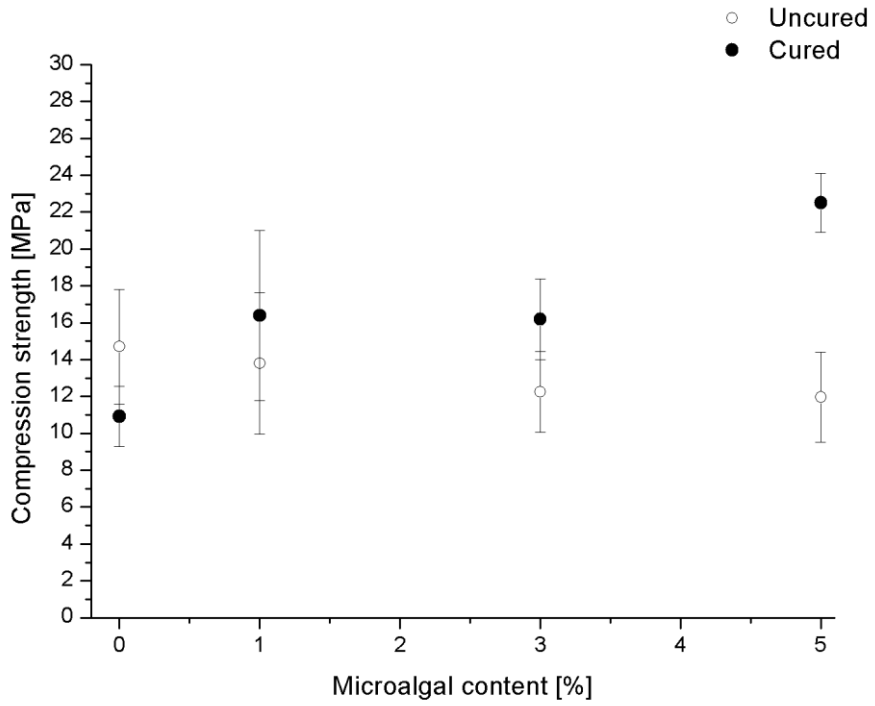

Figure 57. *Compressive strength of thermally cured and uncured 3D-prited samples with different content of Spirulina after 7 days of ambient curing.*

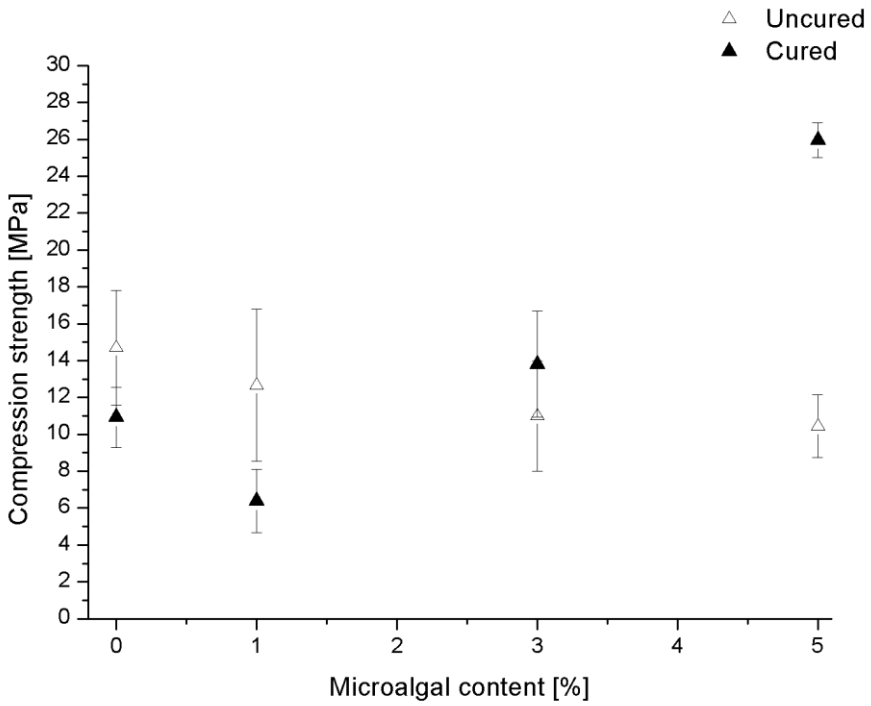

Figure 58. *Compressive strength of thermally cured and uncured 3D-printed samples with different content of Tetraselmis after 7 days of ambient curing.*

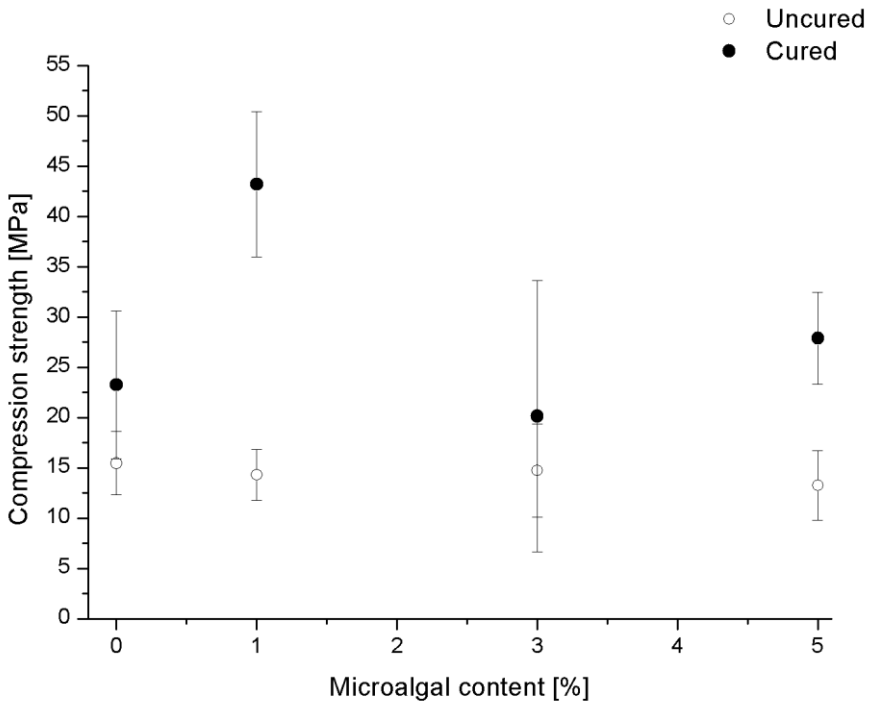

Figure 59. *Compressive strength of thermally cured and uncured 3D-printed samples with different content of Spirulina after 28 days of ambient curing.*

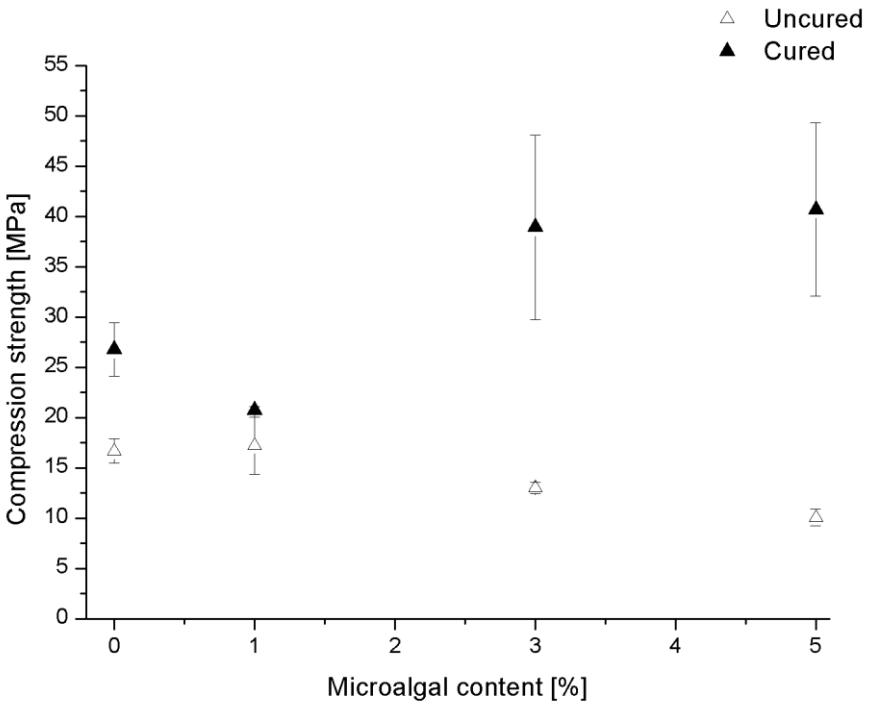

Figure 60. *Compressive strength of thermally cured and uncured 3D-printed samples with different content of Tetraselmis after 28 days of ambient curing.*

In **Figure 57** and **Figure 58**, in the case of 0% of microalgal content, it can be noted that the thermal curing does not have a positive impact on compressive strength, probably due to the fast evaporation of the unreacted water present in the geopolymer structure. While in **Figure 59** and **Figure 60** an increase of compressive strength can be observed, due to a well-crosslinked structure with lower amount of unreacted water inside it and due to the presence of heat which accelerated the geopolymerization reaction and Si-O-Al bond formation [92]. An increase of compressive strength can be observed by increasing the microalgal content, except for the case of 1% of Spirulina after 28 days of ambient curing (see **Figure 59**).

By considering the syringe-casted samples **Figure 61** and **Figure 62** show the results obtained after 7 and 28 days of ambient curing.

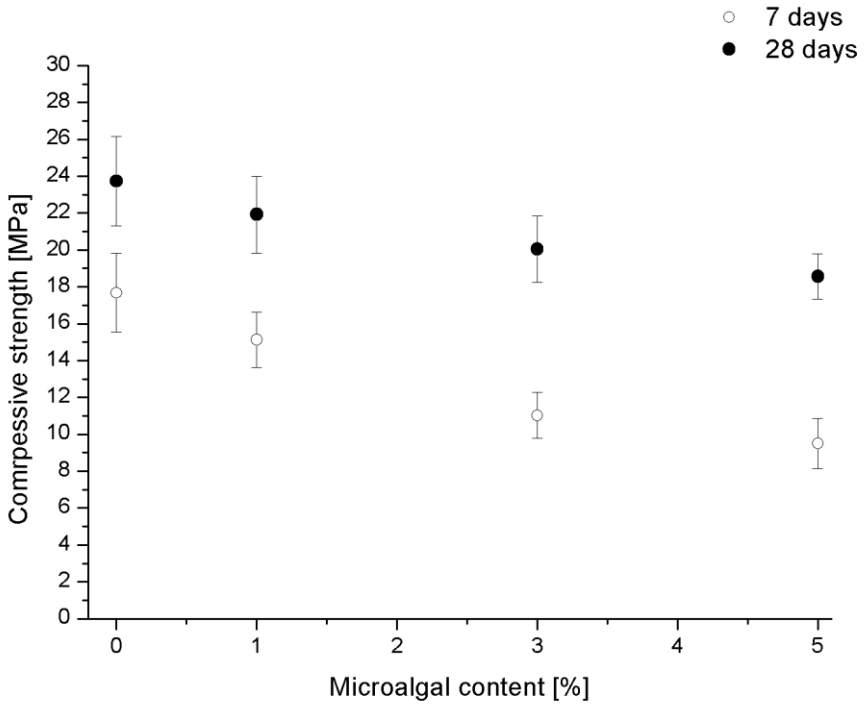

Figure 61. *Compressive strength syringe-casted samples after 7 and 28 days of ambient curing with different content of Spirulina.*

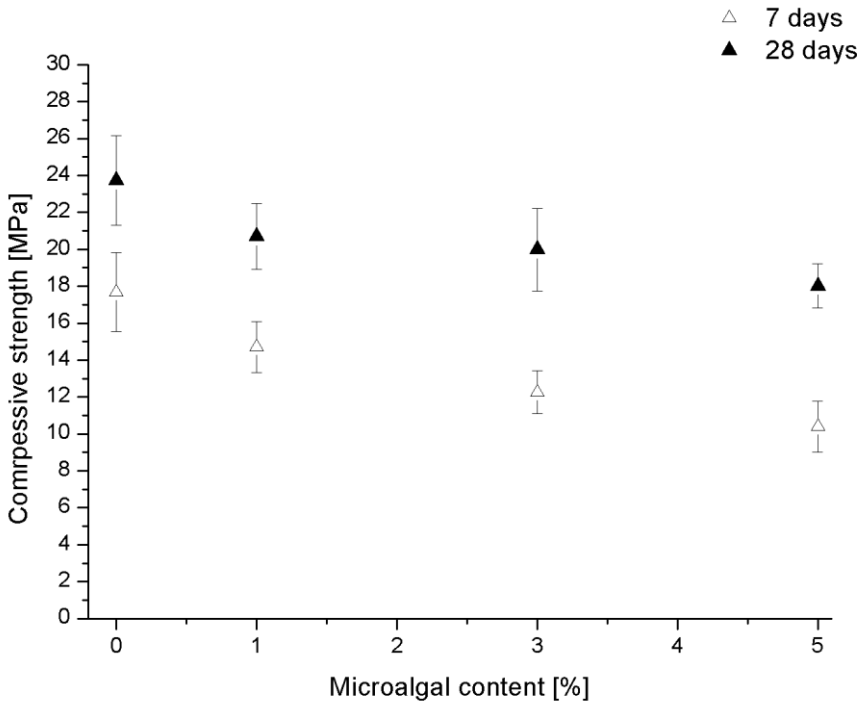

Figure 62. *Compressive strength syringe-casted samples after 7 and 28 days of ambient curing with different content of Tetraselmis.*

The same trend previously shown in the case of 3D-printed samples can be noted. After 28 days of ambient curing the compressive strength of the material increases, regardless from the amount of microalgae.

In the case of casted-samples, the fresh geopolymer paste was inserted and confined in a 1 ml syringe by applying a manual pressure with the plastic syringe piston in order to compact the material, so there is no “layer structure” and the issues associated with the 3D-printing process are not present. A more linear trend can be recognized: the decrease of the compressive strength by increasing he microalgal content can be clearly noted.

The results obtained with thermally cured syringe-casted samples are reported in **Figure 63**, **Figure 64**, **Figure 65** and **Figure 66**.

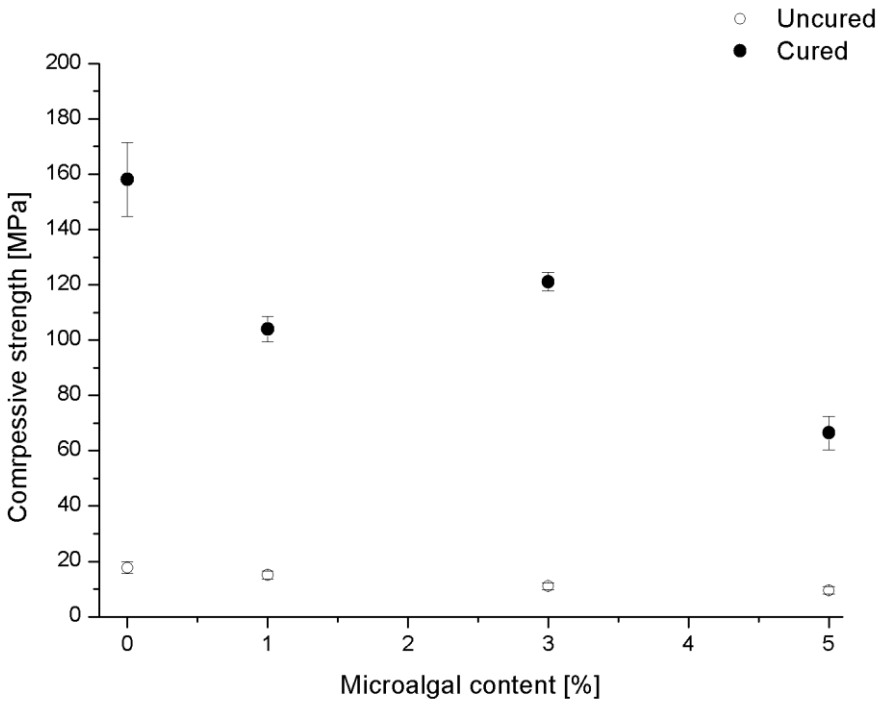

Figure 63. *Compressive strength of thermally cured and uncured syringe-casted samples with different content of Spirulina after 7 days of ambient curing.*

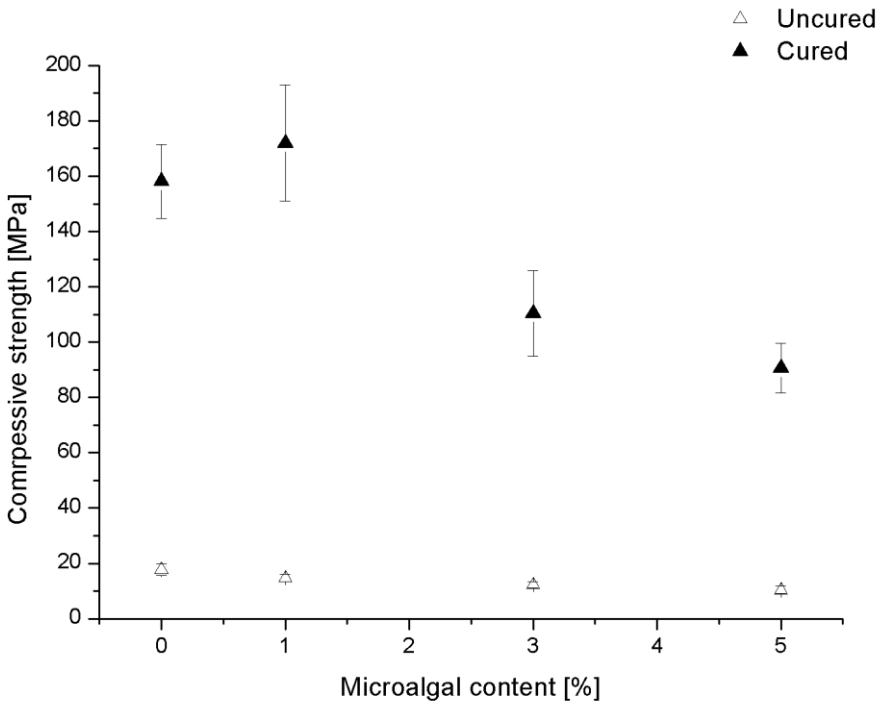

Figure 64. *Compressive strength of thermally cured and uncured syringe-casted samples with different content of Tetraselmis after 7 days of ambient curing.*

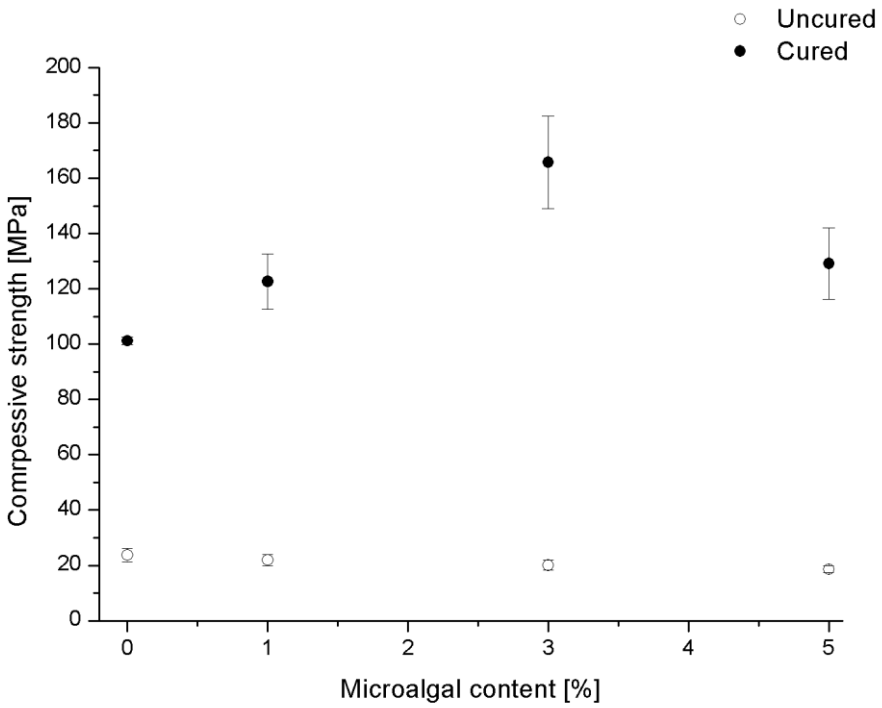

Figure 65. *Compressive strength of thermally cured and uncured syringe-casted samples with different content of Spirulina after 28 days of ambient curing.*

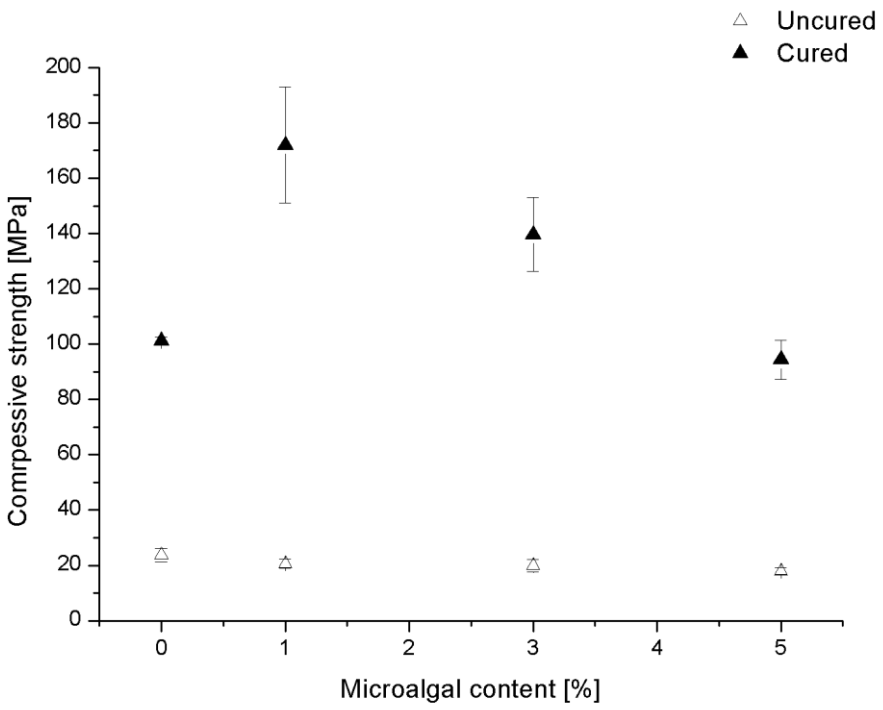

Figure 66. *Compressive strength of thermally cured and uncured syringe-casted samples with different content of Tetraselmis after 28 days of ambient curing.*

A better repeatability was obtained with syringe-casted samples with a significantly lower standard deviation that allows to better appreciate the differences.

In general, all the results show a significantly increase of compression strength after thermal curing at high temperature by considering microalgal content. In the case of syringe-casted samples after 28 days of ambient curing and the additional heat treatment, a compressive strength around 180 MPa was detected (see **Figure 65** and **Figure 66**), that is much higher than the compressive strength of high-strength concrete building (40 MPa) [93].

Mechanical strength of geopolymers changes due to high temperature induced structural and phase composition changes in the material. Structural changes include sintering, densification, melting, cracking and pore size/volume/interconnectivity changes. Phase composition changes include crystal growth and crystal destruction.

In order to have significant changes in the crystal structure of the material and observe the crystallization of some minerals such as nepheline, leucite and

kaliophilite, very high temperatures are required (up to 1000°C). While the densification occurs between 550°C and 650°C. Densification of the geopolymer results in fewer voids and allows for more uniform stress gradients during an applied load, enabling greater mechanical strength. Sintering of the un-reacted material provides increased mechanical strength due to stronger bonding between the particles. Also a crack healing effect occurs during the high temperature exposure that is caused by the viscous sintering of the paste [13].

In case studied, also the degradation of the microalgae during the heat treatment of the samples have to be taken into consideration. The high compression strength showed by some samples with different microalgal content could be related to the formation of a Si-based component, like silicon carbide (SiC).

Several studies have been done in order to find a method for enhancing the compressive strength by incorporating silicon carbide particles or whiskers into a geopolymer matrix [94].

Silicon carbide exists in about 250 crystalline forms [95]. The polymorphism of SiC is characterized by a large family of similar crystalline structures called polytypes. They are variations of the same chemical compound that are identical in two dimensions and differ in the third. Thus, they can be viewed as layers stacked in a certain sequence. Naturally silicon carbide occurs as moissanite and is found merely in very little quantities in certain types of meteorites. The most encountered SiC material is thus man made. Traditionally, SiC material has been produced through the Acheson process, in an Acheson graphite electric resistance furnace, which is still used for production of poly-crystalline SiC. In this process, a solid-state reaction between silica sand and petroleum coke at very high temperature (more the 2500°C) leads to the formation of silicon carbide under the following general reaction:

$$SiO_2(s) + 3C \rightarrow SiC(s) + 2CO(g)$$

Crystalline SiC obtained by the Acheson-Process occurs in different polytypes and varies in purity [96].

Synthetic silicon carbide can be also produced from rice husk ash and coconut shell carbon calcined at 750°C for 2 hours [97]. At the end, the requirements that

could lead to SiC formation are: a high reactive silica and carbon source and a severe heat treatment. In the case studied in this thesis work, all these requirements are present. The reactive metakaolin represent the silica source and the decomposition at 800°C of the organic structure of microalgae (see Paragraph 3.3) could feasible be the carbon source.

More and detailed studies like X-ray photoelectron spectroscopy (XPS) or Infrared spectroscopy (IR) have to be done in order to better study the SiC formation and to exactly determinate the geopolymer-SiC structure.

3.9 Rheological study results

Several rheological tests have been performed in order to understand the influence of microalgae as filler in the geopolymer paste. Initially a paste without bentonite was prepared and the resulting viscosity curves are provided in **Figure 67**.

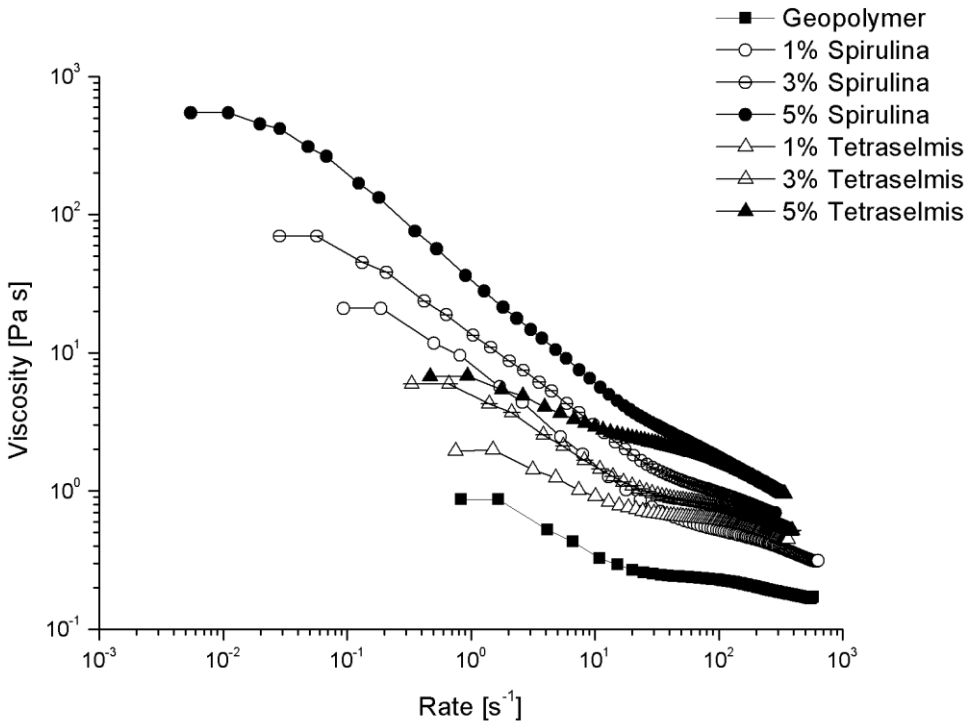

Figure 67. *Viscosity curves of bentonite-free geopolymer paste at different microalgae content.*

As can be seen, geopolymer paste behaves as a cement one [98] by showing a shear thinning behaviour, because of van der Waals colloidal forces dominate

hydrodynamic forces (both viscous and inertial) in the low strain rate regime and a viscosity inversely proportional to the shear rate can be measured. This thixotropic behaviour is present with major evidence also in the case of microalgal addition in the fresh paste. By increasing algal content an increase of viscosity can be noted, in particular with Spirulina species.

Other tests were carried out in order to have a better comparison with a more real 3D-printable fresh geopolymer paste. Due to the high viscosity increase and the measurement instability, only half of bentonite was added in the analysed paste. The resulting curves can be observed in **Figure 68**. Then different measurements using water mixed with microalgae were done (**Figure 69**).

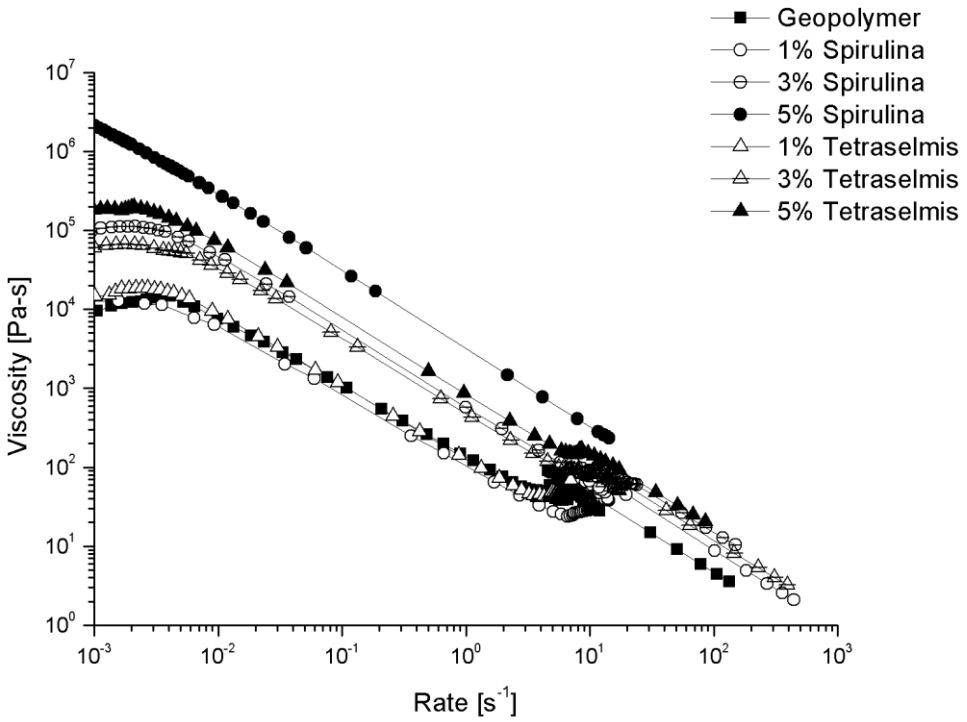

Figure 68. *Viscosity curves of geopolymer paste with half bentonite at different microalgae content.*

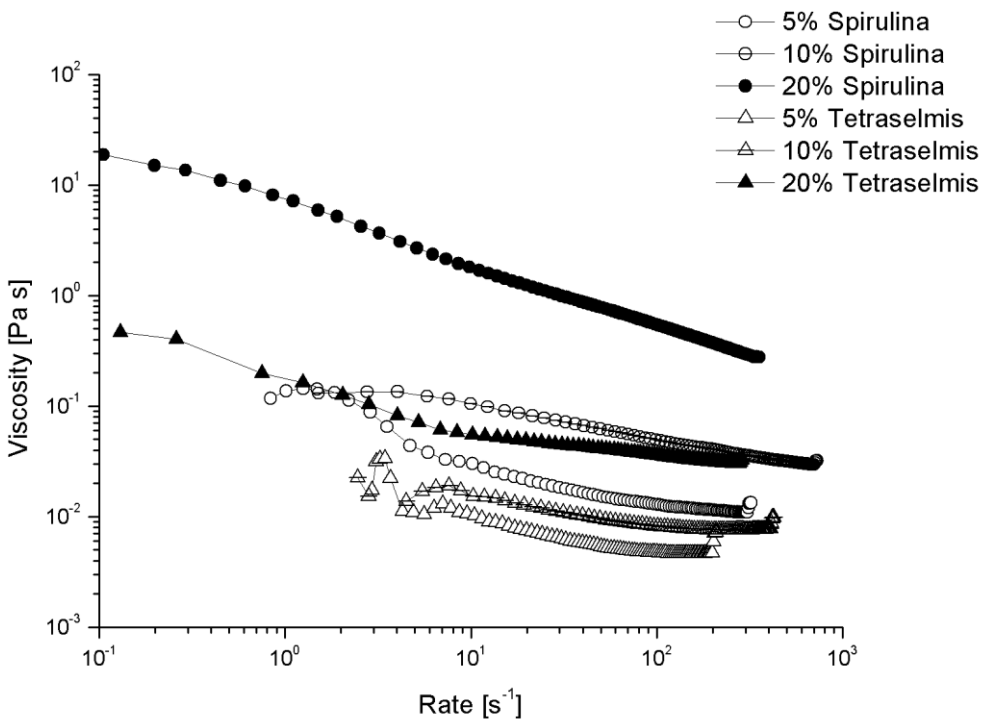

Figure 69. *Viscosity curves of distilled water with different microalgal content.*

Thanks to thixotropic behaviour a printable paste can be obtained and the material can be easily extruded through a plastic syringe. In the case of half-bentonite formulation (see **Figure 68**) the viscosity is greater due to the addition of bentonite as supplementary material.

Figure 69 provides the results of another measurement that was performed with distilled water in order to evaluate the different influence of the two microalgal species on the viscosity. Greater percentages were used to better observe the effect of algae. Spirulina seems to have the major influence on viscosity, also in the case of distilled water. With 20% of Spirulina a drastic increase of viscosity can be noted.

3.10 Printability test results

Interesting results were obtained by printability tests. **Figure 70** and **Figure 71** show some examples obtained with 3D-printed truncated cones at inclination of 65° and 55°.

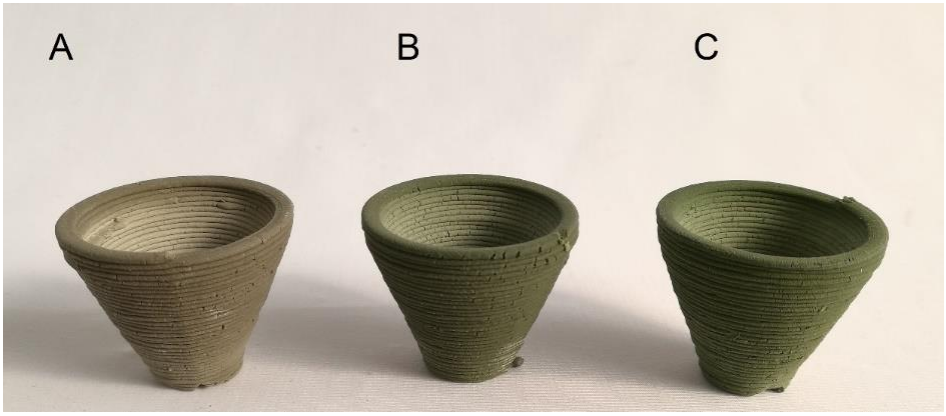

Figure 70. *3D-printed empty truncated cones at 65° of inclination: A geopolymer; B with Spirulina; C with Tetraselmis.*

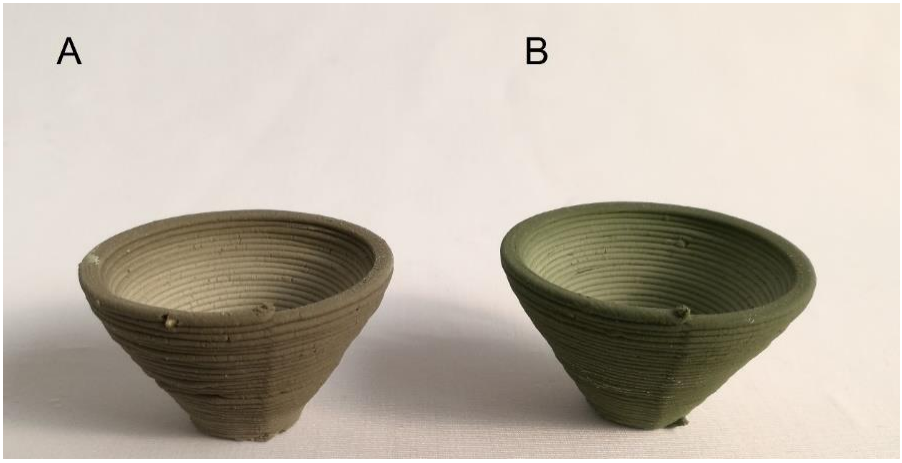

Figure 71. *3D-printed empty truncated cones at 55° of inclination: A geopolymer; B with microalgae.*

As can be noted from the pictures, the addition of microalgae does not have relevant effect on the printing. This can be observed with all the microalgae percentages considered in this study.

By considering a higher inclination at 45°, some differences emerged. The geopolymer paste with no addition of microalgae is not capable to support the high stresses and deformations due to the wall inclination (**Figure 72**). During the print cracks formation occurs through the layers avoiding the completion of the final object.

Figure 72. *3D-printed empty truncated cones at 45° of inclination: A geopolymer; B with microalgae.*

A more compact and printable paste can be obtained with microalgae addition. The object suffers less deformations generated by the nozzle of the syringe during the print thanks also to the higher viscosity.

By considering the rheological study and the printability results previously shown, an experiment by substituting 2% in weight of bentonite with microalgae was made. The result is showed in **Figure 73**.

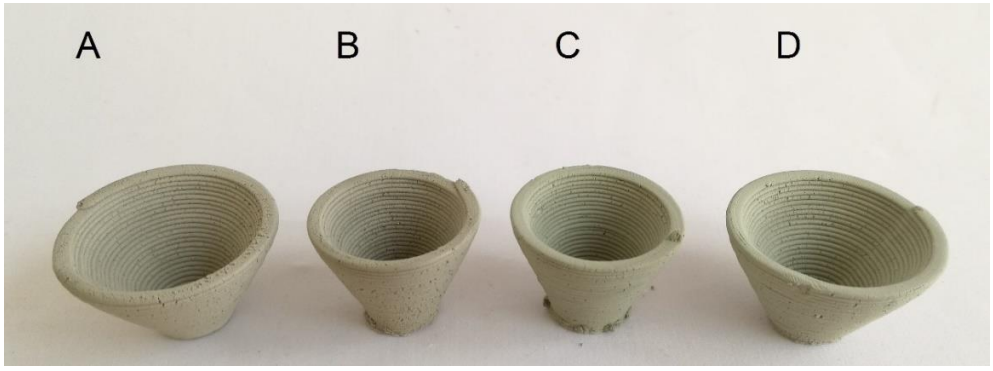

Figure 73. *3D-printed empty truncated cones: A geopolymer at 55°; B geopolymer at 65°; C microalgae at 65°; D microalgae at 55°.*

No difference is recognized except for a mild green colour between the objects. The replacement of a small percentage of bentonite with microalgae does not affect the print and the final printed object. This last result leads at an interesting consideration since an inorganic passive filler in principle may be replaced by an organic one (biomass).

Chapter 4: Conclusions

In this work, several and different geopolymer samples with different microalgal content were prepared by using a commercial metakaolin and bentonite powder and an alkaline solution mainly composed of sodium silicate. Spirulina Platensis and Tetraselmis Seucica microalgae were analysed and used in order to study and evaluate the effect of an organic filler on mechanical and rheological properties of the geopolymer paste. Subsequently, a severe thermal treatment was performed at 800°C in order to carried out additional compression tests and observe the influence on compressive strength of the green-blue microalgae into the geopolymer matrix.

By considering geopolymer samples after ambient curing and without thermal treatment, following concluding remarks have been made on basis of the work conducted:

- Thermogravimetric analysis shows that the decomposition temperature of the two microalgal species is around 600°C. After this temperature, the TGA curve becomes flat and no weight losses is anymore detected by the instrument;
- the organic filler (microalgae) does not exhibit any chemical linkage with the aluminosilicate matrix at room temperature. The results obtained with infrared spectroscopy analysis shows that there is no chemical interaction and formation of new peaks in the analysed spectra. In this case, microalgae act as passive filler, without taking part in the geopolymerization reaction. This assumption is also proved by the shear tests done on fresh geopolymeric paste. The presence of microalgae does not significantly affect the evolution of the Storage Modulus versus time;
- microalgae addition does not have a positive effect on the flexural strength of the geopolymer material that slightly decreases by increase the microalgal content.

- compressive strength of geopolymer increases with increasing ambient curing time, regardless the microalgae content, due to a well-crosslinked structure;
- by considering the microalgal addition, a decrease of the compressive strength with increasing microalgal content can be observed, both in the case of ambient curing after 7 days or 28 days.

More interested results are obtained by considering the samples after the thermal curing at 800°C: very high compressive strength (160 – 180 MPa) was registered in the case of samples with different microalgal content, but more detailed studies have to be carried out due to no-linear or predictable trend obtained from the data. In particular, the probable formation of silicon-carbon-based compounds have to be investigated with proper analysis.

Regarding the rheological study and the promising 3D-printing technology, other conclusions remarks are listed below:

- Microalgal content significantly affect the viscosity of a fresh geopolymer paste. The viscosity increases with increasing microalgal content. The increase of viscosity is more remarkable in the case of Spirulina Platensis;
- the greater influence of Spirulina on viscosity is also proved in the case of water measurements;
- the addition of microalgae does not modify the thixotropic behaviour of the fresh geopolymer paste and the obtained paste can be easily extruded trough a plastic syringe;
- a better mechanical stability during the 3D-print was observed in presence of microalgae in the geopolymer paste;
- based on rheological studies, several printability tests by substituting 2% wt/wt of bentonite with microalgae were done and no difference is recognized on the final 3D-printed objects based on a post-printing visual inspection.

4.1 Feature developments

A wide range of applications could be feasible on basis of the obtained results.

Advanced 3D-printing technology using geopolymer as building material by exploiting the good printability properties conferred by the organic filler obtained from exhaust microalgae could be developed. The first residential building was already built in 24 hours by a Russian company (Apis Core®). They used a 3D-printer of 1.5 meters height with a maximum operation area of 132 m^2 and a properly pressure-system to enhance the extrusion of the geopolymer paste (**Figure 74**) [99].

Abrasive and resistant tools could also be developed in order to exploit the properties of thermally cured geopolymer mixed with microalgae, and so on.

Figure 74. *Advanced 3D-printer developed by Apis Core company* [99].

More and detailed studies are needed in order to clarify and better understand the complex field of alkali-activated binders and the possible application of biomass as organic filler with a high added value. It should be also noted that all the results were obtained by using freeze drying green-blue microalgae. Following feature developments are needed:

- To understand the variation of geopolymer chemical structure with different NaOH and Na_2SiO_3 ratio in the alkaline solution used as activator;

- to perform infrared spectroscopy and X-ray photoelectron spectroscopy (XPS) analysis on the samples after the thermal curing at 800°C, in order to detect the chemical changes related to the formation of new chemical bonds in the geopolymer matrix;
- to better explore the possibility of substituting a low amount of standard supplementary aluminosilicate material as bentonite with microalgae for 3D-printing applications without significantly affect the final mechanical propertis of the material;
- to study the effect of microalgae on geopolymer paste in terms of porosity and shrinkage;
- to explore different species of microalgae with the aim to find the optimal one in terms of chemical composition for geopolymer applications;
- finally, to develop and build up all the process steps starting from the biological wastewater treatment by using microalgae to the next use of the obtained exhaust biomass as organic filler in geopolymer paste.

List of Figures

List of Tables

Bibliography

[1] I. Journal, C. P. Kiran, and R. Tagore, "Conceptual Utilisation of Additive Manufacturing With ' 3D - Printing ,'" vol. 5, no. 7, 2016.

[2] N. Guo and M. C. Leu, "Additive manufacturing: Technology, applications and research needs," *Front. Mech. Eng.*, vol. 8, no. 3, pp. 215–243, 2013.

[3] J. Ur, R. Khan, G. R. Kumar, and P. Sammaiah, "3D Printer Ceramic Technology," vol. 2, no. 11, pp. 337–340, 2015.

[4] I. Gibson and D. Rosen, *Additive Manufacturing Technologies: 3D Printing, Rapid Prototyping, and Direct Digital Manufacturing*, Second Edi., vol. 32, no. 2. Springer New York Heidelberg Dordrecht London, 2012.

[5] A. Gebhardt and J.-S. Hotter, *Additive Manufacturing: 3D Printing for Prototyping and Manufacturing*. 2016.

[6] A. Gebhardt and A. Gebhardt, *Understanding additive manufacturing*. 2012.

[7] T. S. Srivatsan and T. S. Sudarshan, *Additive Manufacturing: Innovations, Advances, and Applications*. 2015.

[8] P. J. Kitson, M. D. Symes, V. Dragone, and L. Cronin, "Combining 3D printing and liquid handling to produce user-friendly reactionware for chemical synthesis and purification," *Chem. Sci.*, vol. 4, no. 8, pp. 3099–3103, 2013.

[9] C. R. Tubío *et al.*, "3D printing of a heterogeneous copper-based catalyst," *J. Catal.*, vol. 334, pp. 110–115, 2016.

[10] Amit Bandyopadhyay and S. Bose, *Additive Manufacturing*. 2015.

[11] C. Barnatt, "3D PRINTING Third Edition."

[12] N. Travitzky *et al.*, "Additive manufacturing of ceramic-based materials," *Adv. Eng. Mater.*, vol. 16, no. 6, pp. 729–754, 2014.

[13] J. Provis L. and J. S. J. van Devener, *Geopolymers: Structure, processing, properties and industrial applications*. Woodhead Publishing Limited, 2009.

[14] A. M. Rashad, "Metakaolin as cementitious material : History , scours , production and composition – A comprehensive overview," *Constr. Build. Mater.*, vol. 41, pp. 303–318, 2013.

[15] J. A. L. F. Pacheco-Torgal, A. P. and C. Leonelli, and P. Chindaprasirt, *Handbook*

of Alkali-activated Cements, Mortars and Concretes, vol. 53, no. 9. 2013.

[16] D. Khale and R. Chaudhary, “Mechanism of geopolymerization and factors influencing its development: A review,” *J. Mater. Sci.*, vol. 42, no. 3, pp. 729–746, 2007.

[17] J. Davidovits, “Properties of Geopolymer Cements,” *First Int. Conf. Alkaline Cem. Concr.*, pp. 131–149, 1994.

[18] P. De Silva, K. Sagoe-Crenstil, and V. Sirivivatnanon, “Kinetics of geopolymerization: Role of Al2O3 and SiO2,” *Cem. Concr. Res.*, vol. 37, no. 4, pp. 512–518, 2007.

[19] P. Duxson, A. Fernández-Jiménez, J. L. Provis, G. C. Lukey, A. Palomo, and J. S. J. Van Deventer, “Geopolymer technology: The current state of the art,” *J. Mater. Sci.*, vol. 42, no. 9, pp. 2917–2933, 2007.

[20] P. Duxson, J. L. Provis, G. C. Lukey, S. W. Mallicoat, W. M. Kriven, and J. S. J. Van Deventer, “Understanding the relationship between geopolymer composition, microstructure and mechanical properties,” *Colloids Surfaces A Physicochem. Eng. Asp.*, vol. 269, no. 1–3, pp. 47–58, 2005.

[21] F. Skvara, K. Lubomir, Kj. Nemecek, and Z. Bittnar, “Microstructure of geopolymer materials based on fly ash,” *Ceram. - Silikaty*, vol. 50, no. 4, pp. 208–215, 2006.

[22] P. Duxson, S. W. Mallicoat, G. C. Lukey, W. M. Kriven, and J. S. J. van Deventer, “The effect of alkali and Si/Al ratio on the development of mechanical properties of metakaolin-based geopolymers,” *Colloids Surfaces A Physicochem. Eng. Asp.*, vol. 292, no. 1, pp. 8–20, 2007.

[23] A. Nazari and J. G. Sanjayan, *Handbook of Low Carbon Concrete*. 2017.

[24] H. RAHIER, W. SIMONS, B. VAN MELE, and M. BIESEMANS, “Low-temperature synthesized aluminosilicate glasses: Part III Influence of the composition of the silicate solution on production, structure and properties,” *J. Mater. Sci.*, vol. 32, no. 9, pp. 2237–2247, 1997.

[25] S. Alonso and A. Palomo, “Alkaline activation of metakaolin and calcium hydroxide mixtures: influence of temperature, activator concentration and solids ratio,” 2001.

[26] A. Fernández-Jiménez and A. Palomo, “Composition and microstructure of

alkali activated fly ash binder: Effect of the activator," *Cem. Concr. Res.*, vol. 35, no. 10, pp. 1984–1992, 2005.

[27] I. Nikolić, L. Karanović, I. J. Častvan, V. Radmilović, S. Mentus, and V. Radmilović, "Improved compressive strength of alkali activated slag upon heating," 2014.

[28] F. Puertas and A. Fernández-Jiménez, "Mineralogical and microstructural characterisation of alkali-activated fly ash/slag pastes," *Cem. Concr. Compos.*, vol. 25, no. 3, pp. 287–292, 2003.

[29] J. C. Swanepoel and C. A. Strydom, "Utilisation of fly ash in a geopolymeric material," *Appl. Geochemistry*, vol. 17, no. 8, pp. 1143–1148, 2002.

[30] S. A. Bernal, "Effect of the activator dose on the compressive strength and accelerated carbonation resistance of alkali silicate-activated slag/metakaolin blended materials," *Constr. Build. Mater.*, vol. 98, pp. 217–226, 2015.

[31] N. T. Abdel-Ghani, H. A. Elsayed, and S. AbdelMoied, "Geopolymer synthesis by the alkali-activation of blastfurnace steel slag and its fire-resistance," *HBRC J.*, pp. 1–6, 2016.

[32] F. Pacheco-Torgal, Z. Abdollahnejad, A. F. Camões, M. Jamshidi, and Y. Ding, "Durability of alkali-activated binders: A clear advantage over Portland cement or an unproven issue?," *Constr. Build. Mater.*, vol. 30, pp. 400–405, 2012.

[33] J. W. Phair, "Green chemistry for sustainable cement production and use," *Green Chem.*, vol. 8, no. 9, p. 763, 2006.

[34] A. M. Neville, *Properties of Concrete*. 2011.

[35] M. Brito, E. Case, and W. M. Kriven, *Developments in Porous , Biological and Geopolymer Ceramics*. 2007.

[36] Y. Muntingh, "Durability and diffusive behaviour evaluation of geopolymeric material," no. December, 2006.

[37] M. K. Head and N. R. Buenfeld, "Measurement of aggregate interfacial porosity in complex, multi-phase aggregate concrete: Binary mask production using backscattered electron, and energy dispersive X-ray images," *Cem. Concr. Res.*, vol. 36, no. 2, pp. 337–345, 2006.

[38] Z. K. Abdulsada, "Evaluation of Microalgae for Secondary and Tertiary

Wastewater Treatment," *Dep. Civ. Environ. Eng.*, vol. Environmen, no. August, p. 114, 2014.

[39] K. Larsdotter, "Wastewater treatment with microalgae – a literature review," *Vatten*, vol. 62, pp. 31–38, 2006.

[40] H. Taher, S. Al-Zuhair, A. H. Al-Marzouqi, Y. Haik, and M. M. Farid, "A review of enzymatic transesterification of microalgal oil-based biodiesel using supercritical technology," *Enzym. Res*, vol. 2011, p. 468292, 2011.

[41] L. BARSANTI and P. GUALTIERI, *Algae: Anatomy, Biochemistry, and Biotechnology*. 2014.

[42] W. Klinthong, Y. H. Yang, C. H. Huang, and C. S. Tan, "A Review: Microalgae and their applications in CO<inf>2</inf> capture and renewable energy," *Aerosol Air Qual. Res.*, vol. 15, no. 2, pp. 712–742, 2015.

[43] L. Christenson and R. Sims, "Production and harvesting of microalgae for wastewater treatment, biofuels, and bioproducts," *Biotechnol. Adv.*, vol. 29, no. 6, pp. 686–702, 2011.

[44] Y. Chisti, "Biodiesel from microalgae beats bioethanol," *Trends Biotechnol.*, vol. 26, no. 3, pp. 126–131, 2008.

[45] T. Cai, S. Y. Park, and Y. Li, "Nutrient recovery from wastewater streams by microalgae: Status and prospects," *Renew. Sustain. Energy Rev.*, vol. 19, pp. 360–369, 2013.

[46] M. A. Borowitzka, "Commercial production of microalgae: ponds, tanks, tubes and fermenters," *J. Biotechnol.*, vol. 70, no. 1–3, pp. 313–321, 1999.

[47] A. Ruiz-Marin, L. G. Mendoza-Espinosa, and T. Stephenson, "Growth and nutrient removal in free and immobilized green algae in batch and semi-continuous cultures treating real wastewater," *Bioresour. Technol.*, vol. 101, no. 1, pp. 58–64, 2010.

[48] Y. Cohen, "Biofiltration - The treatment of fluids by microorganisms immobilized into the filter bedding material: a review," *Bioresour. Technol.*, vol. 77, no. 3, pp. 257–274, 2001.

[49] L. E. de-Bashan and Y. Bashan, "Immobilized microalgae for removing pollutants: Review of practical aspects," *Bioresour. Technol.*, vol. 101, no. 6, pp. 1611–1627, 2010.

[50] N. Abdel-Raouf, A. A. Al-Homaidan, and I. B. M. Ibraheem, "Microalgae and wastewater treatment," *Saudi J. Biol. Sci.*, vol. 19, no. 3, pp. 257–275, 2012.

[51] Y. shu Yuan and X. Yuan, "Progress and Prospects of High Salted Wastewater," *Adv. Sci. Eng.*, vol. 6, no. 1, pp. 37–63, 2014.

[52] N. F. Gray, *BIOLOGY OF WASTEWATER TREATMENT*, Second Edi. Imperial College Press, 2004.

[53] W. Ng, *Industrial wastewater treatment*. 2006.

[54] F. J. CERVANTES, S. G. Pavlostathis, and A. C. van Haandel, *Advanced Biological Treatment Processes for Industrial Wastewaters, Principles & Applications*. 2006.

[55] S. Mace and J. Mata-Alvarez, "Utilization of SBR Technology for Wastewater Treatment: An Overview," *Ind. Eng. Chem. Res.*, vol. 41, no. 23, pp. 5539–5553, 2002.

[56] M. Von Sperling, *Wastewater characteristics, treatment & Disposal, Volume 1*. 2007.

[57] M. Von Sperling, *Activated sludge and aerobic biofilm reactors*. IWA Publishing, 2007.

[58] M. Henze, P. Harremoes, J. la C. Jansen, and E. Arvin, *Wastewater Treatment: Biological and Chemical Processes*, Second Edi. Springer-Verlag Berlin Heidelberg New York, 1997.

[59] M. Kesaano, "Characterization and Performance of Algal Biofilms for Wastewater Treatment and Industrial Applications," p. 171, 2015.

[60] L. Guardabassi, D. M. A. Lo Fo Wong, and A. Dalsgaard, "The effects of tertiary wastewater treatment on the prevalence of antimicrobial resistant bacteria," *Water Res.*, vol. 36, no. 8, pp. 1955–1964, 2002.

[61] N. Qureshi, B. A. Annous, T. C. Ezeji, P. Karcher, and I. S. Maddox, "Biofilm reactors for industrial bioconversion processes: employing potential of enhanced reaction rates.," *Microb. Cell Fact.*, vol. 4, no. 1, p. 24, 2005.

[62] S. Sriram and R. Seenivasan, "Microalgae Cultivation in Wastewater for Nutrient Removal," vol. 3, no. 2, pp. 9–13, 2012.

[63] G. Roeselers, M. C. M. Van Loosdrecht, and G. Muyzer, "Phototrophic biofilms and their potential applications," *J. Appl. Phycol.*, vol. 20, no. 3, pp. 227–235,

2008.

[64] E. Flores and a Herrero, “Nitrogen assimilation and nitrogen control in cyanobacteria.,” *Biochem. Soc. Trans.*, vol. 33, no. Pt 1, pp. 164–167, 2005.

[65] M. D. Doran and W. C. Boyle, “Phosphorus removal by activated algae,” *Water Res.*, vol. 13, no. 8, pp. 805–812, 1979.

[66] D. Version, “Master Programme Energy and Environmental Sciences University of Groningen The use of microalgae as method for phosphorus removal from a human derived waste stream From a lab scale to a household scale cultivation system,” 2012.

[67] B. Singh, K. Bauddh, and F. Bux, *Algae and Environmental Sustainability*, vol. 7, no. Kant 2012. 2015.

[68] N. Das, R. Vimala, and P. Karthika, “Biosorption of heavy metals - An overview,” *Indian J. Biotechnol.*, vol. 7, no. 2, pp. 159–169, 2008.

[69] L. Travieso *et al.*, “Heavy metal removal by microalgae,” *Bull. Environ. Contam. Toxicol.*, vol. 62, no. 2, pp. 144–151, 1999.

[70] D. Kaplan, “Absorption and Adsorption of Heavy Metals by Microalgae,” *Handb. Microalgal Cult. Appl. Phycol. Biotechnol.*, pp. 602–611, 2013.

[71] S. K. Mehta and J. P. Gaur, “Use of algae for removing heavy metal ions from wastewater: progress and prospects.,” *Crit. Rev. Biotechnol.*, vol. 25, no. 3, pp. 113–152, 2005.

[72] P. Spolaore, C. Joannis-Cassan, E. Duran, and A. Isambert, “Commercial applications of microalgae,” *J. Biosci. Bioeng.*, vol. 101, no. 2, pp. 87–96, 2006.

[73] S. Sekar and M. Chandramohan, “Phycobiliproteins as a commodity: Trends in applied research, patents and commercialization,” *J. Appl. Phycol.*, vol. 20, no. 2, pp. 113–136, 2008.

[74] T. M. Mata, A. A. Martins, and N. S. Caetano, “Microalgae for biodiesel production and other applications: A review,” *Renew. Sustain. Energy Rev.*, vol. 14, no. 1, pp. 217–232, 2010.

[75] I. Rawat, R. Ranjith Kumar, T. Mutanda, and F. Bux, “Dual role of microalgae: Phycoremediation of domestic wastewater and biomass production for sustainable biofuels production,” *Appl. Energy*, vol. 88, no. 10, pp. 3411–3424, 2011.

[76] J. K. Pittman, A. P. Dean, and O. Osundeko, “Bioresource Technology The potential of sustainable algal biofuel production using wastewater resources,” *Bioresour. Technol.*, vol. 102, no. 1, pp. 17–25, 2011.

[77] S. Mobin and F. Alam, “Biofuel Production from Algae Utilizing Wastewater,” *19th Australas. Fluid Mech. Conf.*, no. December, 2014.

[78] M. Hu, X. Zhu, and F. Long, “Alkali-activated fly ash-based geopolymers with zeolite or bentonite as additives,” *Cem. Concr. Compos.*, vol. 31, no. 10, pp. 762–768, 2009.

[79] T. Mettler, “Dynamic Mechanical Analysis: sets new standards.” Instrument Service SNC.

[80] PerkinElmer Inc, “Dynamic Mechanical Analysis (DMA) - A Beginner’s Guide,” *Introd. to DMA*, pp. 1–23, 2008.

[81] G. W. Ehrenstein, G. Riedel, and P. Trawiel, “Chapter 6 Dynamic Mechanical Analysis,” *Therm. Anal. Plast. Theory Pract.*, pp. 236–299, 2004.

[82] F. W. Materials, C. Axial, and F. Application, “Standard Test Method for Monotonic Compressive Strength of Advanced Ceramics at,” vol. 10, no. 2015, pp. 1–13, 2016.

[83] A. Marcilla, A. Gómez-Siurana, C. Gomis, E. Chápuli, M. C. Catalá, and F. J. Valdés, “Characterization of microalgal species through TGA/FTIR analysis: Application to nannochloropsis sp.,” *Thermochim. Acta*, vol. 484, no. 1–2, pp. 41–47, 2009.

[84] “Principles of X-ray Diffraction.”

[85] H. J. Liu *et al.*, “Analysis and identification of irradiated Spirulina powder by a three-step infrared macro-fingerprint spectroscopy,” *Radiat. Phys. Chem.*, vol. 85, pp. 210–217, 2013.

[86] S. C. Corporation, “An Introductory guide to Rheology,” vol. VII, 1995.

[87] E. Perez, Barbosa-Cánovas, Gustavo V, A. Ibarz, E. Castell-Perez, and G. V Barbosa-Cánovas, “Newtonian and non-Newtonian flow.”

[88] C. Y. Heah *et al.*, “Study on solids-to-liquid and alkaline activator ratios on kaolin-based geopolymers,” *Constr. Build. Mater.*, vol. 35, pp. 912–922, 2012.

[89] M. Seynou *et al.*, “Production and Characterization of Pozzolan with Raw Clay from Burkina Faso,” *J. Miner. Mater. Charact. Eng.*, vol. 4, no. 3, pp. 195–209,

2016.

[90] C. Leonelli, E. Kamseu, and V. M. Sglavo, “Bi-Axial Four Points Flexural and Compressive Strength of Geopolymer Materials Based Na2O-K2O-Al2O3-SiO2 Systems,” pp. 155–164.

[91] A. M. Rajesh, M. A. Joe, and R. Mammen, “Study of the Strength Geopolymer Concrete with Alkaline Solution of Varying Molarity,” vol. 4, no. 6, pp. 19–24, 2014.

[92] Y. Y. Kim, B. J. Lee, V. Saraswathy, and S. J. Kwon, “Strength and durability performance of alkali-activated rice husk ash geopolymer mortar,” *Sci. World J.*, vol. 2014, 2014.

[93] K. Sisomphon and L. Franke, “Carbonation rates of concretes containing high volume of pozzolanic materials,” vol. 37, pp. 1647–1653, 2007.

[94] F. P. Du *et al.*, “Microstructure and compressive properties of silicon carbide reinforced geopolymer,” *Compos. Part B Eng.*, vol. 105, pp. 93–100, 2016.

[95] R. Cheunq, *Silicon Carbide Micro Electromechanical Systems*. Imperial College Press, 2006.

[96] H. Abderrazak, E. Selmane, and B. Hadj, “Silicon Carbide : Synthesis and Properties,” *Prop. Appl. Silicon Carbide*, no. C, pp. 361–389, 2011.

[97] S. Singh *et al.*, “Characteristics of Commercial SiC and Synthetic SiC as an aggregate in Geopolymer composites,” *J. Phys. Conf. Ser.*, vol. 755, p. 11001, 2016.

[98] A. Favier, J. Hot, G. Habert, N. Roussel, and J.-B. d’Espinose de Lacaillerie, “Flow properties of MK-based geopolymer pastes. A comparative study with standard Portland cement pastes,” *Soft Matter*, vol. 10, no. 8, p. 1134, 2014.

[99] “3D printer | Apis Cor. We print buildings.” [Online]. Available: http://apis-cor.com/en/3d-printer. [Accessed: 19-Jun-2017].